Chapter 7

Complex Analysis and Conformal Mapping

The term "complex analysis" refers to the calculus of complex-valued functions $f(z)$ depending on a single complex variable z. To the novice, it may seem that this subject should merely be a simple reworking of standard real variable theory that you learned in first year calculus. However, this naïve first impression could not be further from the truth! Complex analysis is the culmination of a deep and far-ranging study of the fundamental notions of complex differentiation and integration, and has an elegance and beauty not found in the real domain. For instance, complex functions are necessarily *analytic*, meaning that they can be represented by convergent power series, and hence are infinitely differentiable. Thus, difficulties with degree of smoothness, strange discontinuities, subtle convergence phenomena, and other pathological properties of real functions never arise in the complex realm.

The driving force behind many of the applications of complex analysis is the remarkable connection between complex functions and harmonic functions of two variables, a.k.a. solutions of the planar Laplace equation. To wit, the real and imaginary parts of any complex analytic function are automatically harmonic. In this manner, complex functions provide a rich lode of additional solutions to the two-dimensional Laplace equation, which can be exploited in a wide range of physical and mathematical applications. One of the most useful consequences stems from the elementary observation that the composition of two complex functions is also a complex function. We re-interpret this operation as a complex change of variables, producing a *conformal mapping* that preserves (signed) angles in the Euclidean plane. Conformal mappings can be effectively used for constructing solutions to the Laplace equation on complicated planar domains that appear in a wide range of physical problems, including fluid mechanics, aerodynamics, thermomechanics, electrostatics, and elasticity.

In this chapter, we will develop the basic techniques and theorems of complex analysis that impinge on the solution to boundary value problems associated with the planar Laplace and Poisson equations. We refer the novice to Appendix A for a quick review of the basics of complex numbers and complex arithmetic, and commence our exposition with the basics of complex functions and their differential calculus. We then proceed to develop the theory and applications of conformal mappings. The final section contains a brief introduction to complex integration and a few of its applications. Further developments and additional details and results can be found in a wide variety of texts devoted to complex analysis, including [**4**, **56**, **103**, **104**].

7.1. Complex Functions.

Our principal objects of study are complex-valued functions $f(z)$, depending on a single complex variable $z = x + \mathrm{i}\, y$. In general, the function $f\colon \Omega \to \mathbb{C}$ will be defined on an open subdomain, $z \in \Omega \subset \mathbb{C}$, of the complex plane.

Any complex function can be uniquely written as a complex combination

$$f(z) = f(x + \mathrm{i}\, y) = u(x, y) + \mathrm{i}\, v(x, y), \tag{7.1}$$

of two real functions, each depending on the two real variables x, y:

its *real part* $\quad u(x, y) = \operatorname{Re} f(z) \quad$ and its *imaginary part* $\quad v(x, y) = \operatorname{Im} f(z)$.

For example, the monomial function $f(z) = z^3$ can be expanded and written as

$$z^3 = (x + \mathrm{i}\, y)^3 = (x^3 - 3\, x\, y^2) + \mathrm{i}\, (3\, x^2 y - y^3),$$

and so

$$\operatorname{Re} z^3 = x^3 - 3\, x\, y^2, \qquad\qquad \operatorname{Im} z^3 = 3\, x^2 y - y^3.$$

Many of the well-known functions appearing in real-variable calculus — polynomials, rational functions, exponentials, trigonometric functions, logarithms, and many more — have natural complex extensions. For example, complex polynomials

$$p(z) = a_n\, z^n + a_{n-1}\, z^{n-1} + \cdots + a_1\, z + a_0 \tag{7.2}$$

are complex linear combinations (meaning that the coefficients a_k are allowed to be complex numbers) of the basic monomial functions $z^k = (x + \mathrm{i}\, y)^k$. Similarly, we have already made use of complex exponentials such as

$$e^z = e^{x + \mathrm{i}\, y} = e^x \cos y + \mathrm{i}\, e^x \sin y,$$

when solving differential equations and in Fourier analysis. Further examples will appear shortly.

There are several ways to motivate the link between harmonic functions $u(x, y)$, meaning solutions of the two-dimensional Laplace equation

$$\Delta u = \frac{\partial^2 u}{\partial x^2} + \frac{\partial^2 u}{\partial y^2} = 0, \tag{7.3}$$

and complex functions $f(z)$. One natural starting point is to return to the d'Alembert solution (2.82) of the one-dimensional wave equation, which was based on the factorization

$$\Box = \partial_t^2 - c^2\, \partial_x^2 = (\partial_t - c\, \partial_x)\, (\partial_t + c\, \partial_x)$$

of the linear wave operator (2.68). The two-dimensional Laplace operator $\Delta = \partial_x^2 + \partial_y^2$ has essentially the same form, except for an ostensibly unimportant change in sign[†]. The

[†] Although this "trivial" change in sign has significant ramifications for the analytical properties of (real) solutions. Section 4.3 discusses some of the profound differences between the elliptic Laplace equation and the hyperbolic wave equation.

Laplace operator admits a complex factorization,

$$\Delta = \partial_x^2 + \partial_y^2 = (\partial_x - \mathrm{i}\,\partial_y)\,(\partial_x + \mathrm{i}\,\partial_y),$$

into a product of first order differential operators, with complex "wave speeds" $c = \pm\,\mathrm{i}$. Mimicking our previous solution formula (2.75) for the wave equation, we anticipate that the solutions to the Laplace equation (7.3) should be expressed in the form

$$u(x,y) = f(x + \mathrm{i}\,y) + g(x - \mathrm{i}\,y), \tag{7.4}$$

i.e., a linear combination of functions of the complex variable $z = x + \mathrm{i}\,y$ and its complex conjugate $\overline{z} = x - \mathrm{i}\,y$. The functions $f(x + \mathrm{i}\,y)$ and $g(x - \mathrm{i}\,y)$ formally satisfy the first order complex partial differential equations

$$\frac{\partial f}{\partial x} = -\,\mathrm{i}\,\frac{\partial f}{\partial y}\,, \qquad\qquad \frac{\partial g}{\partial x} = \mathrm{i}\,\frac{\partial g}{\partial y}\,, \tag{7.5}$$

and hence (7.4) does indeed define a complex-valued solution to the Laplace equation.

In most applications, we are searching for real solutions, and so our complex d'Alembert-type formula (7.4) is not entirely satisfactory. As we know, a complex number $z = x + \mathrm{i}\,y$ is real if and only if it equals its own conjugate: $z = \overline{z}$. Thus, the solution (7.4) will be real if and only if

$$f(x + \mathrm{i}\,y) + g(x - \mathrm{i}\,y) = u(x,y) = \overline{u(x,y)} = \overline{f(x + \mathrm{i}\,y)} + \overline{g(x - \mathrm{i}\,y)}.$$

Now, the complex conjugation operation interchanges $x + \mathrm{i}\,y$ and $x - \mathrm{i}\,y$, and so we expect the first term $\overline{f(x + \mathrm{i}\,y)}$ to be a function of $x - \mathrm{i}\,y$, while the second term $\overline{g(x - \mathrm{i}\,y)}$ will be a function of $x + \mathrm{i}\,y$. Therefore†, to equate the two sides of this equation, we should require

$$g(x - \mathrm{i}\,y) = \overline{f(x + \mathrm{i}\,y)},$$

and so

$$u(x,y) = f(x + \mathrm{i}\,y) + \overline{f(x + \mathrm{i}\,y)} = 2\,\mathrm{Re}\,f(x + \mathrm{i}\,y).$$

Dropping the inessential factor of 2, we conclude that a real solution to the two-dimensional Laplace equation can be written as the *real part* of a complex function. A more direct proof of the following key result will appear below.

Proposition 7.1. *If $f(z)$ is a complex function, then its real part*

$$u(x,y) = \mathrm{Re}\,f(x + \mathrm{i}\,y) \tag{7.6}$$

is a harmonic function.

† We are ignoring the fact that f and g are not quite uniquely determined since one can add and subtract a common constant. This does not affect the argument in any significant way.

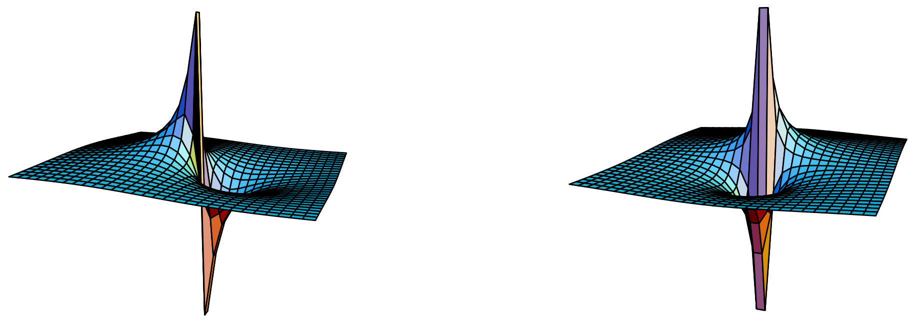

$\mathrm{Re}\,\frac{1}{z}$ $\qquad\qquad$ $\mathrm{Im}\,\frac{1}{z}$

Figure 7.1. Real and Imaginary Parts of $f(z) = \dfrac{1}{z}$.

The *imaginary part* of a complex function is also harmonic. This is because

$$\mathrm{Im}\, f(z) = \mathrm{Re}\left[\, -\,\mathrm{i}\, f(z)\,\right]$$

is the real part of the complex function

$$-\,\mathrm{i}\, f(z) = -\,\mathrm{i}\,[\,u(x,y) + \mathrm{i}\, v(x,y)\,] = v(x,y) - \mathrm{i}\, u(x,y).$$

Therefore, if $f(z)$ is any complex function, we can write it as a complex combination

$$f(z) = f(x + \mathrm{i}\, y) = u(x,y) + \mathrm{i}\, v(x,y),$$

of two inter-related real harmonic functions: $u(x,y) = \mathrm{Re}\, f(z)$ and $v(x,y) = \mathrm{Im}\, f(z)$.

Before delving into the many remarkable properties of complex functions, let us look at some of the most basic examples. In each case, the reader can directly check that the harmonic functions provided by the real and imaginary parts of the complex function are indeed solutions to the two-dimensional Laplace equation.

Examples of Complex Functions

(a) *Harmonic Polynomials*: As noted above, any complex polynomial is a linear combination, as in (7.2), of the basic complex monomials

$$z^n = (x + \mathrm{i}\, y)^n = u_n(x,y) + \mathrm{i}\, v_n(x,y). \tag{7.7}$$

Their real and imaginary parts, $u_n(x,y), v_n(x,y)$, are the *harmonic polynomials* that we previously constructed by applying separation of variables to the polar coordinate form of the Laplace equation (4.104). The general formula can be found in (4.120).

(b) *Rational Functions*: Ratios

$$f(z) = \frac{p(z)}{q(z)} \tag{7.8}$$

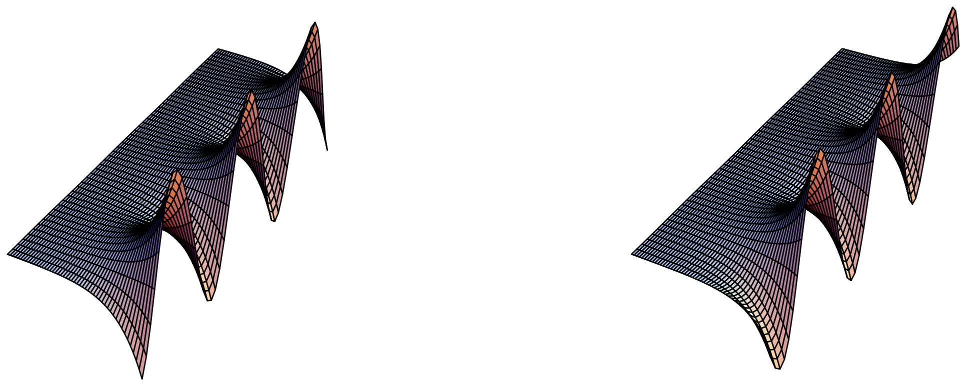

Figure 7.2. Real and Imaginary Parts of e^z.

of complex polynomials provide a large variety of harmonic functions. The simplest case is

$$\frac{1}{z} = \frac{x}{x^2+y^2} - \mathrm{i}\,\frac{y}{x^2+y^2}\,, \tag{7.9}$$

whose real and imaginary parts are graphed in Figure 7.1. Note that these functions have an interesting singularity at the origin $x = y = 0$, but are harmonic everywhere else.

A slightly more complicated example is the function

$$f(z) = \frac{z-1}{z+1}\,. \tag{7.10}$$

To write out (7.10) in standard form (7.1), we multiply and divide by the complex conjugate of the denominator, leading to

$$f(z) = \frac{z-1}{z+1} = \frac{(z-1)(\overline{z}+1)}{(z+1)(\overline{z}+1)} = \frac{|\,z\,|^2 + z - \overline{z} - 1}{|\,z+1\,|^2} = \frac{x^2+y^2-1}{(x+1)^2+y^2} \;+\; \mathrm{i}\,\frac{2\,y}{(x+1)^2+y^2}\,. \tag{7.11}$$

Again, the real and imaginary parts are both harmonic functions away from the singularity at $x=-1$, $y=0$. Incidentally, the preceding maneuver can always be used to find the real and imaginary parts of general rational functions.

(*c*) *Complex Exponentials*: *Euler's formula*

$$e^z = e^x \cos y + \mathrm{i}\, e^x \sin y \tag{7.12}$$

for the complex exponential yields two important harmonic functions: $e^x \cos y$ and $e^x \sin y$, which are graphed in Figure 7.2. More generally, writing out $e^{c\,z}$ for a complex constant $c = a + \mathrm{i}\, b$ produces the complex exponential function

$$e^{c\,z} = e^{a\,x-b\,y}\cos(b\,x+a\,y) + \mathrm{i}\, e^{a\,x-b\,y}\sin(b\,x+a\,y), \tag{7.13}$$

whose real and imaginary parts are harmonic functions for arbitrary $a, b \in \mathbb{R}$. Some of these were found by applying the separation of variables method to the planar Laplace equation in Cartesian coordinates.

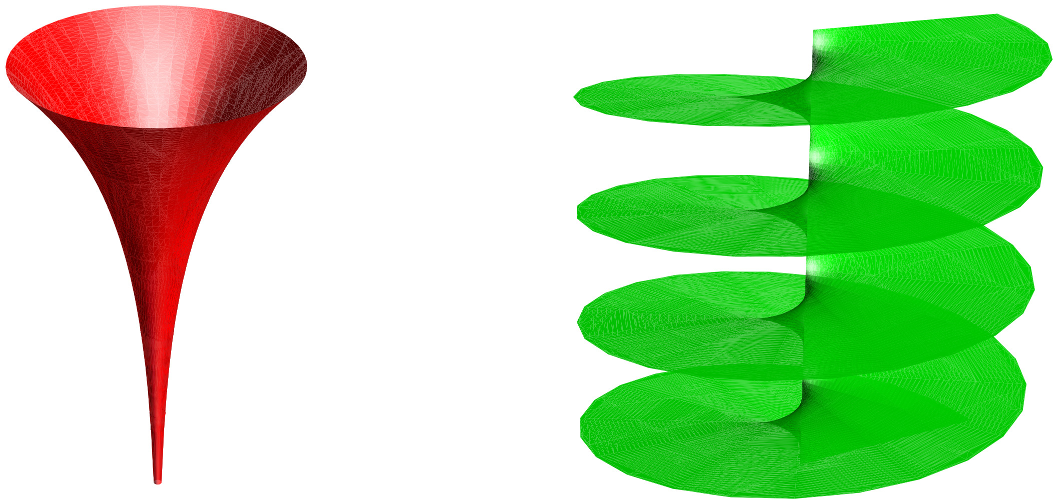

$\mathrm{Re}\,(\log z) = \log|\,z\,|$ $\qquad\qquad$ $\mathrm{Im}\,(\log z) = \mathrm{ph}\, z$

Figure 7.3. Real and Imaginary Parts of $\log z$.

(*d*) *Complex Trigonometric Functions*: These are defined in terms of the complex exponential by adapting our earlier formulae (3.60):

$$\begin{aligned} \cos z &= \frac{e^{\,\mathrm{i}\,z} + e^{-\,\mathrm{i}\,z}}{2} = \cos x \cosh y - \,\mathrm{i}\, \sin x \sinh y, \\ \sin z &= \frac{e^{\,\mathrm{i}\,z} - e^{-\,\mathrm{i}\,z}}{2\,\mathrm{i}} = \sin x \cosh y + \,\mathrm{i}\, \cos x \sinh y. \end{aligned} \tag{7.14}$$

The resulting harmonic functions are products of trigonometric and hyperbolic functions, and can all be written as linear combinations of the harmonic functions (7.13) derived from the complex exponential. Note that when $z = x$ is real, so $y = 0$, these functions reduce to the usual real trigonometric functions $\cos x$ and $\sin x$.

(*e*) *Complex Logarithm*: In a similar fashion, the complex logarithm is a complex extension of the usual real natural (i.e., base e) logarithm. In terms of polar coordinates $z = r\,e^{\,\mathrm{i}\,\theta}$, the complex logarithm has the form

$$\log z = \log(r\,e^{\,\mathrm{i}\,\theta}) = \log r + \log e^{\,\mathrm{i}\,\theta} = \log r + \,\mathrm{i}\,\theta. \tag{7.15}$$

Thus, the logarithm of a complex number has real part

$$\mathrm{Re}\,(\log z) = \log r = \log|\,z\,| = \tfrac{1}{2}\log(x^2 + y^2),$$

which is a well-defined harmonic function on all of $\mathbb{R}^2$ save for a logarithmic singularity at the origin $x = y = 0$. It is, up to multiple, the logarithmic potential (6.104) corresponding to a delta function forcing concentrated at the origin, that played a key role in our construction of the Green's function for the Poisson equation.

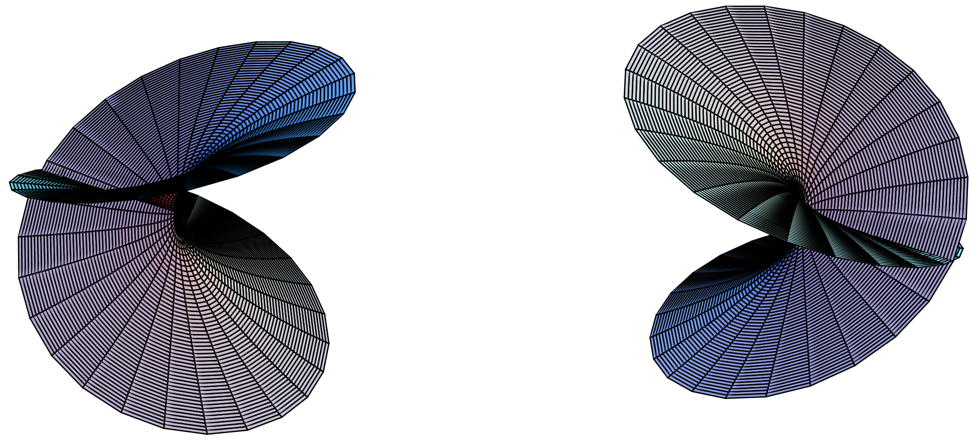

Figure 7.4. Real and Imaginary Parts of $\sqrt{z}$.

The imaginary part

$$\operatorname{Im}(\log z) = \theta = \operatorname{ph} z$$

of the complex logarithm is the polar angle, known in complex analysis as the *phase* or *argument* of z. (Although most texts use the latter name, we much prefer the former, for reasons outlined in the introduction.) It is also not defined at the origin $x = y = 0$. Moreover, the phase is a multiply-valued harmonic function elsewhere, since it is only specified up to integer multiples of 2π. Each nonzero complex number $z \neq 0$ has an infinite number of possible values for its phase, and hence an infinite number of possible complex logarithms $\log z$, differing from each other by an integer multiple of $2\pi\,\mathrm{i}$, which reflects the fact that $e^{2\pi\,\mathrm{i}} = 1$. In particular, if $z = x > 0$ is real and positive, then $\log z = \log x$ agrees with the real logarithm, *provided* we choose $\operatorname{ph} x = 0$. Alternative choices append some integer multiple of $2\pi\,\mathrm{i}$, and so ordinary real, positive numbers $x > 0$ also have complex logarithms! On the other hand, if $z = x < 0$ is real and negative, then $\log z = \log |\,x\,| + (2\,k+1)\,\pi\,\mathrm{i}$, for $k \in \mathbb{Z}$, is complex no matter which value of $\operatorname{ph} z$ is chosen. (This explains why one avoids defining the logarithm of a negative number in first year calculus!)

As the point z circles once around the origin in a counter-clockwise direction, $\operatorname{Im} \log z = \operatorname{ph} z = \theta$ increases by 2π. Thus, the graph of $\operatorname{ph} z$ can be likened to a parking ramp with infinitely many levels, spiraling ever upwards as one circumambulates the origin; Figure 7.3 attempts to illustrate it. At the origin, the complex logarithm exhibits a type of singularity known as a *logarithmic branch point*, the “branches” referring to the infinite number of possible values that can be assigned to $\log z$ at any nonzero point.

(*f*) *Roots and Fractional Powers*: A similar branching phenomenon occurs with the fractional powers and roots of complex numbers. The simplest case is the square root function $\sqrt{z}$. Every nonzero complex number $z \neq 0$ has two different possible square roots: $\sqrt{z}$ and $-\sqrt{z}$. Writing $z = r\,e^{\,\mathrm{i}\,\theta}$ in polar coordinates, we find that

$$\sqrt{z} = \sqrt{r\,e^{\,\mathrm{i}\,\theta}} = \sqrt{r}\,e^{\,\mathrm{i}\,\theta/2} = \sqrt{r}\,\left(\cos\frac{\theta}{2} + \mathrm{i}\,\sin\frac{\theta}{2}\right), \tag{7.16}$$

i.e., we take the square root of the modulus and halve the phase:

$$\left|\,\sqrt{z}\,\right| = \sqrt{|\,z\,|} = \sqrt{r}\,, \qquad\qquad \mathrm{ph}\,\sqrt{z} = \tfrac{1}{2}\,\mathrm{ph}\,z = \tfrac{1}{2}\,\theta.$$

Since $\theta = \mathrm{ph}\,z$ is only defined up to an integer multiple of 2π, the angle $\frac{1}{2}\theta$ is only defined up to an integer multiple of π. The even and odd multiples account for the two possible values of the square root.

In this case, if we start at some $z \neq 0$ and circle once around the origin, we increase $\mathrm{ph}\,z$ by 2π, but $\mathrm{ph}\,\sqrt{z}$ only increases by π. Thus, at the end of our circuit, we arrive at the other square root $-\sqrt{z}$. Circling the origin again increases $\mathrm{ph}\,z$ by a further 2π, and hence brings us back to the original square root $\sqrt{z}$. Therefore, the graph of the multiply-valued square root function will look like a parking ramp with only two interconnected levels, as sketched in Figure 7.4. The origin represents a *branch point* of *degree* 2 for the square root function.

The preceding list of elementary examples is far from exhaustive. Lack of space will preclude us from studying the remarkable properties of complex versions of the gamma function, Airy functions, Bessel functions, and Legendre functions that appear later in the text, as well as the Riemann zeta function (3.58), elliptic functions, modular functions, and many, many other important and fascinating functions arising in complex analysis and its manifold applications. The interested reader is referred to [**92**, **93**, **122**].

7.2. Complex Differentiation.

The bedrock of complex function theory is the notion of the complex derivative. Complex differentiation is defined in the same manner as the usual calculus limit definition of the derivative of a real function. Yet, despite a superficial similarity, complex differentiation is a profoundly different theory, displaying an elegance and depth not shared by its real progenitor.

Definition 7.2. A complex function $f(z)$ is *differentiable* at a point $z \in \mathbb{C}$ if and only if the following limiting difference quotient exists:

$$f'(z) = \lim_{w \to z} \frac{f(w) - f(z)}{w - z}\,. \tag{7.17}$$

The key feature of this definition is that the limiting value $f'(z)$ of the difference quotient must be *independent* of how w converges to z. On the real line, there are only two directions to approach a limiting point — either from the left or from the right. These lead to the concepts of left- and right-handed derivatives and their equality is required for the existence of the usual derivative of a real function. In the complex plane, there are an infinite variety of directions to approach the point z, and the definition requires that all

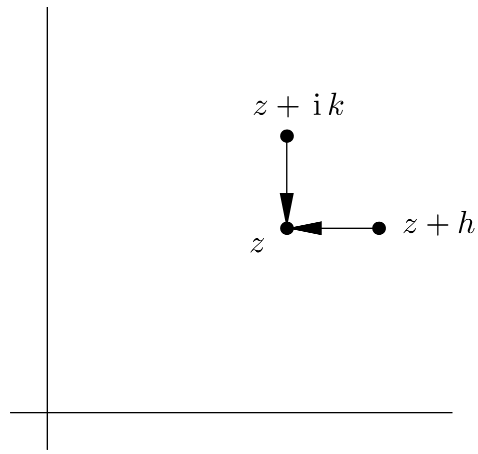

Figure 7.5. Complex Derivative Directions.

of these "directional derivatives" must agree. This requirement imposes severe restrictions on complex derivatives, and is the source of their remarkable properties.

To understand the consequences of this definition, let us first see what happens when we approach z along the two simplest directions — horizontal and vertical. If we set

$$w = z + h = (x + h) + \mathrm{i}\, y, \qquad \text{where } h \text{ is real,}$$

then $w \to z$ along a horizontal line as $h \to 0$, as sketched in Figure 7.5. If we write out

$$f(z) = u(x, y) + \mathrm{i}\, v(x, y)$$

in terms of its real and imaginary parts, then we must have

$$\begin{aligned} f'(z) &= \lim_{h \to 0} \frac{f(z+h) - f(z)}{h} = \lim_{h \to 0} \frac{f(x + h + \mathrm{i}\, y) - f(x + \mathrm{i}\, y)}{h} \\ &= \lim_{h \to 0} \left[\frac{u(x+h, y) - u(x, y)}{h} + \mathrm{i}\ \frac{v(x+h, y) - v(x, y)}{h} \right] = \frac{\partial u}{\partial x} + \mathrm{i}\ \frac{\partial v}{\partial x} = \frac{\partial f}{\partial x}\,, \end{aligned}$$

which follows from the usual definition of the (real) partial derivative. On the other hand, if we set

$$w = z + \mathrm{i}\, k = x + \mathrm{i}\,(y + k), \qquad \text{where } k \text{ is real,}$$

then $w \to z$ along a vertical line as $k \to 0$. Therefore, we must also have

$$\begin{aligned} f'(z) &= \lim_{k \to 0} \frac{f(z + \mathrm{i}\, k) - f(z)}{\mathrm{i}\, k} = \lim_{k \to 0} \left[-\mathrm{i}\ \frac{f(x + \mathrm{i}\,(y+k)) - f(x + \mathrm{i}\, y)}{k} \right] \\ &= \lim_{h \to 0} \left[\frac{v(x, y+k) - v(x, y)}{k} - \mathrm{i}\ \frac{u(x, y+k) - u(x, y)}{k} \right] = \frac{\partial v}{\partial y} - \mathrm{i}\ \frac{\partial u}{\partial y} = -\,\mathrm{i}\ \frac{\partial f}{\partial y}\,. \end{aligned}$$

When we equate the real and imaginary parts of these two distinct formulae for the complex derivative $f'(z)$, we discover that the real and imaginary components of $f(z)$ must satisfy a certain homogeneous linear system of partial differential equations, named after Augustin–Louis Cauchy and Bernhard Riemann, two of the founders of modern complex analysis.

Theorem 7.3. *A complex function $f(z) = u(x,y) + \mathrm{i}\, v(x,y)$ depending on $z = x + \mathrm{i}\, y$ has a complex derivative $f'(z)$ if and only if its real and imaginary parts are continuously differentiable and satisfy the* Cauchy–Riemann equations

$$\frac{\partial u}{\partial x} = \frac{\partial v}{\partial y}, \qquad \frac{\partial u}{\partial y} = -\,\frac{\partial v}{\partial x}. \tag{7.18}$$

In this case, the complex derivative of $f(z)$ is equal to any of the following expressions:

$$f'(z) = \frac{\partial f}{\partial x} = \frac{\partial u}{\partial x} + \mathrm{i}\,\frac{\partial v}{\partial x} = -\,\mathrm{i}\,\frac{\partial f}{\partial y} = \frac{\partial v}{\partial y} - \mathrm{i}\,\frac{\partial u}{\partial y}. \tag{7.19}$$

The proof of the converse — that any function whose real and imaginary components satisfy the Cauchy–Riemann equations is differentiable — will be omitted, but can be found in any basic text on complex analysis, e.g., [**4, 56, 104**].

Remark: It is worth pointing out that the Cauchy–Riemann equations (7.19) imply that f satisfies $\dfrac{\partial f}{\partial x} = -\,\mathrm{i}\,\dfrac{\partial f}{\partial y}$, which, reassuringly, agrees with the first equation in (7.5).

Example 7.4. Consider the elementary function

$$z^3 = (x^3 - 3\,x\,y^2) + \mathrm{i}\,(3\,x^2 y - y^3).$$

Its real part $u = x^3 - 3\,x\,y^2$ and imaginary part $v = 3\,x^2 y - y^3$ satisfy the Cauchy–Riemann equations (7.18), since

$$\frac{\partial u}{\partial x} = 3\,x^2 - 3\,y^2 = \frac{\partial v}{\partial y}, \qquad \frac{\partial u}{\partial y} = -\,6\,x\,y = -\,\frac{\partial v}{\partial x}.$$

Theorem 7.3 implies that $f(z) = z^3$ is complex differentiable. Not surprisingly, its derivative turns out to be

$$f'(z) = \frac{\partial u}{\partial x} + \mathrm{i}\,\frac{\partial v}{\partial x} = \frac{\partial v}{\partial y} - \mathrm{i}\,\frac{\partial u}{\partial y} = (3\,x^2 - 3\,y^2) + \mathrm{i}\,(6\,x\,y) = 3\,z^2.$$

Fortunately, the complex derivative obeys all of the usual rules that you learned in real-variable calculus. For example,

$$\frac{d}{dz}\,z^n = n\,z^{n-1}, \qquad \frac{d}{dz}\,e^{c\,z} = c\,e^{c\,z}, \qquad \frac{d}{dz}\log z = \frac{1}{z}, \tag{7.20}$$

and so on. Here, the power n can be non-integral — or even, in view of the identity $z^n = e^{n \log z}$, complex, while c is any complex constant. The exponential formulae (7.14) for the complex trigonometric functions implies that they also satisfy the standard rules

$$\frac{d}{dz}\cos z = -\sin z, \qquad \frac{d}{dz}\sin z = \cos z. \tag{7.21}$$

The formulae for differentiating sums, products, ratios, inverses, and compositions of complex functions are all identical to their real counterparts, with similar proofs. Thus, thankfully, you don't need to learn any new rules for performing complex differentiation!

Remark: There are many examples of seemingly reasonable functions which do *not* have a complex derivative. The simplest is the complex conjugate function

$$f(z) = \overline{z} = x - \mathrm{i}\, y.$$

Its real and imaginary parts do *not* satisfy the Cauchy–Riemann equations, and hence $\overline{z}$ does *not* have a complex derivative. More generally, any function $f(z, \overline{z})$ that explicitly depends on the complex conjugate variable $\overline{z}$ is *not* complex-differentiable.

Power Series and Analyticity

A remarkable feature of complex differentiation is that the existence of one complex derivative automatically implies the existence of infinitely many! All complex functions $f(z)$ are infinitely differentiable and, in fact, analytic where defined. The reason for this surprising and profound fact will, however, not become evident until we learn the basics of complex integration in Section 7.6. In this section, we shall take analyticity as a given, and investigate some of its principal consequences.

Definition 7.5. A complex function $f(z)$ is called *analytic* at a point $z_0 \in \mathbb{C}$ if it has a power series expansion

$$f(z) = a_0 + a_1 (z - z_0) + a_2 (z - z_0)^2 + a_3 (z - z_0)^3 + \cdots = \sum_{n=0}^{\infty} a_n \, (z - z_0)^n \,, \qquad (7.22)$$

that converges for all z sufficiently close to z_0.

In practice, the standard ratio or root tests for convergence of (real) series that you learned in ordinary calculus, [**4**, **8**, **114**], can be applied to determine where a given (complex) power series converges. We note that if $f(z)$ and $g(z)$ are analytic at a point z_0, so is their sum $f(z) + g(z)$, product $f(z)\, g(z)$ and, provided $g(z_0) \neq 0$, ratio $f(z)/g(z)$.

Example 7.6. All of the real power series found in elementary calculus carry over to the complex versions of the functions. For example,

$$e^z = 1 + z + \tfrac{1}{2} z^2 + \tfrac{1}{6} z^3 + \cdots = \sum_{n=0}^{\infty} \frac{z^n}{n!} \qquad (7.23)$$

is the power series for the exponential function based at $z_0 = 0$. A straightforward application of the ratio test proves that the series converges for all z. On the other hand, the power series

$$\frac{1}{z^2 + 1} = 1 - z^2 + z^4 - z^6 + \cdots = \sum_{k=0}^{\infty} (-1)^k \, z^{2k} \,, \qquad (7.24)$$

converges inside the unit disk, where $|\, z \,| < 1$, and diverges outside, where $|\, z \,| > 1$. Again, convergence is established through the ratio test. The ratio test is inconclusive when $|\, z \,| = 1$, and we shall leave the more delicate question of precisely where on the unit disk this complex series converges to a more advanced treatment, e.g., [**4**, **56**].

In general, there are three possible options for the domain of convergence of a complex power series (7.22):

(a) The series converges for all z.

(b) The series converges inside a disk $|\,z - z_0\,| < \rho$ of radius $\rho > 0$ centered at z_0 and diverges for all $|\,z - z_0\,| > \rho$ outside the disk. The series may converge at some (but not all) of the points on the boundary of the disk where $|\,z - z_0\,| = \rho$.

(c) The series only converges, trivially, at $z = z_0$.

The number ρ is known as the *radius of convergence* of the series. In case (a), we say $\rho = \infty$, while in case (c), $\rho = 0$, and the series does *not* represent an analytic function. An example that has $\rho = 0$ is the power series $\sum n!\, z^n$, as you are asked to show in Exercise ■. The proof of the general result is the subject of Exercise ■; see also [**4**, **56**, **104**] for further details.

Remarkably, the radius of convergence for the power series of a known analytic function $f(z)$ can be determined by inspection, without recourse to any fancy convergence tests! Namely, ρ is equal to the distance from z_0 to the nearest *singularity* of $f(z)$, meaning a point where the function fails to be analytic. In particular, the radius of convergence $\rho = \infty$ if and only if $f(z)$ is an *entire function*, meaning that it is analytic for all $z \in \mathbb{C}$ and has no singularities; examples include polynomials, e^z, $\cos z$, and $\sin z$. On the other hand, the rational function

$$f(z) = \frac{1}{z^2+1} = \frac{1}{(z+\mathrm{i}\,)(z-\mathrm{i}\,)}$$

has singularities at $z = \pm\,\mathrm{i}$, and so its power series (7.24) has radius of convergence $\rho = 1$, which is the distance from $z_0 = 0$ to the singularities. Thus, the extension of the theory of power series to the complex plane serves to explain the apparent mystery of why, as a real function, $(1+x^2)^{-1}$ is well-defined and analytic for all real x, but its power series only converges on the interval $(-1,1)$. It is the *complex* singularities that prevent its convergence when $|\,x\,| > 1$. If we expand $(z^2+1)^{-1}$ in a power series at some other point, say $z_0 = 1 + 2\,\mathrm{i}$, then we need to determine which singularity is closest. We compute $|\,\mathrm{i} - z_0\,| = |\,-1-\mathrm{i}\,| = \sqrt{2}$, while $|\,-\mathrm{i} - z_0\,| = |\,-1-3\,\mathrm{i}\,| = \sqrt{10}$, and so the radius of convergence $\rho = \sqrt{2}$ is the smaller. This allows us to determine the radius of convergence in the absence of any explicit formula for its (rather complicated) Taylor expansion at $z_0 = 1 + 2\,\mathrm{i}$.

There are, in fact, only three possible types of singularities of a complex function $f(z)$:

- *Pole*. A singular point $z = z_0$ is called a *pole* of *order* $0 < n \in \mathbb{Z}$ if and only if

$$f(z) = \frac{h(z)}{(z-z_0)^n}\,, \tag{7.25}$$

where $h(z)$ is analytic at $z = z_0$ and $h(z_0) \neq 0$. The simplest example of such a function is $f(z) = a\,(z-z_0)^{-n}$ for $a \neq 0$ a complex constant.

- *Branch point*. We have already encountered the two basic types: *algebraic branch points*, such as the function $\sqrt[n]{z}$ at $z_0 = 0$, and *logarithmic branch points* such as $\log z$ at $z_0 = 0$. The *degree* of the branch point is n in the first case and ∞ in the second. In general, the power function $z^a = e^{a \log z}$ is analytic at $z_0 = 0$ if $a \in \mathbb{Z}$ is an integer; has a algebraic branch point of degree q the origin if $a = p/q \in \mathbb{Q} \setminus \mathbb{Z}$ is rational, non-integral with $0 \neq p \in \mathbb{Z}$ and $2 \leq q \in \mathbb{Z}$ having no common factors, and a logarithmic branch point of infinite degree at $z = 0$ when $a \in \mathbb{C} \setminus \mathbb{Q}$ is not rational.

- *Essential singularity*. By definition, a singularity is *essential* if it is not a pole or a branch point. The quintessential example is the essential singularity of the function $e^{1/z}$ at $z_0 = 0$. The behavior of a complex function near an essential singularity is quite complicated, [**4**].

Example 7.7. The complex function

$$f(z) = \frac{e^z}{z^3 - z^2 - 5\,z - 3} = \frac{e^z}{(z-3)(z+1)^2}$$

is analytic everywhere except for singularities at the points $z = 3$ and $z = -1$, where its denominator vanishes. Since

$$f(z) = \frac{h_1(z)}{z-3}, \qquad \text{where} \qquad h_1(z) = \frac{e^z}{(z+1)^2}$$

is analytic at $z = 3$ and $h_1(3) = \frac{1}{16}\, e^3 \neq 0$, we conclude that $z = 3$ is a simple (order 1) pole. Similarly,

$$f(z) = \frac{h_2(z)}{(z+1)^2}, \qquad \text{where} \qquad h_2(z) = \frac{e^z}{z-3}$$

is analytic at $z = -1$ with $h_2(-1) = -\frac{1}{4}\, e^{-1} \neq 0$, we see that the point $z = -1$ is a double (order 2) pole.

A complicated complex function can have a variety of singularities. For example, the function

$$f(z) = \frac{e^{-1/(z-1)^2}}{(z^2+1)\,(z+2)^{2/3}} \tag{7.26}$$

has simple poles at $z = \pm\,\mathrm{i}$, a branch point of degree 3 at $z = -2$, and an essential singularity at $z = 1$.

As in the real case, and unlike Fourier series, convergent power series can always be repeatedly term-wise differentiated. Therefore, given the convergent series (7.22), we have the corresponding series

$$\begin{aligned} f'(z) &= a_1 + 2\,a_2(z - z_0) + 3\,a_3(z - z_0)^2 + 4\,a_4(z - z_0)^3 + \cdots \\ &= \sum_{n=0}^{\infty} (n+1)\,a_{n+1}(z - z_0)^n, \\ f''(z) &= 2\,a_2 + 6\,a_3(z - z_0) + 12\,a_4(z - z_0)^2 + 20\,a_5(z - z_0)^3 + \cdots \\ &= \sum_{n=0}^{\infty} (n+1)(n+2)\,a_{n+2}(z - z_0)^n, \end{aligned} \tag{7.27}$$

and so on, for its derivatives. In Exercise ■ you are asked to prove that the differentiated series all have the same radius of convergence as the original. As a consequence, we deduce the following important result.

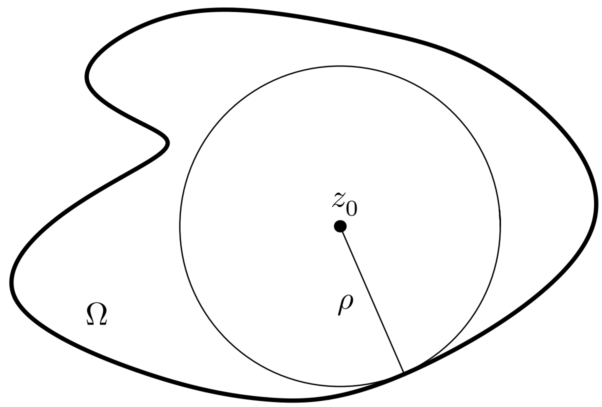

Figure 7.6. Radius of Convergence.

Theorem 7.8. *Any analytic function is infinitely differentiable.*

In particular, when we substitute $z = z_0$ into the successively differentiated series, we discover that $a_0 = f(z_0)$, $a_1 = f'(z_0)$, $a_2 = \frac{1}{2} f''(z_0)$, and, in general,

$$a_n = \frac{f^{(n)}(z)}{n!}\,. \tag{7.28}$$

Therefore, a convergent power series (7.22) is, inevitably, the usual *Taylor series*

$$f(z) = \sum_{n=0}^{\infty} \frac{f^{(n)}(z_0)}{n!}\,(z - z_0)^n\,, \tag{7.29}$$

for the function $f(z)$ at the point z_0.

Let us conclude this section by summarizing the fundamental theorem that characterizes complex functions. A complete, rigorous proof relies on complex integration theory, which is the topic of Section 7.6.

Theorem 7.9. *Let $\Omega \subset \mathbb{C}$ be an open set. The following properties are equivalent:*

(*a*) *The function $f(z)$ has a continuous complex derivative $f'(z)$ for all $z \in \Omega$.*

(*b*) *The real and imaginary parts of $f(z)$ have continuous partial derivatives and satisfy the Cauchy–Riemann equations* (7.18) *in Ω.*

(*c*) *The function $f(z)$ is analytic for all $z \in \Omega$, and so is infinitely differentiable and has a convergent power series expansion at each point $z_0 \in \Omega$. The radius of convergence ρ is at least as large as the distance from z_0 to the boundary $\partial\Omega$, as in Figure 7.6.*

From now on, we reserve the term *complex function* to signifiy one that satisfies the conditions of Theorem 7.9. Sometimes one of the equivalent adjectives "analytic" or "holomorphic" is added for emphasis. From now on, all complex functions are assumed to be analytic everywhere on their domain of definition, except, possibly, at certain singularities.

7.3. Harmonic Functions.

We began this chapter by motivating the analysis of complex functions through applications to the solution of the two-dimensional Laplace equation. Let us now formalize the precise relationship between the two subjects.

Theorem 7.10. *If $f(z) = u(x,y) + \mathrm{i}\,v(x,y)$ is any complex analytic function, then its real and imaginary parts, $u(x,y), v(x,y)$, are both harmonic functions.*

Proof: Differentiating[†] the Cauchy–Riemann equations (7.18), and invoking the equality of mixed partial derivatives, we find that

$$\frac{\partial^2 u}{\partial x^2} = \frac{\partial}{\partial x}\left(\frac{\partial u}{\partial x}\right) = \frac{\partial}{\partial x}\left(\frac{\partial v}{\partial y}\right) = \frac{\partial^2 v}{\partial x\,\partial y} = \frac{\partial}{\partial y}\left(\frac{\partial v}{\partial x}\right) = \frac{\partial}{\partial y}\left(-\,\frac{\partial u}{\partial y}\right) = -\,\frac{\partial^2 u}{\partial y^2}\,.$$

Therefore, u is a solution to the Laplace equation $u_{xx} + u_{yy} = 0$. The proof for v is similar. *Q.E.D.*

Thus, every complex function gives rise to two harmonic functions. It is, of course, of interest to know whether we can invert this procedure. Given a harmonic function $u(x,y)$, does there exist a harmonic function $v(x,y)$ such that $f = u + \mathrm{i}\,v$ is a complex analytic function? If so, the harmonic function $v(x,y)$ is known as a *harmonic conjugate* to u. The harmonic conjugate is found by solving the Cauchy–Riemann equations

$$\frac{\partial v}{\partial x} = -\,\frac{\partial u}{\partial y}\,, \qquad \frac{\partial v}{\partial y} = \frac{\partial u}{\partial x}\,, \tag{7.30}$$

which, for a prescribed function $u(x,y)$, constitutes an inhomogeneous linear system of partial differential equations for $v(x,y)$. As such, it is usually not hard to solve, as the following example illustrates.

Example 7.11. As the reader can verify, the harmonic polynomial

$$u(x,y) = x^3 - 3\,x^2 y - 3\,x\,y^2 + y^3$$

satisfies the Laplace equation everywhere. To find a harmonic conjugate, we solve the Cauchy–Riemann equations (7.30). First of all,

$$\frac{\partial v}{\partial x} = -\,\frac{\partial u}{\partial y} = 3\,x^2 + 6\,x\,y - 3\,y^2,$$

and hence, by direct integration with respect to x,

$$v(x,y) = x^3 + 3\,x^2 y - 3\,x\,y^2 + h(y),$$

where $h(y)$ — the "constant of integration" — is a function of y alone. To determine h we substitute our formula into the second Cauchy–Riemann equation:

$$3\,x^2 - 6\,x\,y + h'(y) = \frac{\partial v}{\partial y} = \frac{\partial u}{\partial x} = 3\,x^2 - 6\,x\,y - 3\,y^2.$$

[†] Theorem 7.9 allows us to differentiate u and v as often as desired.

Therefore, $h'(y) = -3y^2$, and so $h(y) = -y^3 + c$, where c is a real constant. We conclude that every harmonic conjugate to $u(x,y)$ has the form

$$v(x,y) = x^3 + 3x^2 y - 3x y^2 - y^3 + c.$$

Note that the corresponding complex function

$$\begin{aligned} u(x,y) + \mathrm{i}\, v(x,y) &= (x^3 - 3x^2 y - 3x y^2 + y^3) + \mathrm{i}\,(x^3 + 3x^2 y - 3x y^2 - y^3 + c) \\ &= (1 - \mathrm{i}\,) z^3 + c \end{aligned}$$

turns out to be a complex cubic polynomial.

Remark: On a connected domain $\Omega \subset \mathbb{R}^2$, the harmonic conjugates (if any) to a given function $u(x,y)$ differ from each other by a constant: $\widetilde{v}(x,y) = v(x,y) + c$; see Exercise ∎.

Although most harmonic functions have harmonic conjugates, unfortunately this is not always the case. Interestingly, the existence or non-existence of a harmonic conjugate can depend on the underlying topology of its domain of definition. If the domain is simply connected, and so contains no holes, then one can *always* find a harmonic conjugate. On non-simply connected domains, there may not exist a single-valued harmonic conjugate to serve as the imaginary part of a complex function $f(z)$.

Example 7.12. The simplest example where the latter possibility occurs is the logarithmic potential

$$u(x,y) = \log r = \tfrac{1}{2} \log(x^2 + y^2).$$

This function is harmonic on the non-simply connected domain $\Omega = \mathbb{C} \setminus \{0\}$, but is not the real part of any single-valued complex function. Indeed, according to (7.15), the logarithmic potential is the real part of the multiply-valued complex logarithm $\log z$, and so its harmonic conjugate[†] is $\operatorname{ph} z = \theta$, which cannot be consistently and continuously defined on all of Ω. On the other hand, on any simply connected subdomain $\widetilde{\Omega} \subset \Omega$, one can select a continuous, single-valued branch of the angle $\theta = \operatorname{ph} z$, which is then a bona fide harmonic conjugate to $\log r$ restricted to this subdomain.

The harmonic function

$$u(x,y) = \frac{x}{x^2 + y^2}$$

is also defined on the same non-simply connected domain $\Omega = \mathbb{C} \setminus \{0\}$ with a singularity at $x = y = 0$. In this case, there is a single-valued harmonic conjugate, namely

$$v(x,y) = -\,\frac{y}{x^2 + y^2}\,,$$

which is defined on all of Ω. Indeed, according to (7.9), these functions define the real and imaginary parts of the complex function $u + \mathrm{i}\, v = 1/z$. Alternatively, one can directly check that they satisfy the Cauchy–Riemann equations (7.18).

[†] We can, by the preceding remark, add in any constant to the harmonic conjugate, but this does not affect the subsequent argument.

Theorem 7.13. *Every harmonic function $u(x,y)$ defined on a simply connected domain Ω is the real part of a complex valued function $f(z) = u(x,y) + \mathrm{i}\, v(x,y)$ which is defined for all $z = x + \mathrm{i}\, y \in \Omega$.*

Proof: We first rewrite the Cauchy–Riemann equations (7.30) in vectorial form as an equation for the gradient of v:

$$\nabla v = \nabla^{\perp} u, \qquad \text{where} \qquad \nabla^{\perp} u = \begin{pmatrix} -u_y \\ u_x \end{pmatrix} \tag{7.31}$$

is known as the *skew gradient* of u. As in (6.78), it is everywhere orthogonal to the gradient of u and of the same length:

$$\nabla u \cdot \nabla^{\perp} u = 0, \qquad\qquad \| \nabla u \| = \| \nabla^{\perp} u \|.$$

Thus, we have established the important observation that the gradient of a harmonic function and that of its harmonic conjugate are mutually orthogonal vector fields having the same Euclidean lengths:

$$\nabla u \cdot \nabla v \equiv 0, \qquad\qquad \| \nabla u \| \equiv \| \nabla v \|. \tag{7.32}$$

Now, given the harmonic function u, our goal is to construct a solution v to the gradient equation (7.31). A well-known result from vector calculus states the vector field defined by $\nabla^{\perp} u$ has a potential function v if and only if the corresponding line integral is independent of path, which means that

$$0 = \oint_C \nabla v \cdot d\mathbf{x} = \oint_C \nabla^{\perp} u \cdot d\mathbf{x} = \oint_C \nabla u \cdot \mathbf{n}\; ds, \tag{7.33}$$

for every closed curve $C \subset \Omega$. Indeed, if this holds, then a potential function can be devised[†] by integrating the vector field:

$$v(x,y) = \int_{\mathbf{a}}^{\mathbf{x}} \nabla v \cdot d\mathbf{x} = \int_{\mathbf{a}}^{\mathbf{x}} \nabla u \cdot \mathbf{n}\; ds. \tag{7.34}$$

Here $\mathbf{a} \in \Omega$ is any fixed point, and, in view of path independence, the line integral can be taken over any curve that connects $\mathbf{a}$ to $\mathbf{x} = (x,y)^T$.

If the domain Ω is *simply connected* then every simple closed curve $C \subset \Omega$ bounds a sudomain $D \subset \Omega$ with $C = \partial D$. Applying the *divergence form* of Green's Theorem (6.80), we find

$$\oint_C \nabla u \cdot \mathbf{n}\; ds = \iint_D \nabla \cdot \nabla u \; dx\, dy = \iint_D \Delta u \; dx\, dy = 0,$$

because u is harmonic. Thus, in this situation, we have proved[‡] the existence of a harmonic conjugate function. *Q.E.D.*

[†] This assumes that the domain Ω is connected; if not, we apply our reasoning to each connected component.

[‡] Technically, we have only verified path-independence (7.33) when C is a simple closed curve, but this suffices to establish it for arbitrary closed curves; see the proof of Proposition 7.51 for details.

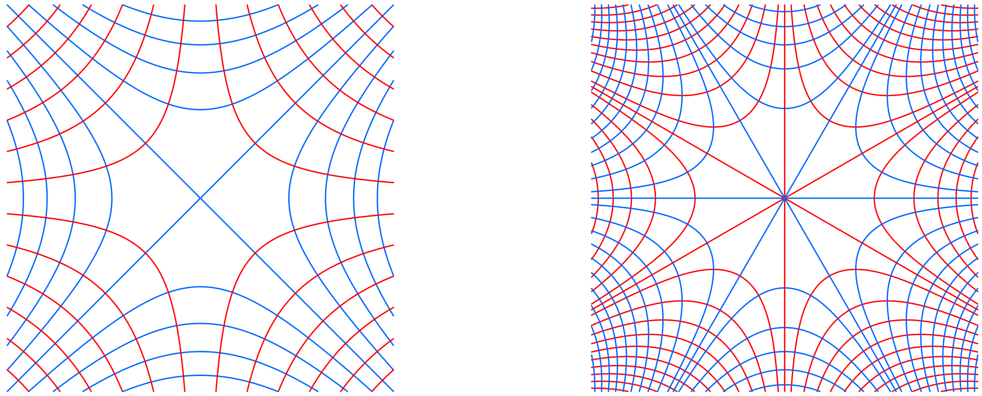

Figure 7.7. Level Curves of the Real and Imaginary Parts of z^2 and z^3.

Remark: As a consequence of (7.19) and the Cauchy–Riemann equations (7.30),

$$f'(z) = \frac{\partial u}{\partial x} - \mathrm{i}\,\frac{\partial u}{\partial y} = \frac{\partial v}{\partial y} + \mathrm{i}\,\frac{\partial v}{\partial x}\,. \tag{7.35}$$

Thus, the individual components of the gradients ∇u and ∇v appear as the real and imaginary parts of the complex derivative $f'(z)$.

The orthogonality (7.31) of the gradient of a function and of its harmonic conjugate has the following important geometric consequence. Recall, [**8**, **114**], that the gradient ∇u of a function $u(x,y)$ points in the normal direction to its *level curves*, that is, the sets $\{\, u(x,y) = c \,\}$ where it assumes a fixed constant value. Since ∇v is orthogonal to ∇u, this must mean that ∇v is *tangent* to the level curves of u. Vice versa, ∇v is normal to its level curves, and so ∇u is tangent to the level curves of its harmonic conjugate v. Since their tangent directions ∇u and ∇v are orthogonal, the level curves of the real and imaginary parts of a complex function form a mutually orthogonal system of plane curves — but with one key exception. If we are at a *critical point*, where $\nabla u = \mathbf{0}$, then $\nabla v = \nabla^{\perp} u = \mathbf{0}$, and the vectors do not define tangent directions. Therefore, the orthogonality of the level curves does not necessarily hold at critical points. It is worth pointing out that, in view of (7.35), the critical points of u are the same as those of v and also the same as the critical points of the corresponding complex function $f(z)$, i.e., those points where its complex derivative vanishes: $f'(z) = 0$.

In Figure 7.7, we illustrate the preceding paragraph by plotting the level curves of the real and imaginary parts of the functions $f(z) = z^2$ and z^3. Note that, except at the origin, where the derivative vanishes, the level curves intersect everywhere at right angles.

Remark: On the "punctured" plane $\Omega = \mathbb{C} \setminus \{0\}$, the logarithmic potential is, in a sense, the only obstruction to the existence of a harmonic conjugate. It can be shown, [**64**], that if $u(x,y)$ is a harmonic function defined on a punctured disk $\Omega_R = \{\, 0 < |\, z\,| < R \,\}$, for $0 < R \leq \infty$, then there exists a constant c such that $\widetilde{u}(x,y) = u(x,y) - c \log \sqrt{x^2 + y^2}$ is also harmonic and possess a single-valued harmonic conjugate $\widetilde{v}(x,y)$. As a result, the function $\widetilde{f} = \widetilde{u} + \mathrm{i}\,\widetilde{v}$ is analytic on all of Ω_R, and so our original function $u(x,y)$ is the real part of the multiply-valued analytic function $f(z) = \widetilde{f}(z) + c \log z$. This fact will be of importance in our subsequent analysis of airfoils.

Applications to Fluid Mechanics

Consider a planar steady state fluid flow, with velocity vector field

$$\mathbf{v}(\mathbf{x}) = \begin{pmatrix} u(x,y) \\ v(x,y) \end{pmatrix} \qquad \text{at the point} \quad \mathbf{x} = \begin{pmatrix} x \\ y \end{pmatrix} \in \Omega.$$

Here $\Omega \subset \mathbb{R}^2$ is the domain occupied by the fluid, while the vector $\mathbf{v}(\mathbf{x})$ represents the instantaneous velocity of the fluid at the point $\mathbf{x} \in \Omega$. Recall that the flow is *incompressible* if and only if it has vanishing divergence:

$$\nabla \cdot \mathbf{v} = \frac{\partial u}{\partial x} + \frac{\partial v}{\partial y} = 0. \tag{7.36}$$

Incompressibility means that the fluid volume does not change as it flows. Most liquids, including water, are, for all practical purposes, incompressible. On the other hand, the flow is *irrotational* if and only if it has vanishing curl:

$$\nabla \times \mathbf{v} = \frac{\partial v}{\partial x} - \frac{\partial u}{\partial y} = 0. \tag{7.37}$$

Irrotational flows have no vorticity, and hence no circulation. A flow that is both incompressible and irrotational is known as an *ideal fluid flow*. In many physical regimes, liquids (and, although less often, gases) behave as *ideal fluids*.

Observe that the two constraints (7.36–37) are almost identical to the Cauchy–Riemann equations (7.18); the only difference is the change in sign in front of the derivatives of v. But this can be easily remedied by replacing v by its negative $-v$. As a result, we establish a profound connection between ideal planar fluid flows and complex functions.

Theorem 7.14. *The velocity vector field* $\mathbf{v} = (\, u(x,y), v(x,y)\,)^T$ *induces an ideal fluid flow if and only if*

$$f(z) = u(x,y) - \mathrm{i}\, v(x,y) \tag{7.38}$$

is a complex analytic function of $z = x + \mathrm{i}\, y$.

Thus, the components $u(x,y)$ and $-v(x,y)$ of the velocity vector field for an ideal fluid flow are necessarily harmonic conjugates. The corresponding complex function (7.38) is, not surprisingly, known as the *complex velocity* of the fluid flow. When using this result, *do not forget* the minus sign that appears in front of the imaginary part of $f(z)$.

Under the flow induced by the velocity vector field $\mathbf{v} = (\, u(x,y), v(x,y)\,)^T$, the fluid particles follow the trajectories $z(t) = x(t) + \mathrm{i}\, y(t)$ obtained by integrating the system of ordinary differential equations

$$\frac{dx}{dt} = u(x,y), \qquad\qquad \frac{dy}{dt} = v(x,y). \tag{7.39}$$

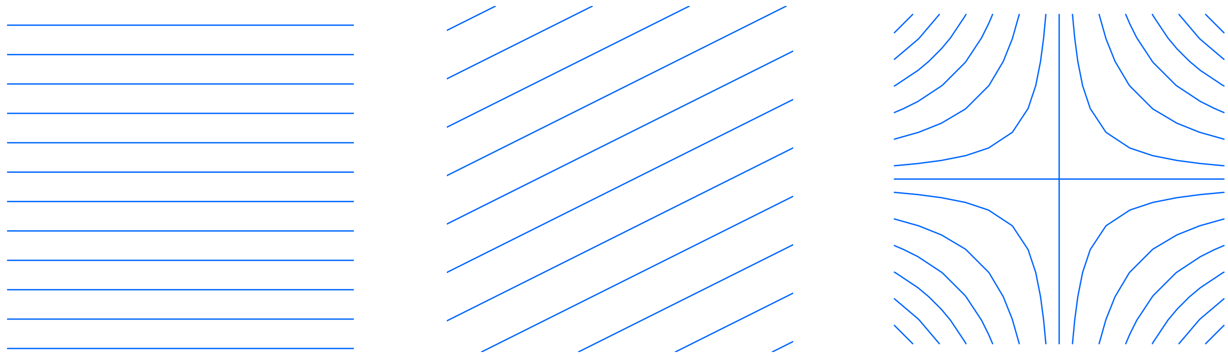

$f(z) = 1$ $\qquad$ $f(z) = 4 + 3\,\mathrm{i}$ $\qquad$ $f(z) = z$

Figure 7.8. Complex Fluid Flows.

In view of the representation (7.38), we can rewrite the preceding system in complex form:

$$\frac{dz}{dt} = \overline{f(z)}\,. \tag{7.40}$$

In fluid mechanics, the curves parametrized by the solutions $z(t)$ are known as the *streamlines* of the fluid flow. Each fluid particle's motion $z(t)$ is uniquely prescribed by its position $z(t_0) = z_0 = x_0 + \mathrm{i}\,y_0$ at an initial time t_0. In particular, if the complex velocity vanishes, $f(z_0) = 0$, then the solution $z(t) \equiv z_0$ to (7.40) is constant, and hence z_0 is a *stagnation point* of the flow. Our steady state assumption, which is reflected in the fact that the ordinary differential equations (7.39) are autonomous, i.e., there is no explicit t dependence, means that, although the fluid is in motion, the stream lines and stagnation points do not change over time. This is a consequence of the standard existence and uniqueness theorems for solutions to ordinary differential equations, [**18**, **24**, **53**].

Example 7.15. The simplest example is when the velocity is constant, corresponding to a uniform, steady flow. Consider first the case

$$f(z) = 1,$$

which corresponds to the horizontal velocity vector field $\mathbf{v} = (\,1, 0\,)^T$. The actual fluid flow is found by integrating the system

$$\dot{z} = 1, \qquad \text{or} \qquad \dot{x} = 1, \qquad \dot{y} = 0.$$

Thus, the solution $z(t) = t + z_0$ represents a uniform horizontal fluid motion whose streamlines are straight lines parallel to the real axis; see Figure 7.8.

Consider next a more general constant velocity

$$f(z) = c = a + \mathrm{i}\,b.$$

The fluid particles will solve the ordinary differential equation

$$\dot{z} = \overline{c} = a - \mathrm{i}\,b, \qquad \text{so that} \qquad z(t) = \overline{c}\,t + z_0.$$

The streamlines remain parallel straight lines, but now at an angle $\theta = \mathrm{ph}\,\overline{c} = -\,\mathrm{ph}\,c$ with the horizontal. The fluid particles move along the streamlines at constant speed $|\,\overline{c}\,| = |\,c\,|$.

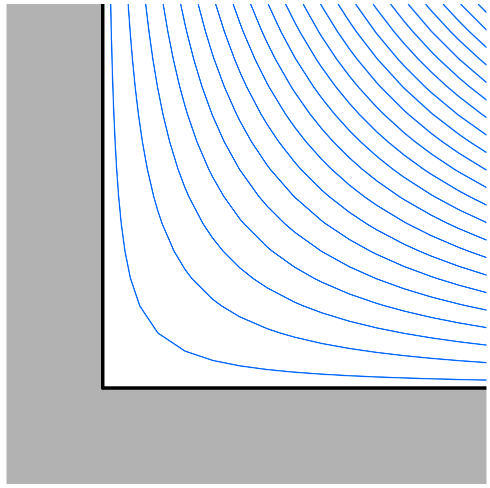

Figure 7.9. Flow Inside a Corner.

The next simplest complex velocity function is

$$f(z) = z = x + \mathrm{i}\, y. \tag{7.41}$$

The corresponding fluid flow is found by integrating the system

$$\dot{z} = \overline{z}, \qquad \text{or, in real form,} \qquad \dot{x} = x, \qquad \dot{y} = -\,y.$$

The origin $x = y = 0$ is a stagnation point. The trajectories of the nonstationary solutions

$$z(t) = x_0\, e^{t} + \mathrm{i}\, y_0\, e^{-t} \tag{7.42}$$

are the hyperbolas $x\,y = c$, along with the positive and negative coordinate semi-axes, as illustrated in Figure 7.8.

On the other hand, if we choose

$$f(z) = -\,\mathrm{i}\, z = y - \mathrm{i}\, x,$$

then the flow is the solution to

$$\dot{z} = \mathrm{i}\, \overline{z}, \qquad \text{or, in real form,} \qquad \dot{x} = y, \qquad \dot{y} = x.$$

The solutions

$$z(t) = (x_0 \cosh t + y_0 \sinh t) + \mathrm{i}\,(x_0 \sinh t + y_0 \cosh t),$$

move along the hyperbolas (and rays) $x^2 - y^2 = c^2$. Observe that this flow can be obtained by rotating the preceding example by 45°.

In general, a solid object in a fluid flow is characterized by the *no-flux condition* that the fluid velocity $\mathbf{v}$ is everywhere tangent to the boundary, and hence no fluid flows into or out of the object. As a result, the boundary will necessarily consist of streamlines and stagnation points of the idealized fluid flow. For example, the boundary of the upper right quadrant $Q = \{\, x > 0, y > 0 \,\} \subset \mathbb{C}$ consists of the positive x and y axes (along with the origin). Since these are streamlines of the flow with complex velocity (7.41), its restriction to Q represents an ideal flow past a 90° interior corner, which is illustrated in Figure 7.9. The individual fluid particles move along hyperbolas as they flow past the corner.

Remark: We could also restrict this flow to the domain $\Omega = \mathbb{C} \setminus \{ x < 0, y < 0 \}$ consisting of three quadrants, corresponding to a 90° exterior corner. However, this flow is not as physically relevant since it has an unphysical asymptotic behavior at large distances. See Exercise ■ for a more realistic flow around an exterior corner.

Now, suppose that the complex velocity $f(z)$ admits a complex anti-derivative, i.e., a complex analytic function

$$\chi(z) = \varphi(x,y) + \mathrm{i}\,\psi(x,y) \qquad \text{that satisfies} \qquad \frac{d\chi}{dz} = f(z). \tag{7.43}$$

Using formula (7.35) for the complex derivative,

$$\frac{d\chi}{dz} = \frac{\partial \varphi}{\partial x} - \mathrm{i}\,\frac{\partial \varphi}{\partial y} = u - \mathrm{i}\,v, \qquad \text{so} \qquad \frac{\partial \varphi}{\partial x} = u, \qquad \frac{\partial \varphi}{\partial y} = v.$$

Thus, $\nabla \varphi = \mathbf{v}$, and hence the real part $\varphi(x,y)$ of the complex function $\chi(z)$ defines a *velocity potential* for the fluid flow. For this reason, the anti-derivative $\chi(z)$ is known as a *complex potential function* for the given fluid velocity field.

Since the complex potential is analytic, its real part — the potential function — is harmonic, and therefore satisfies the Laplace equation $\Delta \varphi = 0$. Conversely, any harmonic function can be viewed as the potential function for some fluid flow. The real fluid velocity is its gradient $\mathbf{v} = \nabla \varphi$, and is automatically incompressible and irrotational. (Why?)

The harmonic conjugate $\psi(x,y)$ to the velocity potential also plays an important role, and, in fluid mechanics, is known as the *stream function*. It also satisfies the Laplace equation $\Delta \psi = 0$, and the potential and stream function are related by the Cauchy–Riemann equations (7.18):

$$\frac{\partial \varphi}{\partial x} = u = \frac{\partial \psi}{\partial y}\,, \qquad \frac{\partial \varphi}{\partial y} = v = -\,\frac{\partial \psi}{\partial x}\,. \tag{7.44}$$

The *level sets* of the velocity potential, $\{ \varphi(x,y) = c \}$, where $c \in \mathbb{R}$ is fixed, are known as *equipotential curves*. The velocity vector $\mathbf{v} = \nabla \varphi$ points in the normal direction to the equipotentials. On the other hand, as we noted above, $\mathbf{v} = \nabla \varphi$ is tangent to the level curves $\{ \psi(x,y) = d \}$ of its harmonic conjugate stream function. But $\mathbf{v}$ is the velocity field, and so tangent to the streamlines followed by the fluid particles. Thus, these two systems of curves must coincide, and we infer that *the level curves of the stream function are the streamlines of the flow*, whence its name! Summarizing, for an ideal fluid flow, the equipotentials $\{ \varphi = c \}$ and streamlines $\{ \psi = d \}$ form two mutually orthogonal families of plane curves. The fluid velocity $\mathbf{v} = \nabla \varphi$ is tangent to the stream lines and normal to the equipotentials, whereas the gradient of the stream function $\nabla \psi = \nabla^{\perp} \varphi$ is tangent to the equipotentials and normal to the streamlines.

The discussion in the preceding paragraph implicitly relied on the fact that the velocity is nonzero, $\mathbf{v} = \nabla \varphi \neq 0$, which means we are not at a stagnation point, where the fluid is not moving. While streamlines and equipotentials might begin or end at a stagnation point, there is no guarantee, and, indeed, it is not generally the case that they meet at mutually orthogonal directions there.

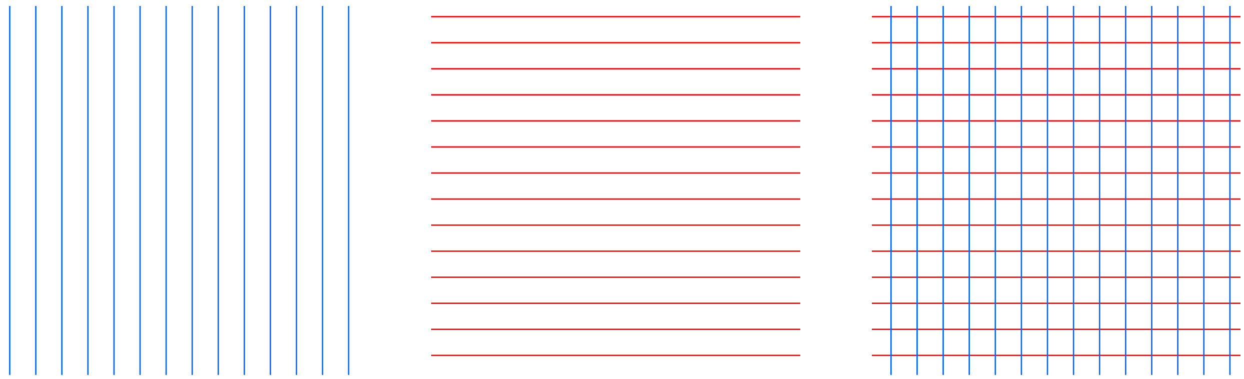

Figure 7.10. Equipotentials and Streamlines for $\chi(z) = z$.

Example 7.16. The simplest example of a complex potential function is

$$\chi(z) = z = x + \mathrm{i}\, y.$$

Thus, the velocity potential is $\varphi(x,y) = x$, while its harmonic conjugate stream function is $\psi(x,y) = y$. The complex derivative of the potential is the complex velocity,

$$f(z) = \frac{d\chi}{dz} = 1,$$

which corresponds to the uniform horizontal fluid motion considered first in Example 7.15. Note that the horizontal stream lines coincide with the level sets $\{y = d\}$ of the stream function, whereas the equipotentials $\{x = c\}$ are the orthogonal system of vertical lines; see Figure 7.10.

Next, consider the complex potential function

$$\chi(z) = \tfrac{1}{2}\, z^2 = \tfrac{1}{2}\,(x^2 - y^2) + \mathrm{i}\, x\, y.$$

The associated complex velocity

$$f(z) = \chi'(z) = z = x + \mathrm{i}\, y$$

leads to the hyperbolic flow (7.42). The hyperbolic streamlines $x\,y = d$ are the level curves of the stream function $\psi(x,y) = x\,y$. The equipotential lines $\frac{1}{2}\,(x^2 - y^2) = c$ form a system of orthogonal hyperbolas. Figure 7.11 shows (some of) the equipotentials in the first plot, the stream lines in the second, and combines them together in the third picture.

Example 7.17. *Flow Around a Disk.* Consider the complex potential function

$$\chi(z) = z + \frac{1}{z} = \left(x + \frac{x}{x^2 + y^2} \right) + \mathrm{i} \left(y - \frac{y}{x^2 + y^2} \right), \tag{7.45}$$

whose real and imaginary parts are individually solutions to the two-dimensional Laplace equation. The corresponding complex fluid velocity is

$$f(z) = \frac{d\chi}{dz} = 1 - \frac{1}{z^2} = 1 - \frac{x^2 - y^2}{(x^2 + y^2)^2} \;+\; \mathrm{i}\, \frac{2\,x\,y}{(x^2 + y^2)^2}\,. \tag{7.46}$$

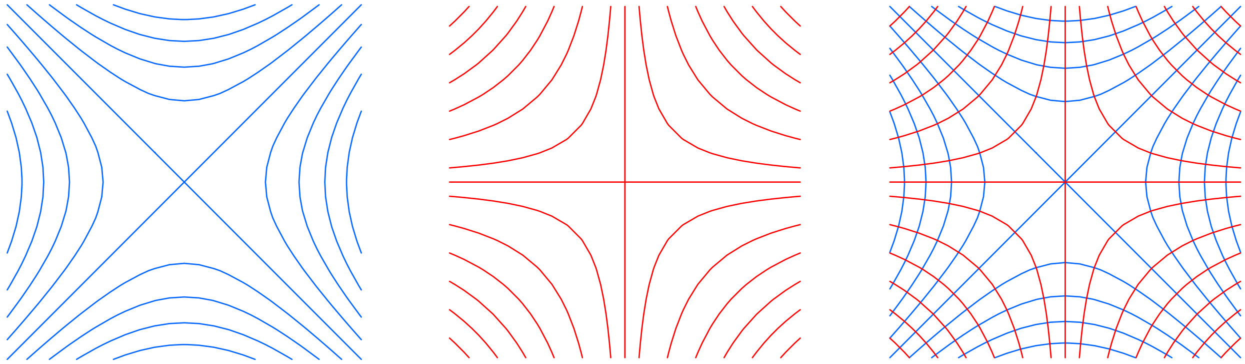

Figure 7.11. Equipotentials and Streamlines for $\chi(z) = \frac{1}{2}\, z^2$.

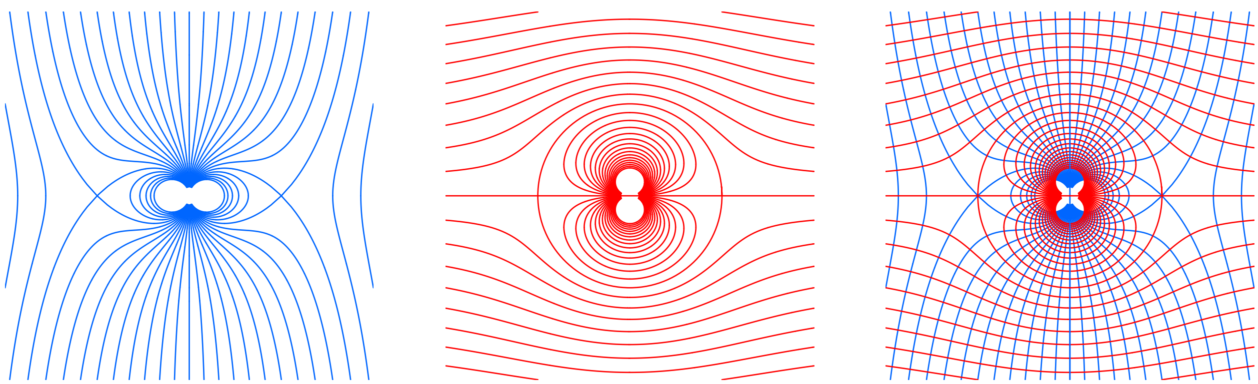

Figure 7.12. Equipotentials and Streamlines for $z + \dfrac{1}{z}$.

The equipotential curves and streamlines are plotted in Figure 7.12. The points $z = \pm 1$ are stagnation points of the flow, while $z = 0$ is a singularity. In particular, fluid particles that move along the positive x axis approach the leading stagnation point $z = 1$ as $t \to \infty$. Note that the streamlines

$$\psi(x, y) = y - \frac{y}{x^2 + y^2} = d$$

are asymptotically horizontal at large distances, and hence, far away from the origin, the flow is indistinguishable from a uniform horizontal motion, from left to right, with unit complex velocity $f(z) \equiv 1$.

The level curve for the particular value $d = 0$ consists of the unit circle $|\, z\,| = 1$ and the real axis $y = 0$. In particular, the unit circle consists of two semicircular stream lines combined with the two stagnation points. The flow velocity vector field $\mathbf{v} = \nabla\varphi$ is everywhere tangent to the unit circle, and hence satisfies the no flux condition $\mathbf{v} \cdot \mathbf{n} = 0$ along the boundary of the unit disk. Thus, we can interpret (7.46), when restricted to the domain $\Omega = \left\{\, |\, z\,| > 1 \,\right\}$, as the complex velocity of a uniformly moving fluid around the outside of a solid circular disk of radius 1, as illustrated in Figure 7.13. In three dimensions, this would correspond to the steady flow of a fluid around a solid cylinder.

Remark: In this section, we have focused on the fluid mechanical roles of a harmonic function and its conjugate. An analogous interpretation applies when $\varphi(x, y)$ represents

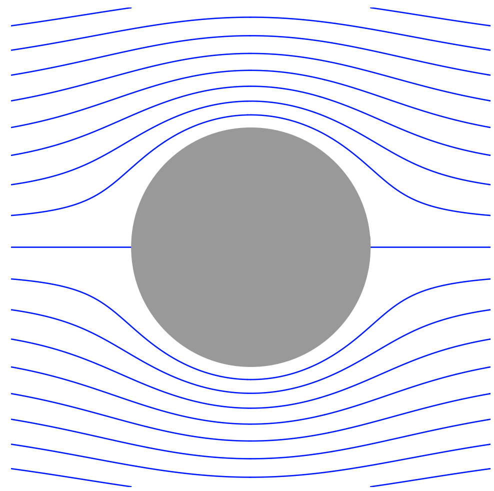

Figure 7.13. Flow Past a Solid Disk.

an electromagnetic potential function; the level curves of its harmonic conjugate $\psi(x,y)$ are the paths followed by charged particles under the electromotive force field $\mathbf{v} = \nabla\varphi$. Similarly, if $\varphi(x,y)$ represents the equilibrium temperature distribution in a planar domain, its level lines represent the *isotherms* — curves of constant temperature, while the level lines of its harmonic conjugate are the curves along which heat energy flows. Finally, if $\varphi(x,y)$ represents the height of a deformed membrane, then its level curves are the contour lines of elevation. The level curves of its harmonic conjugate are the curves of *steepest descent*, that is, the paths followed by, say, a stream of water flowing down the membrane[†].

7.4. Conformal Mapping.

As we now know, complex functions provide an almost inexhaustible supply of harmonic functions, that is, solutions to the the two-dimensional Laplace equation. Thus, to solve an associated boundary value problem, we "merely" find the complex function whose real part matches the prescribed boundary conditions. Unfortunately, even for relatively simple domains, this remains a daunting task.

The one case where we do have an explicit solution is that of a circular disk, where the Poisson integral formula (4.126) provides a complete solution to the Dirichlet boundary value problem. (See also Exercise ■ for the Neumann problem.) Thus, an evident solution strategy for the corresponding boundary value problem on a more complicated domain would be to transform it into a solved case by an inspired change of variables.

Analytic Maps

The intimate connections between complex analysis and solutions to the Laplace equation inspires us to look at changes of variables defined by complex functions. To this end,

[†] This interpretation ignores any inertial effects in the fluid flow.

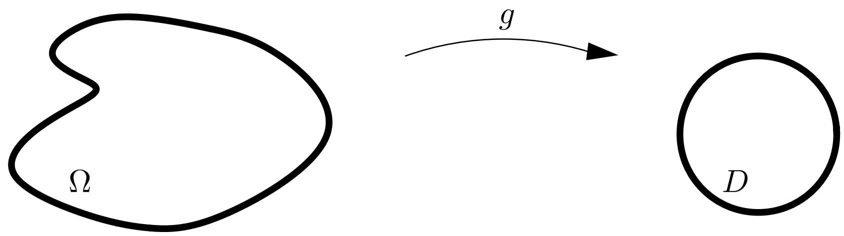

Figure 7.14. Mapping to the Unit Disk.

we will re-interpret a complex analytic function

$$\zeta = g(z) \qquad \text{or} \qquad \xi + \mathrm{i}\,\eta = p(x,y) + \mathrm{i}\,q(x,y) \tag{7.47}$$

as a *mapping* that takes a point $z = x + \mathrm{i}\,y$ belonging to a prescribed domain $\Omega \subset \mathbb{C}$ to a point $\zeta = \xi + \mathrm{i}\,\eta$ belonging to the image domain $D = g(\Omega) \subset \mathbb{C}$. In many cases, the image domain D is the unit disk, as in Figure 7.14, but the method can also be applied to more general domains. In order to unambigouously relate functions on Ω to functions on D, we require that the analytic mapping (7.47) be one-to-one, so that each point $\zeta \in D$ comes from a unique point $z \in \Omega$. As a result, the inverse function $z = g^{-1}(\zeta)$ is a well-defined map from D back to Ω, which we assume is also analytic on all of D. The calculus formula for the derivative of the inverse function

$$\frac{d}{d\zeta}\, g^{-1}(\zeta) = \frac{1}{g'(z)} \qquad \text{at} \qquad \zeta = g(z), \tag{7.48}$$

remains valid for complex functions. It implies that the derivative of $g(z)$ must be nonzero everywhere in order that $g^{-1}(\zeta)$ be differentiable. This condition,

$$g'(z) \neq 0 \qquad \text{at every point} \qquad z \in \Omega, \tag{7.49}$$

will play a crucial role in the development of the method. Finally, in order to match the boundary conditions, we will assume that the mapping extends continuously to the boundary $\partial\Omega$ and maps it, one-to-one, to the boundary ∂D of the image domain.

Before trying to apply this idea to solve boundary value problems for the Laplace equation, let us look at some of the most basic examples of analytic mappings.

Example 7.18. The simplest nontrivial analytic maps are the *translations*

$$\zeta = z + \beta = (x + a) + \mathrm{i}\,(y + b), \tag{7.50}$$

where $\beta = a + \mathrm{i}\,b$ is a fixed complex number. The effect of (7.50) is to translate the entire complex plane in the direction and distance prescribed by the vector $(a,b)^T$. In particular, (7.50) maps the disk $\Omega = \{\, |\, z + \beta\,| < 1 \,\}$ of radius 1 and center at the point $-\beta$ to the unit disk $D = \{\, |\, \zeta\,| < 1\,\}$.

Example 7.19. There are two types of linear analytic maps. First are the *scalings*

$$\zeta = \rho\, z = \rho\, x + \mathrm{i}\,\rho\, y, \tag{7.51}$$

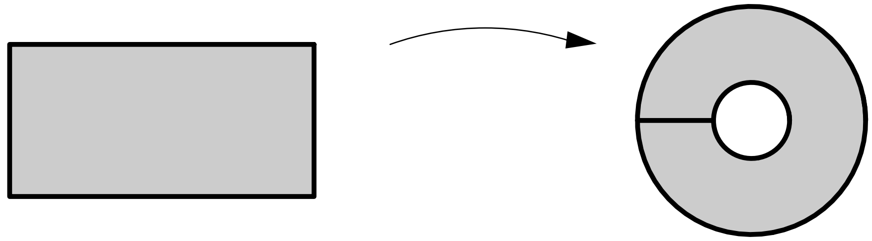

Figure 7.15. The mapping $\zeta = e^z$.

where $\rho \neq 0$ is a fixed nonzero real number. This maps the disk $|\,z\,| < 1/|\,\rho\,|$ to the unit disk $|\,\zeta\,| < 1$. Second are the *rotations*

$$\zeta = e^{\,\mathrm{i}\,\phi}\, z = (x\cos\phi - y\sin\phi) + \,\mathrm{i}\,(x\sin\phi + y\cos\phi), \tag{7.52}$$

which rotates the complex plane around the origin by a fixed (real) angle ϕ. These all map the unit disk to itself.

Example 7.20. Any non-constant *affine transformation*

$$\zeta = \alpha\, z + \beta, \qquad\qquad \alpha \neq 0, \tag{7.53}$$

defines an invertible analytic map on all of $\mathbb{C}$, whose inverse $z = \alpha^{-1}(\zeta - \beta)$ is also affine. Writing $\alpha = \rho\, e^{\,\mathrm{i}\,\phi}$ in polar coordinates, we see that the affine map (7.53) can be viewed as the composition of a rotation (7.52), followed by a scaling (7.51), followed by a translation (7.50). As such, it takes the disk $|\,\alpha\, z + \beta\,| < 1$ of radius $1/|\,\alpha\,| = 1/|\,\rho\,|$ and center $-\beta/\alpha$ to the unit disk $|\,\zeta\,| < 1$.

Example 7.21. A more interesting example is the complex function

$$\zeta = g(z) = \frac{1}{z}\,, \qquad \text{or} \qquad \xi = \frac{x}{x^2+y^2}\,, \qquad \eta = -\,\frac{y}{x^2+y^2}\,, \tag{7.54}$$

which defines an *inversion*† of the complex plane. The inversion is a one-to-one analytic map everywhere except at the origin $z = 0$; indeed $g(z)$ is its own inverse: $g^{-1}(\zeta) = 1/\zeta$. Since $g'(z) = -1/z^2$ is never zero, the derivative condition (7.49) is satisfied everywhere. Note that $|\,\zeta\,| = 1/|\,z\,|$, while $\operatorname{ph}\zeta = -\operatorname{ph} z$. Thus, if $\Omega = \{\, |\,z\,| > \rho\,\}$ denotes the exterior of the circle of radius ρ, then the image points $\zeta = 1/z$ satisfy $|\,\zeta\,| = 1/|\,z\,|$, and hence the image domain is the *punctured disk* $D = \{\, 0 < |\,\zeta\,| < 1/\rho\,\}$. In particular, the inversion maps the outside of the unit disk to its inside, but with the origin removed, and vice versa. The reader may enjoy seeing what the inversion does to other domains, e.g., the unit square $S = \{\, z = x + \mathrm{i}\, y \mid 0 < x, y < 1\,\}$.

† This is slightly different than the real inversion (6.128); see Exercise ■.

Example 7.22. The complex exponential

$$\zeta = g(z) = e^z\,, \qquad \text{or} \qquad \xi = e^x \cos y, \quad \eta = e^x \sin y, \tag{7.55}$$

satisfies the condition $g'(z) = e^z \neq 0$ everywhere. Nevertheless, it is *not* one-to-one because $e^{z+2\pi\,\mathrm{i}} = e^z$, and so points that differ by an integer multiple of $2\pi\,\mathrm{i}$ are all mapped to the same point. We deduce that condition (7.49) is necessary, but not sufficient for invertibility.

Under the exponential map, the horizontal line $\operatorname{Im} z = b$ is mapped to the curve $\zeta = e^{x+\mathrm{i}\,b} = e^x(\cos b + \mathrm{i}\,\sin b)$, which, as x varies from $-\infty$ to ∞, traces out the ray emanating from the origin that makes an angle $\operatorname{ph}\zeta = b$ with the real axis. Therefore, the exponential map will map a horizontal strip

$$S_{a,b} = \{\, a < \operatorname{Im} z < b \,\} \quad \text{to a wedge-shaped domain} \quad \Omega_{a,b} = \{\, a < \operatorname{ph}\zeta < b \,\},$$

and is one-to-one provided $|\, b - a \,| < 2\pi$. In particular, the horizontal strip

$$S_{-\pi/2,\pi/2} = \left\{\, -\tfrac{1}{2}\pi < \operatorname{Im} z < \tfrac{1}{2}\pi \,\right\}$$

of width π centered around the real axis is mapped, in a one-to-one manner, to the right half plane

$$R = \Omega_{-\pi/2,\pi/2} = \left\{\, -\tfrac{1}{2}\pi < \operatorname{ph}\zeta < \tfrac{1}{2}\pi \,\right\} = \{\, \operatorname{Im}\zeta > 0 \,\},$$

while the horizontal strip $S_{-\pi,\pi} = \left\{\, -\pi < \operatorname{Im} z < \pi \,\right\}$ of width 2π is mapped onto the domain

$$\Omega_* = \Omega_{-\pi,\pi} = \{\, -\pi < \operatorname{ph}\zeta < \pi \,\} = \mathbb{C} \setminus \{\, \operatorname{Im} z = 0,\ \operatorname{Re} z \leq 0 \,\}$$

obtained by slitting the complex plane along the negative real axis.

On the other hand, vertical lines $\operatorname{Re} z = a$ are mapped to circles $|\,\zeta\,| = e^a$. Thus, a vertical strip $a < \operatorname{Re} z < b$ is mapped to an annulus $e^a < |\,\zeta\,| < e^b$, albeit many-to-one, since the strip is effectively wrapped around and around the annulus. The rectangle $R = \{\, a < x < b,\ -\pi < y < \pi \,\}$ of height 2π is mapped in a one-to-one fashion on an annulus that has been cut along the negative real axis, as illustrated in Figure 7.15. Finally, we note that no domain is mapped to the unit disk $D = \{\, |\,\zeta\,| < 1 \,\}$ (or, indeed, any other domain that contains 0) because the exponential function is never zero: $\zeta = e^z \neq 0$.

Example 7.23. The squaring map

$$\zeta = g(z) = z^2, \qquad \text{or} \qquad \xi = x^2 - y^2, \quad \eta = 2\,x\,y, \tag{7.56}$$

is analytic on all of $\mathbb{C}$, but is not one-to-one. Its inverse is the square root function $z = \sqrt{\zeta}$, which, as we noted in Section 7.1, is doubly-valued, except at the origin $z = 0$. Furthermore, its derivative $g'(z) = 2\,z$ vanishes at $z = 0$, violating the invertibility condition (7.49). However, once we restrict $g(z)$ to a simply connected subdomain Ω that does not contain 0, the function $g(z) = z^2$ does define a one-to-one mapping, whose inverse $z = g^{-1}(\zeta) = \sqrt{\zeta}$ is a well-defined, analytic and single-valued branch of the square root function.

The effect of the squaring map on a point z is to square its modulus, $|\,\zeta\,| = |\,z\,|^2$, while doubling its phase, $\operatorname{ph}\zeta = \operatorname{ph} z^2 = 2\ \operatorname{ph} z$. Thus, for example, the upper right quadrant

$$Q = \{\, x > 0,\ y > 0 \,\} = \left\{\, 0 < \operatorname{ph} z < \tfrac{1}{2}\pi \,\right\}$$

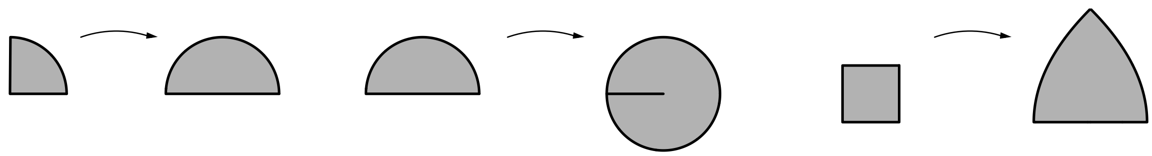

Figure 7.16. The Effect of $\zeta = z^2$ on Various Domains.

is mapped onto the upper half plane

$$U = g(Q) = \{\, \eta = \operatorname{Im} \zeta > 0 \,\} = \{\, 0 < \operatorname{ph} \zeta < \pi \,\}.$$

The inverse function maps a point $\zeta \in U$ back to its unique square root $z = \sqrt{\zeta}$ that lies in the quadrant Q. Similarly, a quarter disk

$$Q_\rho = \left\{\, 0 < |\, z \,| < \rho,\ 0 < \operatorname{ph} z < \tfrac{1}{2}\pi \,\right\}$$

of radius ρ is mapped to a half disk

$$U_{\rho^2} = g(\Omega) = \{\, 0 < |\, \zeta \,| < \rho^2,\ \operatorname{Im} \zeta > 0 \,\}$$

of radius ρ^2. On the other hand, the unit square $S = \{\, 0 < x < 1,\ 0 < y < 1 \,\}$ is mapped to a curvilinear triangular domain, as indicated in Figure 7.16; the edges of the square on the real and imaginary axes map to the two halves of the straight base of the triangle, while the other two edges become its curved sides.

Example 7.24. A particularly important example is the analytic map

$$\zeta = \frac{z-1}{z+1} = \frac{x^2+y^2-1}{(x+1)^2+y^2} \ + \ \mathrm{i}\ \frac{2\,y}{(x+1)^2+y^2}\,, \tag{7.57}$$

where we established the formulae for its real and imaginary parts in (7.11). The map is one-to-one with analytic inverse

$$z = \frac{1+\zeta}{1-\zeta} = \frac{1-\xi^2-\eta^2}{(1-\xi)^2+\eta^2} \ + \ \mathrm{i}\ \frac{2\,\eta}{(1-\xi)^2+\eta^2}\,, \tag{7.58}$$

provided $z \neq -1$ and $\zeta \neq 1$. This particular analytic map has the important property of mapping the right half plane $R = \{\, x = \operatorname{Re} z > 0 \,\}$ to the unit disk $D = \{\, |\,\zeta\,|^2 < 1 \,\}$. Indeed, by (7.58)

$$|\,\zeta\,|^2 = \xi^2 + \eta^2 < 1 \qquad \text{if and only if} \qquad x = \frac{1-\xi^2-\eta^2}{(1-\xi)^2+\eta^2} > 0.$$

Note that the denominator does not vanish on the interior of the disk D.

The complex functions (7.53, 54, 57) are all particular examples of *linear fractional transformations*

$$\zeta = \frac{\alpha\, z + \beta}{\gamma\, z + \delta}\,, \tag{7.59}$$

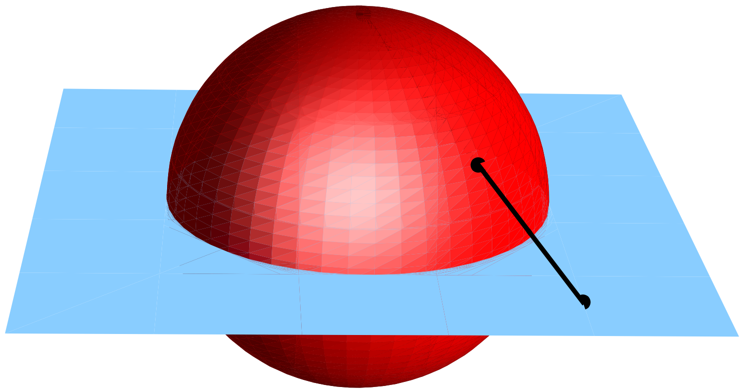

Figure 7.17. Stereographic Projection.

which form one of the most important classes of analytic maps. Here $\alpha, \beta, \gamma, \delta$ are complex constants, subject only to the restriction

$$\alpha\,\delta - \beta\,\gamma \neq 0,$$

since otherwise (7.59) reduces to a trivial constant (and non-invertible) map. (Why?) The map is well defined except when $\gamma \neq 0$ and $z = -\,\delta/\gamma$, which, by convention, is said to be mapped to the point $\zeta = \infty$. On the other hand, the linear fractional transformation maps $z = \infty$ to $\zeta = \alpha/\gamma$ (or ∞ when $\gamma = 0$), the value following from an evident limiting process. Thus, every linear fractional transformation defines a one-to-one, analytic map from the *Riemann sphere* $\mathbb{S} \equiv \mathbb{C} \cup \{\,\infty\,\}$ obtained by adjoining the point at infinity to the complex plane. The resulting space is identified with a two-dimensional sphere via stereographic projection $\pi\colon \mathbb{S} \to \mathbb{C}$, [**4**, **104**], which is one-to-one (and conformal) except at the north pole, where it is not defined and which is thus identified with the point ∞; see Figure 7.17. In complex analysis, one treats the point at infinity on an equal footing with all other complex points, using the map $\zeta = 1/z$, say, to analyze the behavior of analytic functions there.

Example 7.25. The linear fractional transformation

$$\zeta = \frac{z - \alpha}{\overline{\alpha}\, z - 1}\,, \qquad \text{with} \qquad |\,\alpha\,| < 1, \tag{7.60}$$

maps the unit disk to itself, moving the origin $z = 0$ to the point $\zeta = \alpha$. To prove this, we note that

$$\begin{aligned} |\, z - \alpha\,|^2 &= (z - \alpha)(\overline{z} - \overline{\alpha}) &&= |\,z\,|^2 - \alpha\,\overline{z} - \overline{\alpha}\,z + |\,\alpha\,|^2, \\ |\,\overline{\alpha}\,z - 1\,|^2 &= (\overline{\alpha}\,z - 1)(\alpha\,\overline{z} - 1) &&= |\,\alpha\,|^2\,|\,z\,|^2 - \alpha\,\overline{z} - \overline{\alpha}\,z + 1. \end{aligned}$$

Subtracting these two formulae,

$$|\,z - \alpha\,|^2 - |\,\overline{\alpha}\,z - 1\,|^2 = \bigl(\,1 - |\,\alpha\,|^2\,\bigr)\,\bigl(\,|\,z\,|^2 - 1\,\bigr) < 0, \quad \text{whenever} \quad |\,z\,| < 1, \quad |\,\alpha\,| < 1.$$

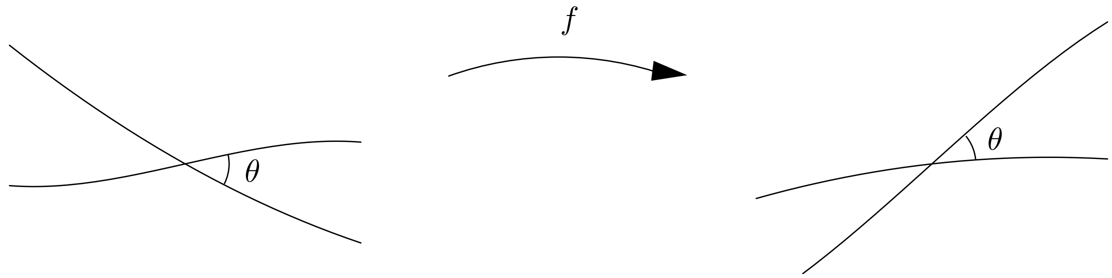

Figure 7.18. A Conformal Map.

Thus, $|\, z - \alpha \,| < |\, \overline{\alpha}\, z - 1 \,|$, which implies that

$$|\,\zeta\,| = \frac{|\, z-\alpha \,|}{|\, \overline{\alpha}\, z - 1 \,|} < 1 \qquad \text{provided} \qquad |\, z \,| < 1, \qquad |\, \alpha \,| < 1,$$

and hence, as promised, ζ lies within the unit disk.

The rotations (7.52) also map the unit disk to itself, while leaving the origin fixed. It can be proved, [**4**, **56**, **104**], that the only invertible analytic mappings that take the unit disk to itself are obtained by composing the preceding linear fractional transformation (7.60) with a rotation.

Proposition 7.26. *If $\zeta = g(z)$ is a one-to-one analytic map that takes the unit disk to itself, then*

$$g(z) = e^{\,\mathrm{i}\,\phi}\, \frac{z-\alpha}{\overline{\alpha}\, z - 1} \qquad \textit{for some} \qquad |\, \alpha \,| < 1, \qquad -\pi < \phi \leq \pi. \tag{7.61}$$

Additional properties of linear fractional transformations are outlined in the exercises.

Conformality

A remarkable geometrical property enjoyed by all complex analytic functions is that, at non-critical points, they preserve angles, and therefore define *conformal mappings*. Conformality makes sense for any inner product space, although in practice one usually deals with Euclidean space equipped with the standard dot product. In the two-dimensional plane, we can assign a sign to the angle between two vectors, whereas in higher dimensions only the absolute value of the angle can be consistently defined.

Definition 7.27. A function $g\colon \mathbb{R}^n \to \mathbb{R}^n$ is called *conformal* if it preserves angles.

But what does it mean to "preserve angles"? In the Euclidean norm, the angle between two vectors is defined by their dot product. However, most analytic maps are nonlinear, and so will not map vectors to vectors since they will typically map straight lines to curves. However, if we interpret "angle" to mean the angle between two curves[†], as illustrated in Figure 7.18, then we can make sense of the conformality requirement. Thus, in order to

[†] Or, more precisely, the angle between their tangent vectors at the point of intersection; see below for details.

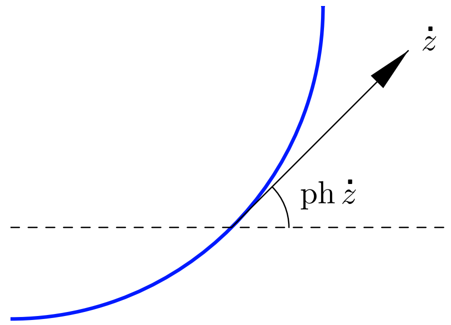

Figure 7.19. Complex Curve and Tangent.

realize complex functions as conformal maps, we first need to understand their effect on curves.

In general, a *curve* $C \in \mathbb{C}$ in the complex plane is parametrized by a complex-valued function

$$z(t) = x(t) + \mathrm{i}\, y(t), \qquad a \leq t \leq b, \tag{7.62}$$

that depends on a *real* parameter t. Note that there is no essential difference between a complex curve (7.62) and a real plane curve; we have merely switched from vector notation $\mathbf{x}(t) = (x(t), y(t))^T$ to complex notation $z(t) = x(t) + \mathrm{i}\, y(t)$. All the usual vectorial curve terminology — closed, simple (non-self intersecting), piecewise smooth, etc. — is employed without modification. In particular, the *tangent vector* to the curve at the point $z(t) = x(t) + \mathrm{i}\, y(t)$ can be identified with the complex number $\dot z(t) = \dot x(t) + \mathrm{i}\, \dot y(t)$, where we use dots to indicated derivatives with respect to the parameter t. Smoothness of the curve is guaranteed by the requirement that $\dot z(t) \neq 0$.

Example 7.28. (a) The curve

$$z(t) = e^{\mathrm{i}\, t} = \cos t + \mathrm{i}\, \sin t, \qquad \text{for} \qquad 0 \leq t \leq 2\pi,$$

parametrizes the unit circle $|\, z\,| = 1$ in the complex plane. Its complex tangent $\dot z(t) = \mathrm{i}\, e^{\mathrm{i}\, t} = \mathrm{i}\, z(t)$ is obtained by rotating $z(t)$ through 90°.

(*b*) The complex curve

$$z(t) = \cosh t + \mathrm{i}\, \sinh t = \frac{1+\mathrm{i}}{2}\, e^{t} + \frac{1-\mathrm{i}}{2}\, e^{-t}, \qquad -\infty < t < \infty,$$

parametrizes the right hand branch of the hyperbola $\operatorname{Re} z^2 = x^2 - y^2 = 1$. Its complex tangent vector is $\dot z(t) = \sinh t + \mathrm{i}\, \cosh t = \mathrm{i}\, \overline{z}(t)$.

When we interpret the curve as the motion of a particle in the complex plane, so that $z(t)$ is the position of the particle at time t, the tangent $\dot z(t)$ represents its instantaneous velocity. The modulus of the tangent, $|\, \dot z\,| = \sqrt{\dot x^2 + \dot y^2}$, indicates the particle's speed, while its phase $\operatorname{ph} \dot z$ measures the direction of motion, as prescribed by the angle that the curve makes with the horizontal; see Figure 7.19.

The (signed) *angle* between between two curves is defined as the angle between their tangents at the point of intersection $z = z_1(t_1) = z_2(t_2)$. If the curve C_1 is at angle

$\theta_1 = \mathrm{ph}\,\dot z_1(t_1)$ while the curve C_2 is at angle $\theta_2 = \mathrm{ph}\,\dot z_2(t_2)$, then the angle θ between C_1 and C_2 at z is their difference

$$\theta = \theta_2 - \theta_1 = \mathrm{ph}\,\dot z_2 - \mathrm{ph}\,\dot z_1 = \mathrm{ph}\left(\frac{\dot z_2}{\dot z_1}\right). \tag{7.63}$$

Now, consider the effect of an analytic map $\zeta = g(z)$. A curve C parametrized by $z(t)$ will be mapped to a new curve $\Gamma = g(C)$ parametrized by the composition $\zeta(t) = g(z(t))$. The tangent to the image curve is related to that of the original curve by the chain rule:

$$\frac{d\zeta}{dt} = \frac{dg}{dz}\,\frac{dz}{dt}, \qquad \text{or} \qquad \dot\zeta(t) = g'(z(t))\,\dot z(t). \tag{7.64}$$

Therefore, the effect of the analytic map on the tangent vector $\dot z$ is to multiply it by the complex number $g'(z)$. If the analytic map satisfies our key assumption $g'(z) \neq 0$, then $\dot\zeta \neq 0$, and so the image curve is guaranteed to be smooth.

According to equation (7.64),

$$|\,\dot\zeta\,| = |\,g'(z)\,\dot z\,| = |\,g'(z)\,|\,|\,\dot z\,|. \tag{7.65}$$

Thus, the speed of motion along the new curve $\zeta(t)$ is multiplied by a factor $\rho = |\,g'(z)\,| > 0$. Observe that the magnification factor ρ depends only upon the point z and not how the curve passes through it. All curves passing through the point z are speeded up (or slowed down if $\rho < 1$) by the same factor! Similarly, the angle that the new curve makes with the horizontal is given by

$$\mathrm{ph}\,\dot\zeta = \mathrm{ph}\big(g'(z)\,\dot z\big) = \mathrm{ph}\,g'(z) + \mathrm{ph}\,\dot z. \tag{7.66}$$

Therefore, the tangent angle of the curve is increased by an amount $\phi = \mathrm{ph}\,g'(z)$, i.e., its tangent has been rotated through angle ϕ. Again, the increase in tangent angle only depends on the point z, and all curves passing through z are rotated by the same amount ϕ. This immediately implies that the angle between any two curves is preserved. More precisely, if C_1 is at angle θ_1 and C_2 at angle θ_2 at a point of intersection, then their images $\Gamma_1 = g(C_1)$ and $\Gamma_2 = g(C_2)$ are at angles $\psi_1 = \theta_1 + \phi$ and $\psi_2 = \theta_2 + \phi$. The angle between the two image curves is the difference

$$\psi_2 - \psi_1 = (\theta_2 + \phi) - (\theta_1 + \phi) = \theta_2 - \theta_1,$$

which is *the same* as the angle between the original curves. This establishes the conformality or angle-preservation property of analytic maps.

Theorem 7.29. *If $\zeta = g(z)$ is an analytic function and $g'(z) \neq 0$, then g defines a conformal map.*

Remark: The converse is also valid: Every planar conformal map comes from a complex analytic function with nonvanishing derivative. You are asked to find a proof of this fact in Exercise ■.

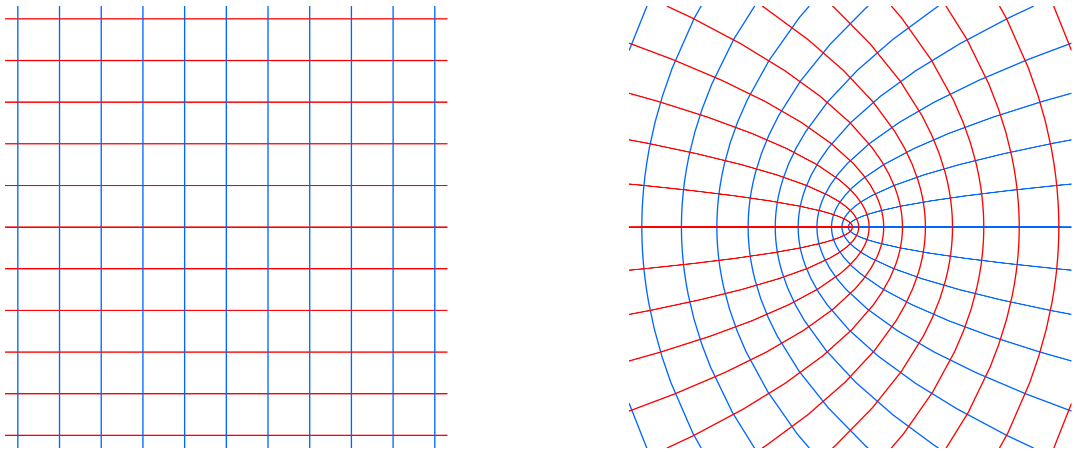

Figure 7.20. Conformality of z^2.

The conformality of analytic functions is all the more surprising when one revisits elementary examples. In Example 7.23, we discovered that the function $w = z^2$ maps a quarter plane to a half plane, and therefore *doubles* the angle between the coordinate axes at the origin! Thus $g(z) = z^2$ is most definitely not conformal at $z = 0$. The explanation is, of course, that $z = 0$ is a critical point, $g'(0) = 0$, and Theorem 7.29 only guarantees conformality when the derivative is nonzero. Amazingly, the map preserves angles everywhere else! Somehow, the angle at the origin is doubled, while angles at all nearby points are preserved. Figure 7.20 illustrates this remarkable and counter-intuitive feat. The left hand figure shows the coordinate grid, while on the right are the images of the horizontal and vertical lines under the map z^2. Note that, except at the origin, the image curves continue to meet at 90° angles, in accordance with conformality.

Example 7.30. A particularly interesting example is the *Joukowski map*

$$\zeta = \frac{1}{2}\left(z + \frac{1}{z}\right). \tag{7.67}$$

It was first employed to study flows around airplane wings by the pioneering Russian aero- and hydro-dynamics researcher Nikolai Zhukovskii (Joukowski). Since

$$\frac{d\zeta}{dz} = \frac{1}{2}\left(1 - \frac{1}{z^2}\right) = 0 \qquad \text{if and only if} \qquad z = \pm 1,$$

the Joukowski map is conformal *except* at the critical points $z = \pm 1$ as well as the singularity $z = 0$, where it is not defined.

If $z = e^{\,\mathrm{i}\,\theta}$ lies on the unit circle, then

$$\zeta = \tfrac{1}{2}\left(e^{\,\mathrm{i}\,\theta} + e^{-\,\mathrm{i}\,\theta}\right) = \cos\theta,$$

lies on the real axis, with $-1 \le \zeta \le 1$. Thus, the Joukowski map squashes the unit circle down to the real line segment $[-1, 1]$. The images of points outside the unit circle fill the rest of the ζ plane, as do the images of the (nonzero) points inside the unit circle. Indeed, if we solve (7.67) for

$$z = \zeta \pm \sqrt{\zeta^2 - 1}\,, \tag{7.68}$$

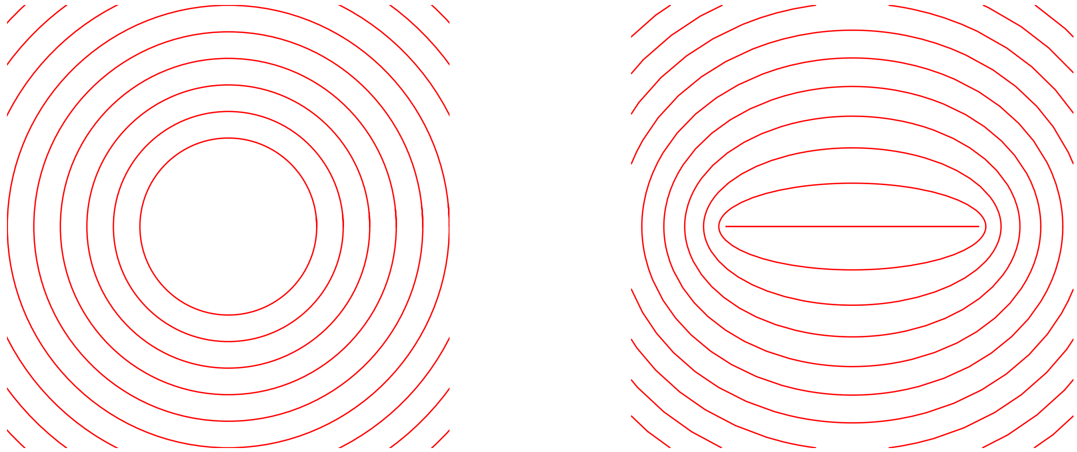

Figure 7.21. The Joukowski Map.

we see that every ζ except ± 1 comes from two different points z; for ζ not on the critical line segment $[-1,1]$, one point (with the minus sign) lies inside and one (with the plus sign) lies outside the unit circle, whereas if $-1 < \zeta < 1$, both points lie on the unit circle and a common vertical line. Therefore, (7.67) defines a one-to-one conformal map from the exterior of the unit circle $\{\, |z| > 1 \,\}$ onto the exterior of the unit line segment $\mathbb{C} \setminus [-1,1]$.

Under the Joukowski map, the concentric circles $|z| = r \neq 1$ are mapped to ellipses with foci at ± 1 in the ζ plane; see Figure 7.21. The effect on circles not centered at the origin is quite interesting. The image curves take on a wide variety of shapes; several examples are plotted in Figure 7.22. If the circle passes through the singular point $z = 1$, then its image is no longer smooth, but has a cusp at $\zeta = 1$; this happens in the last 6 of the figures. Some of the image curves assume the shape of the cross-section through an idealized airplane wing or *airfoil*. Later, we will see how to determine the physical fluid flow around such an airfoil, a construction that was important in early aircraft design.

Composition and the Riemann Mapping Theorem

One of the hallmarks of conformal mapping is that one can assemble a large repertoire of complicated examples by simply composing elementary mappings. This relies on the fact that the composition of two complex analytic functions is also complex analytic.

Proposition 7.31. *If $w = f(z)$ is an analytic function of the complex variable $z = x + \mathrm{i}\,y$, and $\zeta = g(w)$ is an analytic function of the complex variable $w = u + \mathrm{i}\,v$, then the composition*[†] *$\zeta = h(z) \equiv g \circ f(z) = g(f(z))$ is an analytic function of z.*

The proof that the composition of two differentiable functions is differentiable is identical to the real variable version, [**8**, **102**, **114**], and need not be reproduced here. The

[†] Of course, to properly define the composition, we need to ensure that the range of the function $w = f(z)$ is contained in the domain of the function $\zeta = g(w)$.

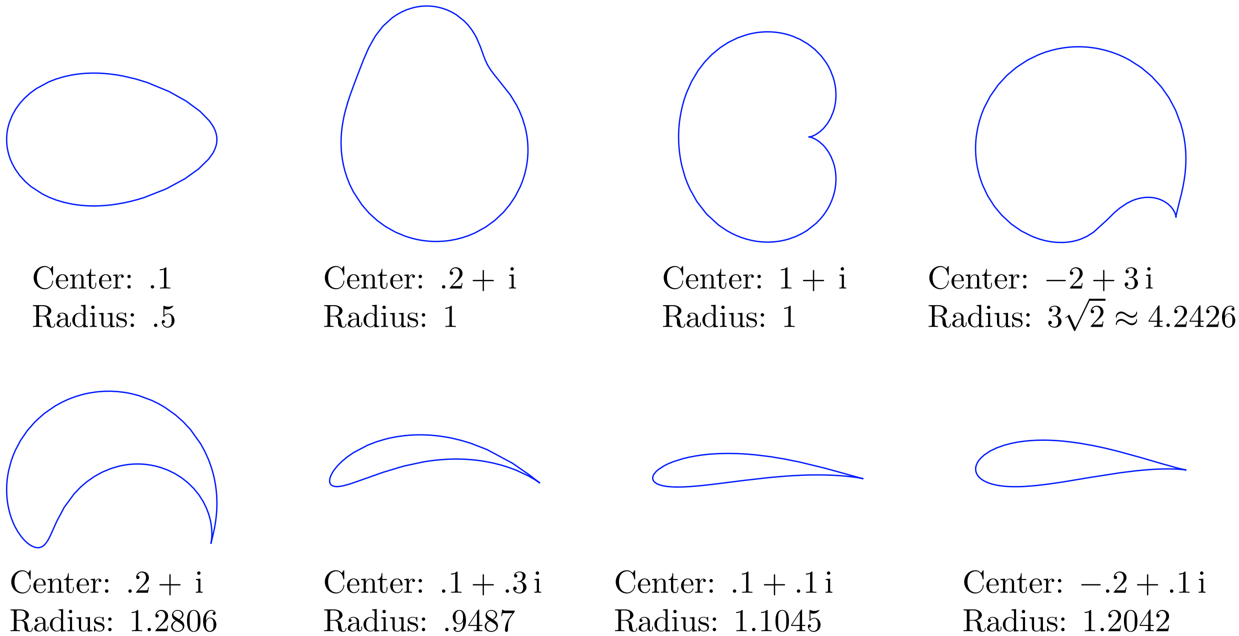

Figure 7.22. Airfoils Obtained from Circles via the Joukowski Map.

derivative of the composition is explicitly given by the usual chain rule:

$$\frac{d}{dz}\, g \circ f(z) = g'(f(z))\, f'(z), \qquad \text{or, in Leibnizian notation,} \qquad \frac{d\zeta}{dz} = \frac{d\zeta}{dw}\,\frac{dw}{dz}\,. \tag{7.69}$$

If both f and g are one-to-one, so is their composition $h = g \circ f$. Moreover, the composition of two conformal maps is also conformal, a fact that is immediate from the definition, or by using the chain rule (7.69) to show that

$$h'(z) = g'(f(z))\, f'(z) \neq 0 \qquad \text{provided} \qquad g'(f(z)) \neq 0 \quad \text{and} \quad f'(z) \neq 0.$$

Example 7.32. As we learned in Example 7.22, the exponential function

$$w = e^z$$

maps the horizontal strip $S = \{ -\frac{1}{2}\pi < \operatorname{Im} z < \frac{1}{2}\pi \}$ conformally onto the right half plane $R = \{ \operatorname{Re} w > 0 \}$. On the other hand, Example 7.24 tells us that the linear fractional transformation

$$\zeta = \frac{w-1}{w+1}$$

maps the right half plane R conformally to the unit disk $D = \{ |\,\zeta\,| < 1 \}$. Therefore, the composition

$$\zeta = \frac{e^z - 1}{e^z + 1} \tag{7.70}$$

is a one-to-one conformal map from the horizontal strip S to the unit disk D, which we illustrate in Figure 7.23.

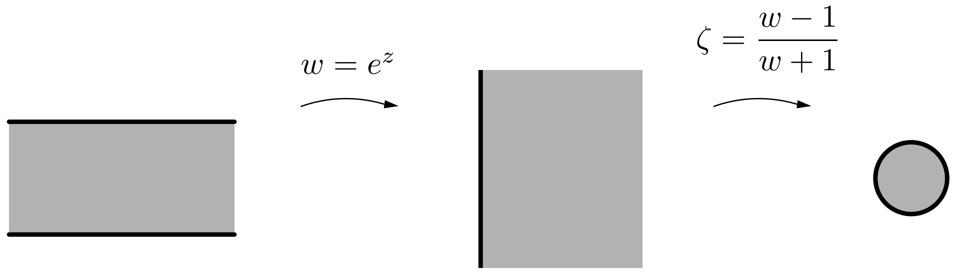

Figure 7.23. Composition of Conformal Maps.

Recall that our aim is to use analytic functions/conformal maps to solve boundary value problems for the Laplace equation on a complicated domain Ω by transforming them to solved boundary value problems on the unit disk. Of course, the key question the student should be asking at this point is: Is there, in fact, a conformal map $\zeta = g(z)$ from a given domain Ω to the unit disk $D = g(\Omega)$? The theoretical answer is the celebrated *Riemann Mapping Theorem*.

Theorem 7.33. *If $\Omega \subsetneq \mathbb{C}$ is any simply connected open subset,* not *equal to the entire complex plane, then there exists a one-to-one complex analytic map $\zeta = g(z)$, satisfying the conformality condition $g'(z) \neq 0$ for all $z \in \Omega$, that maps Ω to the unit disk $D = \{\,|\,\zeta\,| < 1\,\}$.*

Thus, *any* simply connected domain — with one exception, the entire complex plane — can be conformally mapped the unit disk. Note that Ω need *not* be bounded for this to hold. Indeed, the conformal map (7.57) takes the unbounded right half plane $R = \{\operatorname{Re} z > 0\}$ to the unit disk. The proof of this important theorem relies on some more advanced topics in complex analysis, and can be found, for instance, in [**4**].

The Riemann Mapping Theorem guarantees the existence of a conformal map from any simply connected domain to the unit disk, but its proof is not constructive, and so cannot be used to produce an explicit formula for the desired mapping. And, in general, this is not an easy task. In practice, one assembles a collection of useful conformal maps that apply to particular domains of interest. More complicated maps can then be built up by composition of the basic examples. An extensive catalog can be found in [**64**], while numerical schemes for constructing conformal maps are surveyed in [**37**].

Example 7.34. Suppose we are asked to conformally map the upper half plane $U = \big\{\operatorname{Im} z > 0\big\}$ to the unit disk $D = \big\{\,|\,\zeta\,| < 1\,\big\}$. We already know that the linear fractional transformation

$$\zeta = g(w) = \frac{w-1}{w+1}$$

maps the right half plane $R = \big\{\operatorname{Re} w > 0\big\}$ to $D = g(R)$. On the other hand, multiplication by $\mathrm{i} = e^{\mathrm{i}\,\pi/2}$, with $z = h(w) = \mathrm{i}\,w$, rotates the complex plane by 90° and so maps the right half plane R to the upper half plane $U = h(R)$. Its inverse $h^{-1}(z) = -\,\mathrm{i}\,z$ will therefore map U to $R = h^{-1}(U)$. Therefore, to map the upper half plane to the unit disk, we compose these two maps, leading to the conformal map

$$\zeta = g \circ h^{-1}(z) = \frac{-\,\mathrm{i}\,z - 1}{-\,\mathrm{i}\,z + 1} = \frac{\mathrm{i}\,z + 1}{\mathrm{i}\,z - 1} \tag{7.71}$$

from U to D.

In a similar vein, we already know that the squaring map $w = z^2$ maps the upper right quadrant $Q = \left\{ 0 < \operatorname{ph} z < \frac{1}{2}\pi \right\}$ to the upper half plane U. Composing this with our previously constructed map — which requires replacing z by w in (7.71) beforehand — leads to the conformal map

$$\zeta = \frac{\mathrm{i}\, z^2 + 1}{\mathrm{i}\, z^2 - 1} \tag{7.72}$$

that maps the quadrant Q to the unit disk D.

Example 7.35. The goal of this example is to construct an conformal map that takes a half disk

$$D_+ = \{\, |\, z\,| < 1, \quad \operatorname{Im} z > 0 \,\} \tag{7.73}$$

to the full unit disk $D = \{\, |\, \zeta\,| < 1\,\}$. The answer is *not* $\zeta = z^2$ because the image of D_+ omits the positive real axis, resulting in a disk that has a slit cut out of it: $\{\, |\, \zeta\,| < 1,\ 0 < \operatorname{ph} \zeta < 2\pi \,\}$. To obtain the entire disk as the image of the conformal map, we must think a little harder. The first observation is that the map $z = (w-1)/(w+1)$ that we analyzed in Example 7.24 takes the right half plane $R = \{\operatorname{Re} w > 0\}$ to the unit disk. Moreover, it maps the upper right quadrant $Q = \left\{ 0 < \operatorname{ph} w < \frac{1}{2}\pi \right\}$ to the half disk (7.73). Its inverse,

$$w = \frac{z+1}{z-1} \tag{7.74}$$

will therefore map the half disk, $z \in D_+$, to the upper right quadrant $w \in Q$.

On the other hand, we just constructed a conformal map (7.72) that takes the upper right quadrant Q to the unit disk D. Therefore, if compose the two maps — replacing z by w in (7.72) and then using (7.74) — we obtain the desired conformal map:

$$\zeta = \frac{\mathrm{i}\, w^2 + 1}{\mathrm{i}\, w^2 - 1} = \frac{\mathrm{i}\left(\dfrac{z+1}{z-1}\right)^2 + 1}{\mathrm{i}\left(\dfrac{z+1}{z-1}\right)^2 - 1} = \frac{(\mathrm{i}+1)(z^2+1) + 2(\mathrm{i}-1)z}{(\mathrm{i}-1)(z^2+1) + 2(\mathrm{i}+1)z}\,.$$

The formula can be further simplified by multiplying numerator and denominator by $\mathrm{i}+1$, and so

$$\zeta = -\,\mathrm{i}\ \frac{z^2 + 2\,\mathrm{i}\, z + 1}{z^2 - 2\,\mathrm{i}\, z + 1}\,.$$

The leading factor $-\mathrm{i}$ is unimportant and can be omitted, since it merely rotates the disk by -90°, and so

$$\zeta = \frac{z^2 + 2\,\mathrm{i}\, z + 1}{z^2 - 2\,\mathrm{i}\, z + 1} \tag{7.75}$$

is an equally valid solution to our problem.

Finally, as noted in the preceding example, the conformal map guaranteed by the Riemann Mapping Theorem is *not* unique. Since the linear fractional transformations (7.61) map the unit disk to itself, we can compose them with any conformal Riemann

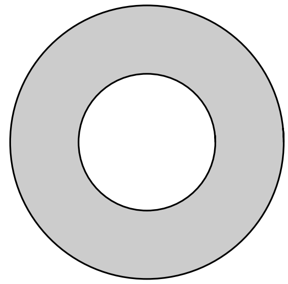

Figure 7.24. An Annulus.

mapping to produce additional conformal maps from a simply connected domain to the unit disk. For example, composing with (7.75) produces the two parameter family of conformal mappings

$$\zeta = e^{\,\mathrm{i}\,\phi}\,\frac{z^2 + 2\,\mathrm{i}\,z + 1 - \alpha\,(z^2 - 2\,\mathrm{i}\,z + 1)}{\overline{\alpha}\,(z^2 + 2\,\mathrm{i}\,z + 1) - z^2 + 2\,\mathrm{i}\,z - 1}\,, \tag{7.76}$$

which, for any $|\,\alpha\,| < 1$, $-\pi < \phi \leq \pi$, take the half disk onto the unit disk. Proposition 7.26 implies that this is the only ambiguity, and so, in this instance, (7.76) forms a complete list of one-to-one conformal maps from D_+ to D.

Annular Domains

The Riemann Mapping Theorem does not apply to non-simply connected domains. For purely topological reasons, a hole cannot be made to disappear under a one-to-one continuous mapping — much less a conformal map — and so it is impossible to map a non-simply connected domain in a one-to-one manner onto the unit disk. So we must look elsewhere for a simple model domain.

The simplest non-simply connected domain is an *annulus* consisting of the points between two concentric circles

$$A_{r,R} = \left\{\, r < |\,\zeta\,| < R \,\right\}, \tag{7.77}$$

which, for simplicity, is centered around the origin; see Figure 7.24. The case $r = 0$ corresponds to a punctured disk, while setting $R = \infty$ gives the exterior of a disk of radius r. It can be proved, [**64**], that any other domain with a single hole can be conformally mapped to an annulus. The annular radii r, R are not uniquely specified; indeed the linear map $\zeta = \alpha\, z$ maps the annulus (7.77) to a rescaled annulus $A_{\rho r, \rho R}$ whose inner and outer radii have both been scaled by the factor $\rho = |\,\alpha\,|$. But the ratio r/R of the inner to outer radius of the annulus is uniquely specified, and annuli with different ratios *cannot* be mapped to each other by a conformal map. Here, if $r = 0$ or $R = \infty$, but not both, then $r/R = 0$ by convention. The punctured plane, where $r = 0$ and $R = \infty$ remains a separate case.

Example 7.36. Let $c > 0$. Consider the domain

$$\Omega = \left\{\, |\,z\,| < 1 \quad \text{and} \quad |\,z - c\,| > c \,\right\}$$

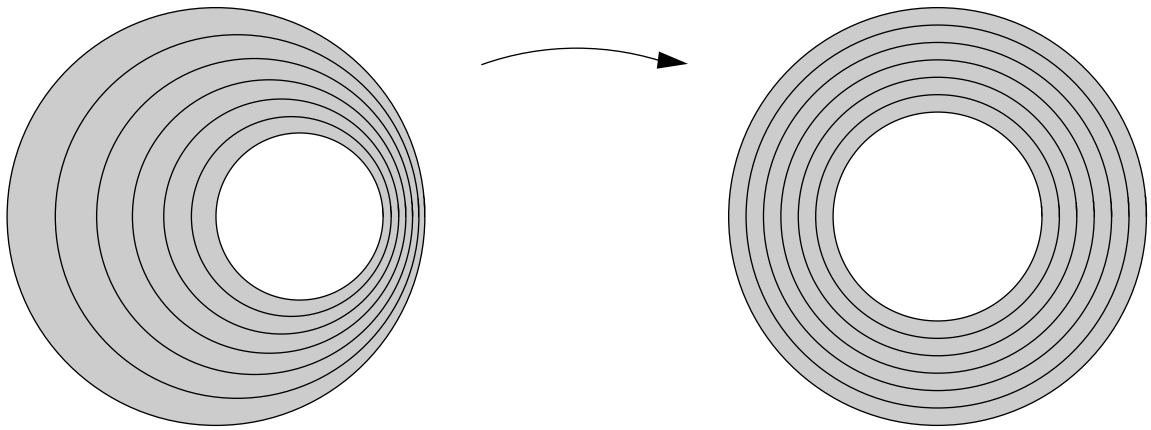

Figure 7.25. Conformal Map for a Non-Concentric Annulus.

contained between two nonconcentric circles. To keep the computations simple, we take the outer circle to have radius 1 (which can always be arranged by scaling, anyway) while the inner circle has center at the point $z = c$ on the real axis and radius c, which means that it passes through the origin. We must restrict $c < \frac{1}{2}$ in order that the inner circle be strictly inside the outer circle. Our goal is to find a conformal map $\zeta = g(z)$ that takes this non-concentric annular domain to a concentric annulus of the form

$$A_{r,1} = \{\, r < |\,\zeta\,| < 1 \,\}.$$

Now, according to Example 7.25, a linear fractional transformation of the form

$$\zeta = g(z) = \frac{z - \alpha}{\overline{\alpha}\, z - 1} \qquad \text{with} \qquad |\,\alpha\,| < 1 \tag{7.78}$$

maps the unit disk to itself. Moreover, as noted above, and demonstrated in Exercise ■, linear fractional transformations always map circles to circles. Therefore, we seek a particular value of α that maps the inner circle $|\,z - c\,| = c$ to a circle of the form $|\,\zeta\,| = r$ centered at the origin. We choose α to be real and try to map the points 0 and $2\,c$ on the inner circle to the points r and $-r$ on the circle $|\,\zeta\,| = r$. This requires

$$g(0) = \alpha = r, \qquad\qquad g(2\,c) = \frac{2\,c - \alpha}{2\,c\alpha - 1} = -\,r. \tag{7.79}$$

Substituting the first into the second leads to the quadratic equation

$$c\alpha^2 - \alpha + c = 0,$$

which has two real solutions:

$$\alpha = \frac{1 - \sqrt{1 - 4\,c^2}}{2\,c} \qquad \text{and} \qquad \alpha = \frac{1 + \sqrt{1 - 4\,c^2}}{2\,c}\,. \tag{7.80}$$

Since $0 < c < \frac{1}{2}$, the second solution gives $\alpha > 1$, and hence is inadmissible. Therefore, the first solution yields the required conformal map

$$\zeta = \frac{z - 1 + \sqrt{1 - 4c^2}}{(1 - \sqrt{1 - 4c^2}\,)\, z - 2c}\,.$$

Note in particular that the radius $r = \alpha$ of the inner circle in $A_{r,1}$ is *not the same* as the radius c of the inner circle in Ω. For example, taking $c = \frac{2}{5}$, equation (7.80) implies $\alpha = \frac{1}{2}$, and hence the linear fractional transformation $\zeta = \dfrac{2z - 1}{z - 2}$ maps the annular domain $\Omega = \left\{ \,|\, z \,|< 1,\ \left|\, z - \frac{2}{5} \,\right| > \frac{2}{5} \,\right\}$ to the concentric annulus $A = A_{1/2,1} = \left\{ \,\frac{1}{2} < |\,\zeta\,| < 1 \,\right\}$. In Figure 7.25, we plot several of the non-concentric circles in Ω that are mapped to concentric circles in the annulus A.

7.5. Applications of Conformal Mapping.

Let us now apply what we have learned about analytic/conformal maps. We begin with boundary value problems for the Laplace equation, and then present some applications in fluid mechanics. We conclude by explaining how to use conformal maps to construct Green's functions for the two-dimensional Poisson equation.

Applications to Harmonic Functions and Laplace's Equation

We are interested in solving a boundary value problem for the Laplace equation on a domain $\Omega \subset \mathbb{R}^2$. Our strategy is to map it to a corresponding boundary value problem on the unit disk D that we know how to solve. To this end, suppose we know a conformal map $\zeta = g(z)$ that takes $z \in \Omega$ to $\zeta \in D$. As we know, the real and imaginary parts of an analytic function $F(\zeta)$ defined on D are harmonic. Moreover, according to Proposition 7.31, the composition $f(z) = F(g(z))$ defines an analytic function whose real and imaginary parts are harmonic functions on Ω. Thus, the conformal mapping can be regarded as a change of variables that preserves the property of harmonicity. In fact, this property does not even require the harmonic function to be the real part of an analytic function, i.e., we need not assume the existence of a harmonic conjugate.

Proposition 7.37. *If $U(\xi, \eta)$ is a harmonic function of ξ, η, and*

$$\zeta = \xi + \mathrm{i}\,\eta = \xi(x, y) + \mathrm{i}\,\eta(x, y) = g(z) \tag{7.81}$$

is any analytic function, then the composition

$$u(x, y) = U(\xi(x, y), \eta(x, y)) \tag{7.82}$$

is a harmonic function of x, y.

Proof: This is a straightforward application of the chain rule:

$$\frac{\partial u}{\partial x} = \frac{\partial U}{\partial \xi}\,\frac{\partial \xi}{\partial x} + \frac{\partial U}{\partial \eta}\,\frac{\partial \eta}{\partial x}\,, \qquad\qquad \frac{\partial u}{\partial y} = \frac{\partial U}{\partial \xi}\,\frac{\partial \xi}{\partial y} + \frac{\partial U}{\partial \eta}\,\frac{\partial \eta}{\partial y}\,,$$

$$\frac{\partial^2 u}{\partial x^2} = \frac{\partial^2 U}{\partial \xi^2}\left(\frac{\partial \xi}{\partial x}\right)^2 + 2\,\frac{\partial^2 U}{\partial \xi\,\partial \eta}\,\frac{\partial \xi}{\partial x}\,\frac{\partial \eta}{\partial x} + \frac{\partial^2 U}{\partial \eta^2}\left(\frac{\partial \eta}{\partial x}\right)^2 + \frac{\partial U}{\partial \xi}\,\frac{\partial^2 \xi}{\partial x^2} + \frac{\partial U}{\partial \eta}\,\frac{\partial^2 \eta}{\partial x^2}\,,$$

$$\frac{\partial^2 u}{\partial y^2} = \frac{\partial^2 U}{\partial \xi^2}\left(\frac{\partial \xi}{\partial y}\right)^2 + 2\,\frac{\partial^2 U}{\partial \xi\,\partial \eta}\,\frac{\partial \xi}{\partial y}\,\frac{\partial \eta}{\partial y} + \frac{\partial^2 U}{\partial \eta^2}\left(\frac{\partial \eta}{\partial y}\right)^2 + \frac{\partial U}{\partial \xi}\,\frac{\partial^2 \xi}{\partial y^2} + \frac{\partial U}{\partial \eta}\,\frac{\partial^2 \eta}{\partial y^2}\,.$$

Using the Cauchy–Riemann equations

$$\frac{\partial \xi}{\partial x} = -\,\frac{\partial \eta}{\partial y}\,, \qquad\qquad \frac{\partial \xi}{\partial y} = \frac{\partial \eta}{\partial x}\,,$$

for the analytic function $\zeta = \xi + \mathrm{i}\,\eta$, we find, after some algebra,

$$\Delta u = \frac{\partial^2 u}{\partial x^2} + \frac{\partial^2 u}{\partial y^2} = \left[\left(\frac{\partial \xi}{\partial x}\right)^2 + \left(\frac{\partial \eta}{\partial x}\right)^2\right]\left[\frac{\partial^2 U}{\partial \xi^2} + \frac{\partial^2 U}{\partial \eta^2}\right] = |\,g'(z)\,|^2\,\Delta U, \tag{7.83}$$

the final expression following from the first formula for the complex derivative in (7.19). We conclude that whenever $U(\xi,\eta)$ is harmonic, and so solves the Laplace equation $\Delta U = 0$ in the ξ,η variables, then $u(x,y)$ is solves the Laplace equation $\Delta u = 0$ in the x,y variables, and is thus also harmonic. *Q.E.D.*

This observation has immediate consequences for boundary value problems arising in physical applications. Suppose we wish to solve the Dirichlet problem

$$\Delta u = 0 \quad \text{in} \quad \Omega, \qquad\qquad u = h \quad \text{on} \quad \partial\Omega, \tag{7.84}$$

in a simply connected domain $\Omega \subsetneq \mathbb{C}$. Let $\zeta = g(z) = p(x,y) + \mathrm{i}\,q(x,y)$ be a one-to-one conformal mapping from the domain Ω to the unit disk D, whose existence is guaranteed by the Riemann Mapping Theorem 7.33. (Although its explicit construction may be problematic.) Then the change of variables formula (7.82) will map the harmonic function $u(x,y)$ on Ω to a harmonic function $U(\xi,\eta)$ on D. Moreover, the boundary values of $U = H$ on the unit circle ∂D correspond to those of $u = h$ on $\partial\Omega$ by the same change of variables formula:

$$h(x,y) = H(p(x,y), q(x,y)) \qquad \text{for} \qquad (x,y) \in \partial\Omega. \tag{7.85}$$

We conclude that $U(\xi,\eta)$ solves the Dirichlet problem

$$\Delta U = 0 \quad \text{in} \quad D, \qquad\qquad U = H \quad \text{on} \quad \partial D. \tag{7.86}$$

But we already know how to solve the Dirichlet problem (7.86) on the unit disk by the Poisson integral formula (4.126)! We conclude that the solution to the original boundary value problem is given by the composition formula $u(x,y) = U\big(p(x,y), q(x,y)\big)$. In summary, the solution to the Dirichlet problem on a unit disk can be used to solve the Dirichlet problem on more complicated planar domains — provided we are in possession of a suitable conformal map.

Example 7.38. According to Example 7.24, the analytic function

$$\xi + \mathrm{i}\,\eta = \zeta = \frac{z-1}{z+1} = \frac{x^2+y^2-1}{(x+1)^2+y^2} + \mathrm{i}\,\frac{2\,y}{(x+1)^2+y^2} \tag{7.87}$$

maps the right half plane $R = \{\, x = \operatorname{Re} z > 0 \,\}$ to the unit disk $D = \{\, |\,\zeta\,| < 1 \,\}$. Proposition 7.37 implies that if $U(\xi,\eta)$ is a harmonic function in the unit disk, then

$$u(x,y) = U\left(\frac{x^2+y^2-1}{(x+1)^2+y^2}\,,\ \frac{2\,y}{(x+1)^2+y^2}\right) \tag{7.88}$$

is a harmonic function on the right half plane. (This can, of course, be checked directly by a rather unpleasant chain rule computation.)

To solve the Dirichlet boundary value problem

$$\Delta u = 0, \qquad x > 0, \qquad\qquad u(0,y) = h(y), \tag{7.89}$$

on the right half plane, we adopt the change of variables (7.87) and use the Poisson integral formula to construct the solution to the transformed Dirichlet problem

$$\Delta U = 0, \qquad \xi^2+\eta^2 < 1, \qquad\qquad U(\cos\phi, \sin\phi) = H(\phi), \tag{7.90}$$

on the unit disk. The transformed boundary data are found as follows. Using the explicit form

$$x + \mathrm{i}\,y = z = \frac{1+\zeta}{1-\zeta} = \frac{(1+\zeta)(1-\overline{\zeta})}{|\,1-\zeta\,|^2} = \frac{1+\zeta-\overline{\zeta}-|\,\zeta\,|^2}{|\,1-\zeta\,|^2} = \frac{1-\xi^2-\eta^2+2\,\mathrm{i}\,\eta}{(\xi-1)^2+\eta^2}$$

for the inverse map, we see that the boundary point $\zeta = \xi + \mathrm{i}\,\eta = e^{\,\mathrm{i}\,\phi}$ on the unit circle ∂D will correspond to the boundary point

$$\mathrm{i}\,y = \frac{2\,\eta}{(\xi-1)^2+\eta^2} = \frac{2\,\mathrm{i}\,\sin\phi}{(\cos\phi-1)^2+\sin^2\phi} = \mathrm{i}\,\cot\frac{\phi}{2} \tag{7.91}$$

on the imaginary axis $\partial R = \{\, \operatorname{Re} z = 0 \,\}$. Thus, the boundary data $h(y)$ on ∂R corresponds to the boundary data

$$H(\phi) = h\bigl(\cot\tfrac{1}{2}\,\phi\bigr)$$

on the unit circle. The Poisson integral formula (4.126) can then be applied to solve (7.90), from which we are able to reconstruct the solution (7.88) to the boundary value problem (7.88) on the half plane.

Let's look at an explicit example. If the boundary data on the imaginary axis is provided by the step function

$$u(0,y) = h(y) \equiv \begin{cases} 1, & y > 0, \\ 0, & y < 0, \end{cases}$$

then the corresponding boundary data on the unit disk is a (periodic) step function

$$H(\phi) = \begin{cases} 1, & 0 < \phi < \pi, \\ 0, & -\pi < \phi < 0. \end{cases}$$

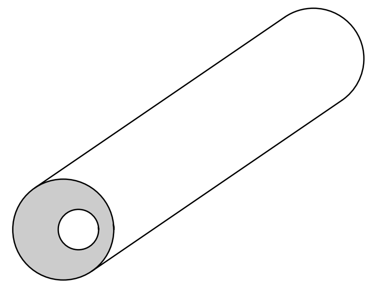

Figure 7.26. A Non–Coaxial Cable.

According to (4.129), the corresponding solution in the unit disk is

$$U(\xi,\eta) = \begin{cases} 1 - \dfrac{1}{\pi}\tan^{-1}\left(\dfrac{1-\xi^2-\eta^2}{2\eta}\right), & \xi^2+\eta^2<1, \quad \eta>0, \\ \frac{1}{2}, & \xi^2+\eta^2<1, \quad \eta=0, \\ -\dfrac{1}{\pi}\tan^{-1}\left(\dfrac{1-\xi^2-\eta^2}{2\eta}\right), & \xi^2+\eta^2<1, \quad \eta<0. \end{cases}$$

After some tedious algebra, we find that the corresponding solution in the right half plane is simply

$$u(x,y) = \frac{1}{2} + \frac{1}{\pi}\,\mathrm{ph}\,z = \frac{1}{2} + \frac{1}{\pi}\,\tan^{-1}\frac{y}{x}\,,$$

an answer that, in hindsight, we should have been able to guess.

Remark: The solution to the preceding Dirichlet boundary value problem is not, in fact, unique, owing to the unboundedness of the domain. The solution that we pick out by using the conformal map to the unit disk is the one that remains bounded at ∞. The unbounded solutions would correspond to solutions on the unit disk that have a singularity in their boundary data at the point -1; see Exercise ■.

Example 7.39. *A non-coaxial cable.* The goal of this example is to determine the electrostatic potential inside a non-coaxial cylindrical cable with prescribed constant potential values on the two bounding cylinders, as illustrated in Figure 7.26. Assume for definiteness that the larger cylinder has radius 1, and is centered at the origin, while the smaller cylinder has radius $\frac{2}{5}$, and is centered at $z=\frac{2}{5}$. The resulting electrostatic potential will be independent of the longitudinal coordinate, and so can be viewed as a planar potential in the annular domain contained between two circles representing the cross-sections of our cylinders. The desired potential must satisfy the Dirichlet boundary value problem

$$\Delta u = 0 \qquad \text{when} \qquad |\,z\,|<1 \quad \text{and} \quad \left|\,z-\tfrac{2}{5}\,\right| > \tfrac{2}{5},$$
$$u=a, \quad \text{when} \quad |\,z\,|=1, \qquad \text{and} \qquad u=b \quad \text{when} \quad \left|\,z-\tfrac{2}{5}\,\right| = \tfrac{2}{5}.$$

According to Example 7.36, the linear fractional transformation

$$\zeta = \frac{2\,z-1}{z-2} \tag{7.92}$$

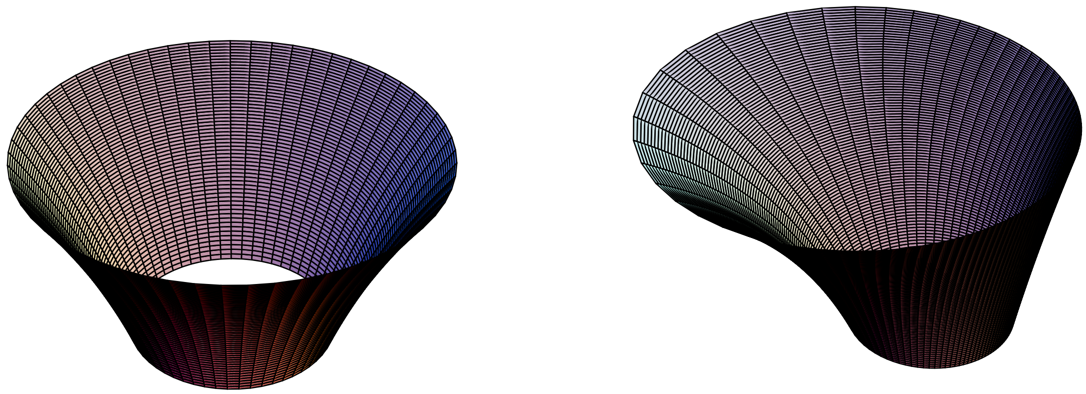

Figure 7.27. Electrostatic Potential Between Coaxial and Non-Coaxial Cylinders.

maps this non-concentric annular domain to the annulus $A_{1/2,1} = \left\{ \frac{1}{2} < |\,\zeta\,| < 1 \right\}$, which is the cross-section of a coaxial cable. The corresponding transformed potential $U(\xi,\eta)$ has the constant Dirichlet boundary conditions

$$U = a, \quad \text{when} \quad |\,\zeta\,| = \tfrac{1}{2}, \qquad \text{and} \qquad U = b \quad \text{when} \quad |\,\zeta\,| = 1. \tag{7.93}$$

Clearly the coaxial potential U must be a radially symmetric solution to the Laplace equation, and hence, according to (6.103), of the form

$$U(\xi,\eta) = \alpha \, \log |\,\zeta\,| + \beta,$$

for constants α, β. A short computation shows that the particular potential function

$$U(\xi,\eta) = \frac{b-a}{\log 2} \, \log |\,\zeta\,| + b = \frac{b-a}{2\log 2} \, \log(\xi^2 + \eta^2) + b$$

satisfies the prescribed boundary conditions (7.93). Therefore, the desired non-coaxial electrostatic potential

$$u(x,y) = \frac{b-a}{\log 2} \, \log \left| \frac{2\,z-1}{z-2} \right| + b = \frac{b-a}{2\log 2} \, \log \left(\frac{(2\,x-1)^2 + y^2}{(x-2)^2 + y^2} \right) + b \tag{7.94}$$

is obtained by composition with the conformal map (7.92). The particular case $a = 0$, $b = 1$, is plotted in Figure 7.27.

Remark: The same harmonic function determines the equilibrium temperature of an annular plate whose inner boundary is kept at a temperature $u = a$ while the outer boundary is kept at temperature $u = b$. One could also interpret this solution as the equilibrium temperature of a three-dimensional cylindrical body contained between two non-coaxial cylinders that are held at fixed temperatures. In this circumstance, the body's temperature (7.94) only depends upon the transverse coordinates x, y, and not upon the longitudinal coordinate z.

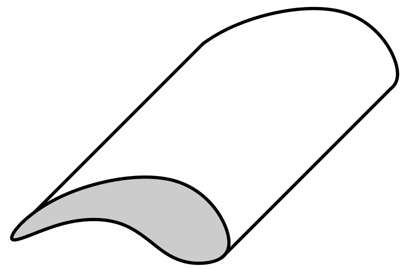

Figure 7.28. Cross Section of Cylindrical Object.

Applications to Fluid Flow

Conformal mappings are particularly apt for the analysis of planar ideal fluid flow. Let $\Theta(\zeta) = \Phi(\xi,\eta) + \mathrm{i}\,\Psi(\xi,\eta)$ be an analytic function representing the complex potential function for a steady state fluid flow in a planar domain $\zeta \in D$. Composing the complex potential $\Theta(\zeta)$ with a one-to-one conformal map $\zeta = g(z)$ leads to a transformed complex potential $\chi(z) = \Theta(g(z)) = \varphi(x,y) + \mathrm{i}\,\psi(x,y)$ on the corresponding domain $\Omega = g^{-1}(D)$. Thus, we can employ conformal maps to construct fluid flows in complicated domains from known flows in simpler domains.

Let us concentrate on fluid flow past a solid object. The ideal flow assumptions of incompressibility and irrotationality are reasonably accurate if the flow is *laminar*, meaning far away from turbulent. In three dimensions, the object is assumed to have a uniform shape in the axial direction, and so we can restrict our attention to a planar fluid flow around a closed, bounded subset $D \subset \mathbb{R}^2 \simeq \mathbb{C}$ representing the cross-section of our cylindrical object, as in Figure 7.28. The (complex) velocity and potential are defined on the complementary domain $\Omega = \mathbb{C} \setminus D$ occupied by the fluid. The velocity potential $\varphi(x,y)$ will satisfy the Laplace equation $\Delta\varphi = 0$ in the exterior domain Ω. For a solid object, we should impose the homogeneous Neumann boundary conditions

$$\frac{\partial \varphi}{\partial \mathbf{n}} = 0 \qquad \text{on the boundary} \qquad \partial\Omega = \partial D, \tag{7.95}$$

indicating that there is no fluid flux into the object. We note that, according to Exercise ■, a conformal map will automatically preserve the Neumann boundary conditions.

In addition, since the flow is taking place on an unbounded domain, we need to specify the fluid motion at large distances. We shall assume our object is placed in a uniform horizontal flow, e.g., a wind tunnel, as sketched in Figure 7.29. Thus, far away, the object will not affect the flow, and so the velocity should approximate the uniform velocity field $\mathbf{v} = (\,1,0\,)^T$, where, for simplicity, we choose our physical units so that the fluid moves from left to right with an asymptotic speed equal to 1. Equivalently, the velocity potential should satisfy

$$\varphi(x,y) \approx x, \qquad \text{so} \qquad \nabla\varphi \approx (\,1,0\,) \qquad \text{when} \qquad x^2+y^2 \gg 0.$$

An alternative physical interpretation is that we are located on an object that is moving horizontally to the left at unit speed through a fluid that is initially at rest. Think of an

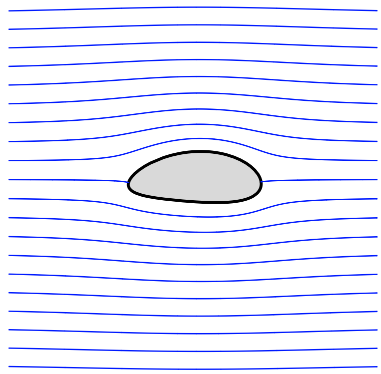

Figure 7.29. Flow Past a Solid Object.

airplane flying through the air at constant speed. If we adopt a moving coordinate system by sitting inside the airplane, then the effect is as if the plane is sitting still while the air is moving towards us at unit speed.

Example 7.40. *Horizontal plate.* The simplest example is a flat plate moving horizontally through the fluid. The plate's cross-section is a horizontal line segment, and, for simplicity, we take it to be the segment $D = [-1, 1]$ lying on the real axis. If the plate is very thin and smooth, it will have no appreciable effect on the horizontal flow of the fluid, and, indeed, the velocity potential is given by

$$\varphi(x, y) = x, \qquad \text{for} \qquad x + \mathrm{i}\, y \in \Omega = \mathbb{C} \setminus [-1, 1].$$

Note that $\nabla\varphi = (1, 0)^T$, and hence this flow satisfies the Neumann boundary conditions (7.95) on the horizontal segment $D = \partial\Omega$. The corresponding complex potential is $\chi(z) = z$, with complex velocity $f(z) = \chi'(z) = 1$.

Example 7.41. *Circular disk.* Recall, from Example 7.30, that the Joukowski conformal map

$$\zeta = g(z) = \frac{1}{2}\left(z + \frac{1}{z} \right) \tag{7.96}$$

squashes the unit circle $|z| = 1$ down to the real line segment $[-1, 1]$ in the ζ plane. Therefore, it will map the fluid flow outside a unit disk to the fluid flow past the line segment, which, according to the previous example, has complex potential $\Theta(\zeta) = \zeta$. The resulting complex potential is

$$\chi(z) = \Theta \circ g(z) = g(z) = \frac{1}{2}\left(z + \frac{1}{z} \right). \tag{7.97}$$

Except for a factor of $\frac{1}{2}$, indicating that the corresponding flow past the disk is half as fast, this agrees with the potential we derived in Example 7.17.

Example 7.42. *Tilted plate.* Let us next consider the case of a tilted plate in a uniformly horizontal fluid flow. The cross-section will be the line segment

$$z(t) = t\, e^{-\mathrm{i}\,\phi}, \qquad\qquad -1 \le t \le 1,$$

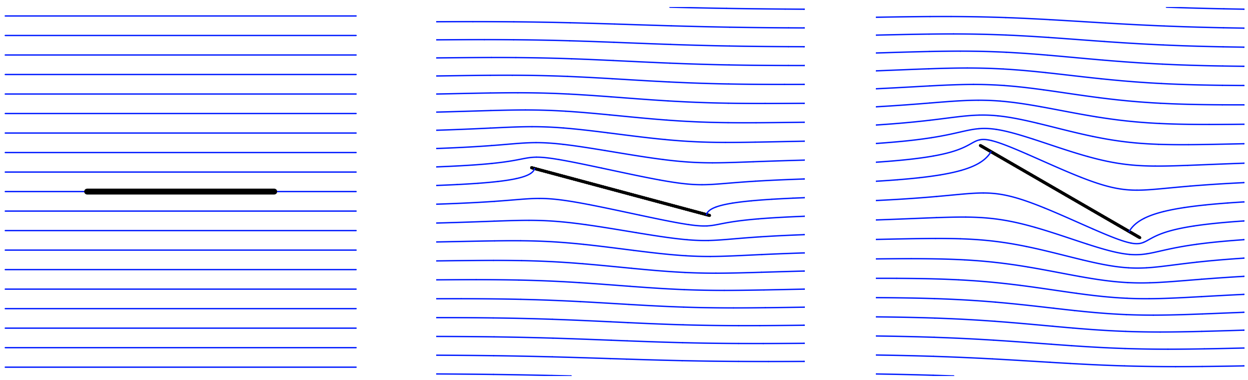

$\phi = 0°$ $\phi = 15°$ $\phi = 30°$

Figure 7.30. Fluid Flow Past a Tilted Plate.

obtained by rotating the horizontal line segment $[-1, 1]$ through an angle $-\phi$, as in Figure 7.30. The goal is to construct a fluid flow past the tilted segment that is asymptotically horizontal at large distance. As before, the air flow will be going from left to right, and so ϕ is called the *attack angle* of the plate or airfoil relative to the flow.

The key observation is that, while the effect of rotating a plate in a fluid flow is not so evident, rotating a circularly symmetric disk has no effect on in the flow around it. Thus, the rotation $w = e^{\mathrm{i}\phi} z$ through angle ϕ maps the disk potential (7.45) to the complex potential

$$\Upsilon(w) = \chi(e^{-\mathrm{i}\phi} w) = e^{-\mathrm{i}\phi} w + \frac{e^{\mathrm{i}\phi}}{w}. \tag{7.98}$$

The streamlines of the induced flow are no longer asymptotically horizontal, but rather at an angle ϕ. If we now apply the original Joukowski map (7.96) (with w replacing z) to the rotated flow, the circle is again squashed down to the horizontal line segment, but the stream lines continue to be at angle ϕ at large distances. Thus, if we then rotate the resulting flow through an angle $-\phi$, the net effect will be to tilt the segment to the desired angle while rotating the streamlines to be asymptotically horizontal. Putting the pieces together, we deduce the final complex potential to be of the form

$$\chi(z) = e^{\mathrm{i}\phi}\left(z \cos\phi - \mathrm{i} \sin\phi \sqrt{z^2 - e^{-2\mathrm{i}\phi}} \right). \tag{7.99}$$

Sample streamlines for the flow at several attack angles are plotted in Figure 7.30.

Example 7.43. *Airfoils.* As we discovered in Example 7.30, applying the Joukowski map to off-center disks will, in favorable configurations, produce airfoil-shaped objects. The fluid motion around such airfoils can thus be obtained from the flow past such an off-center circle.

First, an affine map

$$w = \alpha z + \beta$$

has the effect of moving the unit disk $|z| \le 1$ to the disk

$$|w - \beta| \le |\alpha| \tag{7.100}$$

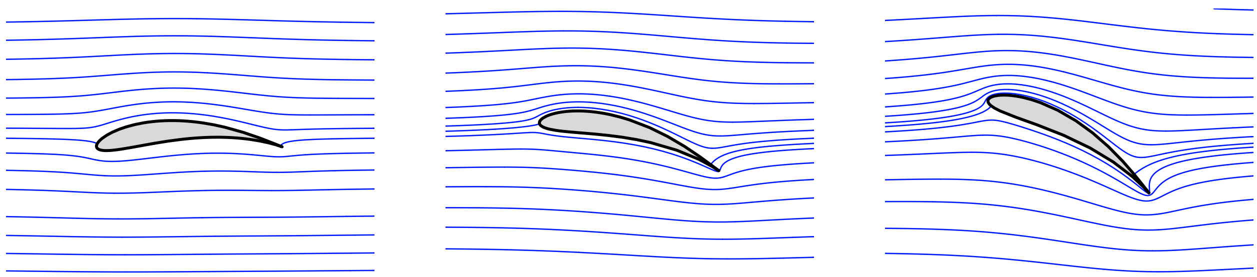

$\phi = 0°$ $\phi = 15°$ $\phi = 30°$

Figure 7.31. Flow Past a Tilted Airfoil.

with center β and radius $|\,\alpha\,|$. In particular, the boundary circle will continue to pass through the point $w = 1$ provided $|\,\alpha\,| = |\,1-\beta\,|$. Moreover, as noted in Example 7.20, the angular component of α has the effect of a rotation, and so the streamlines around the new disk will, asymptotically, be at an angle $\phi = \operatorname{ph}\alpha$ with the horizontal. We then apply the Joukowski transformation

$$\zeta = \frac{1}{2}\left(w + \frac{1}{w}\right) = \frac{1}{2}\left(\alpha\, z + \beta + \frac{1}{\alpha\, z + \beta}\right) \tag{7.101}$$

to map the disk (7.100) to the airfoil shape. The resulting complex potential for the flow past the airfoil is obtained by substituting the inverse map

$$z = \frac{w-\beta}{\alpha} = \frac{\zeta - \beta + \sqrt{\zeta^2 - 1}}{\alpha}\,,$$

into the disk potential (7.45), whereby

$$\Theta(\zeta) = \frac{\zeta - \beta + \sqrt{\zeta^2 - 1}}{\alpha} \;+\; \frac{\alpha\big(\,\zeta - \beta - \sqrt{\zeta^2 - 1}\;\big)}{\beta^2 + 1 - 2\,\beta\,\zeta}\,. \tag{7.102}$$

Finally, to make the streamlines asymptotically horizontal, we replace ζ by $e^{\,\mathrm{i}\,\phi}\zeta$ in the final formula (7.102), which produces an airfoil tilted by the attack angle ϕ to the horizontal flow. Sample streamlines for the airfoil generated by the circle centered at $-.1 + .2\,\mathrm{i}$ and passing through 1, at several attack angles, are shown in Figure 7.31.

Unfortunately, there is a major flaw with the airfoils that we have just designed. As we will discover, potential flows do not produce lift, and hence an airplane with such a wing would not fly. Fortunately, for both birds and the travel industry, physical air flow is not of this nature! In order to understand how lift enters into the picture, we need to study complex integration, and this will be the topic of the final section of this chapter.

Poisson's Equation and the Green's Function

Although designed for solving the homogeneous Laplace equation, the method of conformal mapping can also be used to solve its inhomogeneous counterpart — the Poisson equation. As we learned in Chapter 6, to solve an inhomogeneous boundary value problem it suffices to solve the problem when the right hand side is a delta function concentrated at a single point in the domain:

$$-\Delta u = \delta_\zeta(x,y) = \delta(x-\xi)\,\delta(y-\eta), \qquad\qquad \zeta = \xi + \mathrm{i}\,\eta \in \Omega,$$

subject to homogeneous boundary conditions (Dirichlet or mixed) on $\partial\Omega$. (As usual, we exclude pure Neumann boundary conditions due to lack of existence/uniqueness.) The solution

$$u(x,y) = G_\zeta(x,y) = G(x,y;\xi,\eta)$$

is the *Green's function* for the given boundary value problem. We will sometimes abbreviate it as $G(z;\zeta)$, where $z = x + \mathrm{i}\,y$, $\zeta = \xi + \mathrm{i}\,\eta$. With the Green's function in hand, the solution to the homogeneous boundary value problem under a general external forcing,

$$-\Delta u = f(x,y),$$

is then provided by the Superposition Principle

$$u(x,y) = \iint_\Omega G(x,y;\xi,\eta)\,f(\xi,\eta)\,d\xi\,d\eta. \tag{7.103}$$

For the planar Poisson equation, the important observation is that conformal mappings preserve Green's functions. Specifically:

Theorem 7.44. *Let $w = g(z)$ be a one-to-one conformal map that maps the domain Ω to the domain D, which is also continuous on the boundary: $g\colon \partial\Omega \to \partial D$. Let $\widetilde{G}(w;\omega)$ be the Green's function for the homogeneous Dirichlet boundary value problem for the Poisson equation on D. Then $G(z;\zeta) = \widetilde{G}\big(\,g(z);g(\zeta)\,\big)$ is the corresponding Green's function on Ω.*

Proof: Fixing $\omega = \varphi + \mathrm{i}\,\psi$, we are given that $H(u,v) = \widetilde{G}(w;\omega)$, with $w = u + \mathrm{i}\,v$, solves

$$-\widetilde{\Delta} H(u,v) = \delta_\omega(u,v) = \delta(u-\varphi, v-\psi),$$

where we use $\widetilde{\Delta}$ to denote the Laplacian in the u,v variables, along with the homogeneous Dirichlet boundary conditions on ∂D. We now apply the change of variables $u = p(x,y)$, $v = q(x,y)$, provided by the real and imaginary parts of our conformal map. According to (7.83), the function $h(x,y) = H\big(p(x,y),q(x,y)\big)$ satisfies

$$\Delta h(x,y) = \left[\left(\frac{\partial p}{\partial x}\right)^2 + \left(\frac{\partial q}{\partial x}\right)^2\right]\,\widetilde{\Delta} H\big(p(x,y),q(x,y)\big).$$

On the other hand, at $\omega = g(\zeta)$ with $\zeta = \xi + \mathrm{i}\,\eta$, formula (delta2tr) implies that

$$\delta_\omega\big(p(x,y),q(x,y)\big) = \frac{\delta_\zeta(x,y)}{|\,J(\xi,\eta)\,|}$$

where $J(x,y)$ is the Jacobian determinant of the transformation, namely

$$J(x,y) = \frac{\partial p}{\partial x}\,\frac{\partial q}{\partial y} - \frac{\partial p}{\partial y}\,\frac{\partial q}{\partial x} = \left(\frac{\partial p}{\partial x}\right)^2 + \left(\frac{\partial q}{\partial x}\right)^2,$$

where the second expression follows from the Cauchy–Riemann equations (7.18) for the analytic function $g(z)$. Combining the preceding four formulas, we conclude that

$$-\Delta h = \frac{p_x(x,y)^2 + q_x(x,y)^2}{p_x(\xi,\eta)^2 + q_x(\xi,\eta)^2}\, \delta_\zeta(x,y) = \delta_\zeta(x,y),$$

since the delta function vanishes except when $(x,y) = (\xi,\eta)$, at which point the numerator and denominator in the fraction coincide. Thus, the Laplacian of the transformed function has the correct delta function singularity at the point $\zeta = \xi + \mathrm{i}\,\eta$. The fact that $h(x,y)$ also satisfies homogeneous Dirichlet boundary conditions on $\partial\Omega$ is immediate. *Q.E.D.*

Remark: Exercise ■ implies that Theorem 7.44 also applies to the mixed boundary value problem, provided the conformal map is C^1 on the Neumann part of the boundary.

Now, we know, from Section 6.3, that the logarithmic potential function

$$U(u,v) = \mathrm{Re}\left(-\frac{1}{2\pi}\log w\right) = -\frac{1}{2\pi}\log|\,w\,| = -\frac{1}{4\pi}\log\,(u^2+v^2), \tag{7.104}$$

solves the Dirichlet problem

$$-\widetilde{\Delta} U = \delta(u,v), \qquad (u,v) \in D, \qquad\qquad U = 0 \quad \text{on} \quad \partial D,$$

on the unit disk D for a delta impulse concentrated at the origin. According to Example 7.25, the linear fractional transformation

$$w = g(z) = \frac{z-\zeta}{\overline{\zeta}\,z - 1}\,, \qquad \text{where} \qquad |\,\zeta\,| < 1, \tag{7.105}$$

maps the unit disk to itself, moving the point $z = \zeta$ to the origin $w = g(\zeta) = 0$. The proof of Theorem 7.44 then implies that the transformed function $u(x,y)$ will satisfy

$$-\Delta u = \delta_\zeta(x,y), \qquad (x,y) \in D, \qquad\qquad u = 0 \quad \text{on} \quad \partial D,$$

and hence defines the Green's function at the point $\zeta = \xi + \mathrm{i}\,\eta$. We conclude that

$$G(z;\zeta) = \frac{1}{2\pi}\,\log\left|\,\frac{\overline{\zeta}\,z - 1}{z-\zeta}\,\right| \tag{7.106}$$

is the Green's function for the Dirichlet boundary value problem on the unit disk, which reproduces the Poisson formula (6.131) for the Green's function that we previously derived by the method of images. This identification can be verified by substituting $z = r\,e^{\mathrm{i}\,\theta}$, $\zeta = \rho\,e^{\mathrm{i}\,\phi}$, or, more simply, by noting that the denominator in the logarithmic fraction gives the potential due to a unit impulse at $z = \zeta$, while the numerator represents the image potential at $z = 1/\overline{\zeta}$ required to cancel out the effect of the interior potential on the boundary of the unit disk.

Now that we know the Green's function on the unit disk, we can use the Riemann Mapping Theorem 7.33 and Theorem 7.44 to produce the Green's function for any other simply connected domain $\Omega \subsetneq \mathbb{C}$.

Corollary 7.45. *Let $w = g(z)$ denote a conformal map that takes the simply connected domain $z \in \Omega$ to the unit disk $w \in D$. Then the Green's function for the homogeneous Dirichlet boundary problem for the Poisson equation on Ω is explicitly given by*

$$G(z;\zeta) = \frac{1}{2\pi} \log \left| \frac{\overline{g(\zeta)}\, g(z) - 1}{g(z) - g(\zeta)} \right|. \tag{7.107}$$

Example 7.46. According to Example 7.24, the analytic function

$$w = \frac{z-1}{z+1}$$

maps the right half plane $x = \operatorname{Re} z > 0$ to the unit disk $|\,\zeta\,| < 1$. Therefore, by (7.107), the Green's function for the right half plane has the form

$$G(z;\zeta) = \frac{1}{2\pi} \log \left| \frac{\dfrac{\overline{\zeta}-1}{\overline{\zeta}+1}\;\dfrac{z-1}{z+1} - 1}{\dfrac{z-1}{z+1} - \dfrac{\zeta-1}{\zeta+1}} \right| = \frac{1}{2\pi} \log \left| \frac{(\zeta+1)\,(z+\overline{\zeta}\,)}{(\overline{\zeta}+1)\,(z-\zeta)} \right|. \tag{7.108}$$

One can then write an integral formula for the solution to the Poisson equation on the right half plane in the form of a superposition as in (7.103).

7.6. Complex Integration.

The magic and power of calculus ultimately rests on the amazing fact that differentiation and integration are mutually inverse operations. And, just as complex functions enjoy remarkable differentiability properties not shared by their real counterparts, so the sublime beauty of complex integration goes far beyond its more mundane real progenitor.

Lets begin by motivating the definition of the complex integral. As you know, the (definite) integral of a real function, $\displaystyle\int_a^b f(t)\,dt$, is evaluated on an interval $[\,a,b\,] \subset \mathbb{R}$. In complex function theory, integrals are taken along curves in the complex plane, and are akin to the line integrals appearing in real vector calculus. Indeed, the identification of a complex number $z = x + \mathrm{i}\,y$ with a planar vector $\mathbf{x} = (\,x, y\,)^T$ will serve to connect the two theories.

Consider a curve C in the complex plane, parametrized by $z(t) = x(t) + \mathrm{i}\,y(t)$ for $a \le t \le b$. We define the *integral* of the complex function $f(z)$ along C to be the complex number

$$\int_C f(z)\,dz = \int_a^b f(z(t))\,\frac{dz}{dt}\,dt, \tag{7.109}$$

the right hand side being an ordinary real integral of a complex-valued function. We shall always assume that the integrand $f(z)$ is a well-defined complex function at each point on the curve, and hence the integral is well-defined. Let us write out the integrand

$$f(z) = u(x,y) + \mathrm{i}\,v(x,y)$$

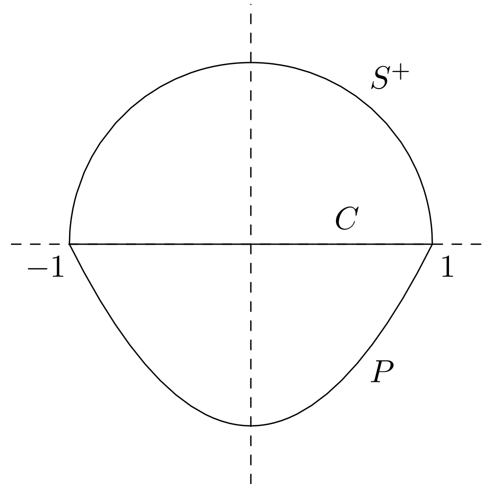

Figure 7.32. Curves for Complex Integration.

in terms of its real and imaginary parts, as well as the differential

$$dz = \frac{dz}{dt}\, dt = \left(\frac{dx}{dt} + \mathrm{i}\, \frac{dy}{dt} \right) dt = dx + \mathrm{i}\, dy.$$

As a result, the complex integral (7.109) splits up into a pair of real line integrals:

$$\int_C f(z)\, dz = \int_C (u + \mathrm{i}\, v)(dx + \mathrm{i}\ dy) = \int_C (u\, dx - v\, dy) + \mathrm{i} \int_C (v\, dx + u\, dy). \qquad (7.110)$$

Example 7.47. Suppose n is an integer. Let us compute complex integrals

$$\int_C z^n\, dz \qquad (7.111)$$

of the monomial function $f(z) = z^n$ along several different curves. We begin with a straight line segment I along the real axis connecting the points -1 and 1, which we parametrize by $z(t) = t$ for $-1 \le t \le 1$. The defining formula (7.109) implies that the complex integral (7.111) reduces to an elementary real integral:

$$\int_I z^n\, dz = \int_{-1}^{1} t^n\, dt = \begin{cases} 0, & 0 < n = 2k+1 \ \text{ odd}, \\ \dfrac{2}{n+1}, & 0 \le n = 2k \ \text{ even}. \end{cases}$$

If $n \le -1$ is negative, then the singularity of the integrand at the origin implies that the integral diverges, and so the complex integral is not defined.

Let us evaluate the same complex integral, but now along a parabolic arc P parametrized by

$$z(t) = t + \mathrm{i}\,(t^2 - 1), \qquad -1 \le t \le 1.$$

Note that, as we see in Figure 7.32, the parabola connects the same two points in $\mathbb{C}$. We again refer back to the basic definition (7.109) to evaluate the integral, so

$$\int_P z^n\, dz = \int_{-1}^{1} \left[\, t + \mathrm{i}\,(t^2 - 1)\,\right]^n (1 + 2\,\mathrm{i}\, t)\, dt.$$

We could, at this point, expand the resulting complex polynomial integrand, and then integrate term by term. A more elegant approach is to recognize that it is an exact derivative:

$$\frac{d}{dt}\,\frac{\bigl[\,t+\mathrm{i}\,(t^2-1)\,\bigr]^{n+1}}{n+1}=\bigl[\,t+\mathrm{i}\,(t^2-1)\,\bigr]^{n}(1+2\,\mathrm{i}\,t),$$

as long as $n\neq -1$. Therefore, we can use the Fundamental Theorem of Calculus (which works equally well for real integrals of complex-valued functions), to evaluate

$$\int_P z^n\,dz=\left.\frac{\bigl[\,t+\mathrm{i}\,(t^2-1)\,\bigr]^{n+1}}{n+1}\,\right|_{t=-1}^{1}=\begin{cases}0, & -1\neq n=2\,k+1\ \ \text{odd},\\[4pt] \dfrac{2}{n+1}, & n=2\,k\ \ \text{even}.\end{cases}$$

Thus, when $n\geq 0$ is a positive integer, we obtain the same result as before. Interestingly, in this case the complex integral is well-defined even when n is a negative integer because, unlike the real line segment, the parabolic path does *not* go through the singularity of z^n at $z=0$. The case $n=-1$ needs to be done slightly differently, and integration of $1/z$ along the parabolic path is left as an exercise for the reader — one that requires some care. We recommend trying the exercise now, and then verifying your answer once we have become a little more familiar with basic complex integration techniques.

Finally, let us try integrating around a semi-circular arc, again with the same endpoints -1 and 1. If we parametrize the semi-circle S^+ by $z(t)=e^{\,\mathrm{i}\,t}$, $0\leq t\leq\pi$, we find

$$\begin{aligned}\int_{S^+} z^n\,dz&=\int_0^\pi z^n\,\frac{dz}{dt}\,dt=\int_0^\pi e^{\,\mathrm{i}\,nt}\ \mathrm{i}\,e^{\,\mathrm{i}\,t}\,dt=\int_0^\pi\ \mathrm{i}\,e^{\,\mathrm{i}\,(n+1)t}\,dt\\&=\left.\frac{e^{\,\mathrm{i}\,(n+1)t}}{n+1}\ \right|_{t=0}^{\pi}=\frac{1-e^{\,\mathrm{i}\,(n+1)\pi}}{n+1}=\begin{cases}0, & -1\neq n=2\,k+1\ \ \text{odd},\\[4pt] -\,\dfrac{2}{n+1}\,, & n=2\,k\ \ \text{even}.\end{cases}\end{aligned}$$

This value is the negative of the previous cases — but this can be explained by the fact that the circular arc is oriented to go *from* 1 *to* -1 whereas the line segment and parabola both go *from* -1 *to* 1. Just as with line integrals, the direction of the curve determines the sign of the complex integral; if we reverse direction, replacing t by $-t$, we end up with the same value as the preceding two complex integrals. Moreover — again provided $n\neq -1$ — it does not matter whether we use the upper semicircle or lower semicircle to go from -1 to 1 — the result is exactly the same. However, the case $n=-1$ is an exception to this "rule". Integrating along the upper semicircle S^+ from 1 to -1 yields

$$\int_{S^+}\frac{dz}{z}=\int_0^\pi\ \mathrm{i}\ dt=\pi\,\mathrm{i}\,, \tag{7.112}$$

whereas integrating along the lower semicircle S^- from 1 to -1 yields the negative

$$\int_{S^-}\frac{dz}{z}=\int_0^{-\pi}\ \mathrm{i}\ dt=-\,\pi\,\mathrm{i}\,. \tag{7.113}$$

Hence, when integrating the function $1/z$, it makes a difference which direction we go around the origin.

Integrating z^n for any integer $n \neq -1$ around an entire circle gives zero — irrespective of the radius. This can be seen as follows. We parametrize a circle of radius r by $z(t) = r e^{\,\mathrm{i}\, t}$ for $0 \leq t \leq 2\pi$. Then, by the same computation,

$$\oint_C z^n \, dz = \int_0^{2\pi} (r^n e^{\,\mathrm{i}\, nt})(r\,\mathrm{i}\, e^{\,\mathrm{i}\, t})\, dt = \int_0^{2\pi} \mathrm{i}\, r^{n+1} e^{\,\mathrm{i}\,(n+1)t}\, dt = \frac{r^{n+1}}{n+1}\, e^{\,\mathrm{i}\,(n+1)t} \,\Big|_{t=0}^{2\pi} = 0, \tag{7.114}$$

provided $n \neq -1$. The circle on the integral sign serves to remind us that we are integrating around a closed curve. The case $n = -1$ remains special. Integrating once around the circle in the counter-clockwise direction yields a nonzero result

$$\oint_C \frac{dz}{z} = \int_0^{2\pi} \mathrm{i}\; dt = 2\pi\,\mathrm{i}\,. \tag{7.115}$$

Let us note that a complex integral does not depend on the particular parametrization of the curve C. It does, however, depend upon its orientation: if we traverse the curve in the reverse direction, then the complex integral changes its sign:

$$\int_{-C} f(z)\, dz = - \int_C f(z)\, dz. \tag{7.116}$$

Moreover, if we chop up the curve into two non-overlapping pieces, $C = C_1 \cup C_2$, with a common orientation, then the complex integral can be decomposed into a sum over the pieces:

$$\int_{C_1 \cup C_2} f(z) = \int_{C_1} f(z)\, dz \; + \int_{C_2} f(z)\, dz. \tag{7.117}$$

For instance, the integral (7.115) of $1/z$ around the circle is the difference of the individual semicircular integrals (7.112, 113); the lower semicircular integral acquires a negative sign to flip its orientation so as to agree with that of the entire circle. All these facts are immediate consequences of the well-known properties of line integrals, or can be proved directly from the defining formula (7.109).

Note: In complex integration theory, a simple closed curve is often referred to as a *contour*, and so complex integration is sometimes referred to as *contour integration*. Unless explicitly stated otherwise, we always go around contours in the *counter-clockwise* direction.

Further experiments lead us to suspect that complex integrals are usually path-independent, and hence evaluate to zero around closed curves. One must be careful, though, as the integral (7.115) makes clear. Path independence, in fact, follows from the complex version of the Fundamental Theorem of Calculus.

Theorem 7.48. *Let $f(z) = F'(z)$ be the derivative of a single-valued complex function $F(z)$ defined on a domain $\Omega \subset \mathbb{C}$. Let $C \subset \Omega$ be any curve with initial point α and final point β. Then*

$$\int_C f(z)\, dz = \int_C F'(z)\, dz = F(\beta) - F(\alpha). \tag{7.118}$$

Proof: This follows immediately from the definition (7.109) and the chain rule:

$$\int_C F'(z)\,dz = \int_a^b F'(z(t))\,\frac{dz}{dt}\,dt = \int_a^b \frac{d}{dt}\,F(z(t))\,dt = F(z(b)) - F(z(a)) = F(\beta) - F(\alpha),$$

where $\alpha = z(a)$ and $\beta = z(b)$ are the endpoints of the curve. *Q.E.D.*

For example, when $n \neq -1$, the function $f(z) = z^n$ is the derivative of the single-valued function $F(z) = \dfrac{1}{n+1}\,z^{n+1}$. Hence

$$\int_C z^n\,dz \;=\; \frac{\beta^{n+1}}{n+1} \;-\; \frac{\alpha^{n+1}}{n+1}$$

whenever C is (almost) any curve connecting α to β. The only restriction is that, when $n < 0$, the curve is not allowed to pass through the singularity at the origin $z = 0$.

In contrast, the function $f(z) = 1/z$ is the derivative of the complex logarithm

$$\log z = \log |\, z\,| + \mathrm{i}\;\,\mathrm{ph}\,z,$$

which is *not* single-valued on all of $\mathbb{C} \setminus \{0\}$, and so Theorem 7.48 cannot be applied directly. However, if our curve is contained within a simply connected subdomain that does not include the origin, $0 \notin \Omega \subset \mathbb{C}$, then we can use *any* single-valued branch of the complex logarithm to evaluate the integral

$$\int_C \frac{dz}{z} = \log\beta - \log\alpha,$$

where α, β are the endpoints of the curve. Since the common multiples of $2\pi\,\mathrm{i}$ cancel, the answer does not depend upon which particular branch of the complex logarithm is selected as long as we are consistent in our choice. For example, on the upper semicircle S^+ of radius 1 going from 1 to -1,

$$\int_{S^+} \frac{dz}{z} = \log(-1) - \log 1 = \pi\,\mathrm{i}\,,$$

where we use the branch of $\log z = \log|\,z\,| + \mathrm{i}\;\mathrm{ph}\,z$ with $0 \leq \mathrm{ph}\,z \leq \pi$. On the other hand, if we integrate on the lower semi-circle S^- going from 1 to -1, we need to adopt a different branch, say that with $-\pi \leq \mathrm{ph}\,z \leq 0$. With this choice, the integral becomes

$$\int_{S^-} \frac{dz}{z} = \log(-1) - \log 1 = -\,\pi\,\mathrm{i}\,,$$

thus reproducing $(7.112, 113)$. Pay particular attention to the different values of $\log(-1)$ used in the two cases!

Cauchy's Theorem

The preceding considerations suggest the following fundamental theorem, due in its general form to Cauchy. Before stating it, we introduce the convention that a complex function $f(z)$ is to be deemed *analytic on a domain* $\Omega \subset \mathbb{C}$ provided it is analytic at every

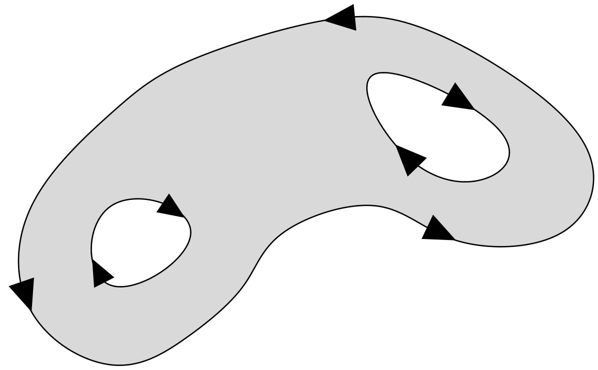

Figure 7.33. Orientation of Domain Boundary.

point inside Ω and, in addition, remains (at least) continuous on the boundary $\partial\Omega$. When Ω is bounded, its boundary $\partial\Omega$ consists of one or more simple closed curves. In general, as in Green's Theorem 6.13, we orient $\partial\Omega$ so that the domain is always on our left hand side. This means that the outermost boundary curve is traversed in the counter-clockwise direction, but those around interior holes take on a clockwise orientation. Our convention is depicted in Figure 7.33.

Theorem 7.49. *If $f(z)$ is analytic on a bounded domain $\Omega \subset \mathbb{C}$, then*

$$\oint_{\partial\Omega} f(z)\,dz = 0. \tag{7.119}$$

Proof: Application of Green's Theorem to the two real line integrals in (7.110) yields

$$\oint_{\partial\Omega} u\,dx - v\,dy = \iint_\Omega \left(-\frac{\partial v}{\partial x} - \frac{\partial u}{\partial y} \right) = 0, \qquad \oint_{\partial\Omega} v\,dx + u\,dy = \iint_\Omega \left(\frac{\partial u}{\partial x} - \frac{\partial v}{\partial y} \right) = 0,$$

both of which vanish by virtue of the Cauchy–Riemann equations (7.18). *Q.E.D.*

If the domain of definition of our complex function $f(z)$ is simply connected, then, by definition, the interior of any closed curve $C \subset \Omega$ is contained in Ω, and hence Cauchy's Theorem 7.49 implies path independence of the complex integral within Ω.

Corollary 7.50. *If $f(z)$ is analytic on a simply connected domain $\Omega \subset \mathbb{C}$, then its complex integral $\displaystyle\int_C f(z)\,dz$ for $C \subset \Omega$ is independent of path. In particular,*

$$\oint_C f(z)\,dz = 0 \tag{7.120}$$

for any closed curve $C \subset \Omega$.

Remark: Simple connectivity of the domain is an essential hypothesis — our evaluation (7.115) of the integral of $1/z$ around the unit circle provides a simple counterexample to (7.120) for the non-simply connected domain $\Omega = \mathbb{C} \setminus \{0\}$. Interestingly, this result also admits a converse: a continuous complex-valued function that satisfies (7.120) for *all* closed curves is necessarily analytic; see [**4**] for a proof.

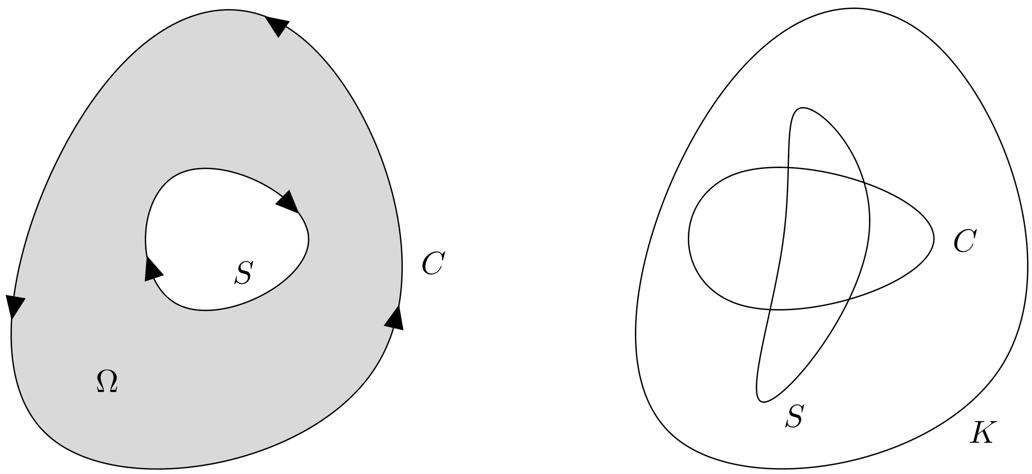

Figure 7.34. Integration Around Two Closed Curves.

We will also require a slight generalization of this result.

Proposition 7.51. *If $f(z)$ is analytic in a domain that contains two simple closed curves S and C, and the entire region lying between them, then, assuming they are oriented in the same direction,*

$$\oint_C f(z)\,dz = \oint_S f(z)\,dz. \tag{7.121}$$

Proof: If C and S do not cross each other, we let Ω denote the domain contained between them, so that $\partial\Omega = C \cup S$; see the first plot in Figure 7.34. According to Cauchy's Theorem 7.49, $\displaystyle\oint_{\partial\Omega} f(z) = 0$. Now, our orientation convention for $\partial\Omega$ means that the outer curve, say C, is traversed in the counter-clockwise direction, while the inner curve S assumes the opposite, clockwise orientation. Therefore, if we assign both curves the same counter-clockwise orientation,

$$0 = \oint_{\partial\Omega} f(z) = \oint_C f(z)\,dz - \oint_S f(z)\,dz,$$

proving (7.121).

If the two curves cross, we can construct a nearby curve $K \subset \Omega$ that neither crosses, as in the second sketch in Figure 7.34. By the preceding paragraph, each integral is equal to that over the third curve,

$$\oint_C f(z)\,dz = \oint_K f(z)\,dz = \oint_S f(z)\,dz,$$

and formula (7.121) remains valid. *Q.E.D.*

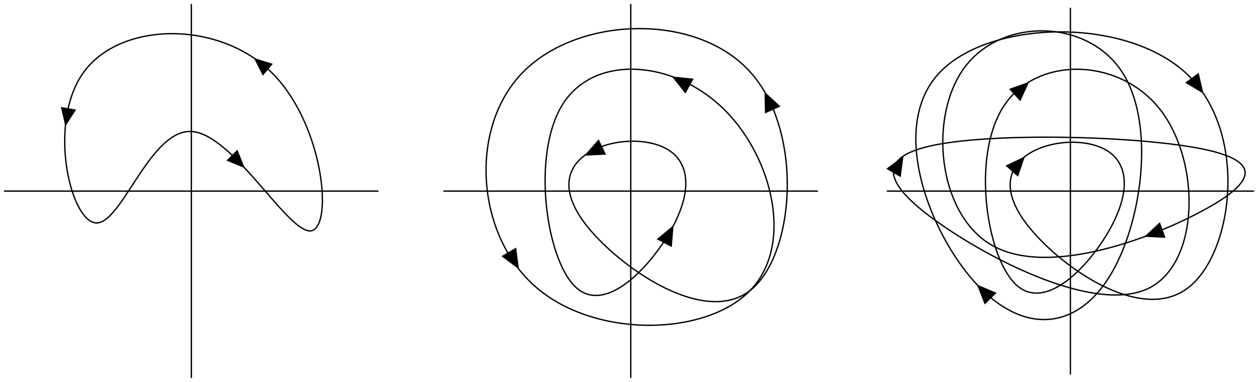

Figure 7.35. Winding Numbers.

Example 7.52. Consider the function $f(z) = z^n$ where n is an integer[†]. In (7.114), we already computed

$$\oint_C z^n \, dz = \begin{cases} 0, & n \neq -1, \\ 2\pi \,\mathrm{i}\,, & n = -1, \end{cases} \tag{7.122}$$

when C is a circle centered at $z = 0$. When $n \geq 0$, Theorem 7.48 immediately implies that the integral of z^n is 0 over *any* closed curve in the plane. The same applies in the cases $n \leq -2$ provided the curve does not pass through the singular point $z = 0$. In particular, the integral is zero around closed curves encircling the origin, even though z^n for $n \leq -2$ has a singularity inside the curve and so Cauchy's Theorem 7.49 does not apply as stated.

The case $n = -1$ has particular significance. Here, Proposition 7.51 implies that the integral is the same as the integral around a circle — provided the curve C also goes once around the origin in a counter-clockwise direction. Thus (7.115) holds for any closed curve that goes counter-clockwise once around the origin. More generally, if the curve goes several times around the origin[‡], then

$$\oint_C \frac{dz}{z} = 2\,k\,\pi\,\mathrm{i} \tag{7.123}$$

is an integer multiple of $2\pi\,\mathrm{i}$. The integer k is called the *winding number* of the curve C, and measures the total number of times C goes around the origin. For instance, if C winds three times around 0 in a counter-clockwise fashion, then $k = 3$, while $k = -5$ indicates that the curve winds 5 times around 0 in a clockwise direction, as in Figure 7.35. In particular, a winding number $k = 0$ indicates that C is not wrapped around the origin. If C represents a loop of string wrapped around a pole (the *pole* of $1/z$ at 0) then a winding number $k = 0$ would indicate that the string can be disentangled from the pole without cutting; nonzero winding numbers would indicate that the string is truly entangled[§].

[†] When n is fractional or irrational, the integrals are not well-defined owing to the multi-valued branch point at the origin.

[‡] Such a curve is undoubtedly not simple and must necessarily cross over itself.

[§] Actually, there are more subtle three-dimensional considerations that come into play, and

Lemma 7.53. *If C is a simple closed curve, and a is any point not lying on C, then*

$$\oint_C \frac{dz}{z-a} = \begin{cases} 2\pi\,\mathrm{i}, & a \ \textit{inside}\ C \\ 0, & a \ \textit{outside}\ C. \end{cases} \tag{7.124}$$

If $a \in C$, then the integral does not converge.

Proof: Note that the integrand $f(z) = 1/(z-a)$ is analytic everywhere except at $z = a$, where it has a simple pole. If a is outside C, then Cauchy's Theorem 7.49 applies, and the integral is zero. On the other hand, if a is inside C, then Proposition 7.51 implies that the integral is equal to the integral around a circle centered at $z = a$. The latter integral can be computed directly by using the parametrization $z(t) = a + r\,e^{\mathrm{i}\,t}$ for $0 \le t \le 2\pi$, as in (7.115). *Q.E.D.*

Example 7.54. Let $D \subset \mathbb{C}$ be a closed and *connected* domain. Let $a, b \in D$ be two points in D. Then

$$\oint_C \left(\frac{1}{z-a} - \frac{1}{z-b} \right) dz = \oint_C \frac{dz}{z-a} - \oint_C \frac{dz}{z-b} = 0$$

for any closed curve $C \subset \Omega = \mathbb{C} \setminus D$ lying outside the domain D. This is because, by connectivity of D, either C contains both points in its interior, in which case both integrals equal $2\pi\,\mathrm{i}$, or C contains neither point, in which case both integrals are 0. The conclusion is that, while the individual logarithms are multiply-valued, their difference

$$F(z) = \log(z-a) - \log(z-b) = \log \frac{z-a}{z-b} \tag{7.125}$$

is a consistent, single-valued complex function on all of $\Omega = \mathbb{C} \setminus D$. The function (7.125) has, in fact, an infinite number of possible values, differing by integer multiples of $2\pi\,\mathrm{i}$; the ambiguity can be resolved by choosing one of its values at a single point in Ω. These conclusions rest on the fact that D is connected, and are *not* valid, say, for the twice-punctured plane $\mathbb{C} \setminus \{a, b\}$.

Circulation and Lift

In fluid mechanical applications, the complex integral can be assigned an important physical interpretation. As above, we consider the steady state flow of an incompressible, irrotational fluid. Let $f(z) = u(x,y) - \mathrm{i}\,v(x,y)$ denote the complex velocity corresponding to the real velocity vector $\mathbf{v} = (\,u(x,y), v(x,y)\,)^T$ at the point $(x,y)^T$.

As we noted in (7.110), the integral of the complex velocity $f(z)$ along a curve C can be written as a pair of real line integrals:

$$\int_C f(z)\,dz = \int_C (u - \mathrm{i}\,v)(dx + \mathrm{i}\ dy) = \int_C (u\,dx + v\,dy) - \mathrm{i} \int_C (v\,dx - u\,dy). \tag{7.126}$$

---

even strings with zero winding number cannot be removed from the pole without cutting if they are knotted in some nontrivial manner. Can you think of an example?

The real part is the *circulation integral*

$$\int_C \mathbf{v} \cdot d\mathbf{x} = \int_C u\,dx + v\,dy, \tag{7.127}$$

while the imaginary part is minus the *flux integral*

$$\int_C \mathbf{v} \cdot \mathbf{n}\; ds = \int_C \mathbf{v} \times d\mathbf{x} = \int_C v\,dx - u\,dy. \tag{7.128}$$

If the complex velocity admits a single-valued complex potential

$$\chi(z) = \varphi(z) - \mathrm{i}\,\psi(z), \qquad \text{where} \qquad \chi'(z) = f(z),$$

which is always the case if its domain of definition is simply connected, then the complex integral is independent of path, and one can use the Fundamental Theorem 7.48 to evaluate it:

$$\int_C f(z)\,dz = \chi(\beta) - \chi(\alpha) \tag{7.129}$$

for any curve C connecting α to β. Path independence of the complex integral reconfirms the path independence of the circulation and flux integrals for ideal fluid flow. The real part of formula (7.129) evaluates the circulation integral

$$\int_C \mathbf{v} \cdot d\mathbf{x} = \int_C \nabla\varphi \cdot d\mathbf{x} = \varphi(\beta) - \varphi(\alpha), \tag{7.130}$$

as the difference in the values of the (real) potential at the endpoints α, β of the curve C. On the other hand, the imaginary part of formula (7.129) computes the flux integral

$$\int_C \mathbf{v} \times d\mathbf{x} = \int_C \nabla\psi \cdot d\mathbf{x} = \psi(\beta) - \psi(\alpha), \tag{7.131}$$

as the difference in the values of the stream function at the endpoints of the curve. The stream function acts as a "flux potential" for the flow. Thus, for ideal flows, the fluid flux through a curve depends only upon its endpoints. In particular, if C is a closed contour, and $\chi(z)$ is analytic on its interior, then

$$\oint_C \mathbf{v} \cdot d\mathbf{x} \;=\; 0 \;=\; \oint_C \mathbf{v} \times d\mathbf{x}, \tag{7.132}$$

and so there is no net circulation or flux along any closed curve in this scenario.

Typically, lift on a body requires a nonzero circulation around it. (The precise relation is spelled out by Blasius' Theorem, the subject of Exercise ■.) Let $D \subset \mathbb{C}$ be a bounded, simply connected domain representing the cross-section of a cylindrical body, e.g., an airplane wing. The velocity vector field $\mathbf{v}$ of a steady state flow around the exterior of the body is defined on the domain $\Omega = \mathbb{C} \setminus \overline{D}$. The no flux boundary conditions $\mathbf{v} \cdot \mathbf{n} = 0$ on $\partial\Omega = \partial D$ indicate that there is no fluid flowing across the boundary of the solid body. The resulting circulation of the fluid around the body is given by the integral $\displaystyle\oint_C \mathbf{v} \cdot d\mathbf{x}$,

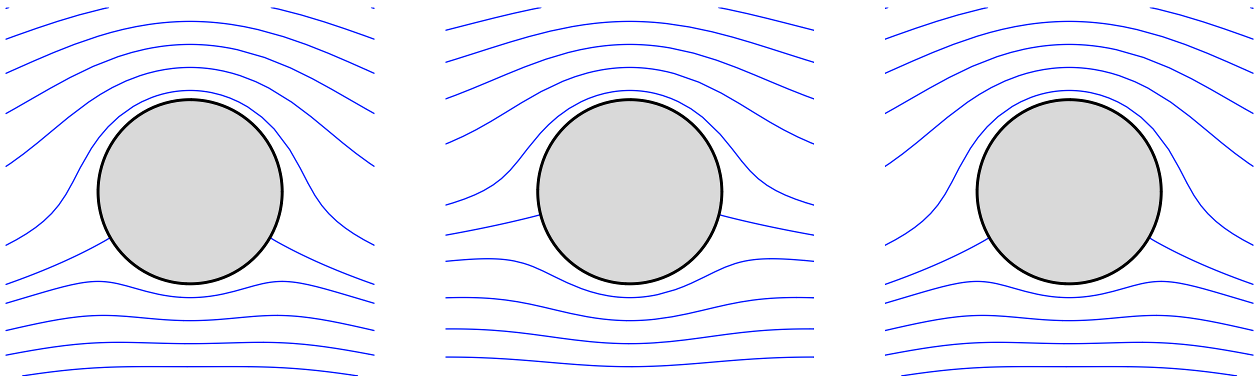

$\gamma = .25$ $\gamma = .5$ $\gamma = .75$

Figure 7.36. Flow with Lift Around a Circle.

where $C \subset \Omega$ is any simple closed contour encircling the body. (Cauchy's theorem, in the form of Proposition 7.51, tells us that the value does not depend upon the choice of contour.) However, if the corresponding complex velocity $f(z)$ admits a single-valued complex potential in Ω, then (7.132) tells us that the circulation integral is automatically zero, and so the body will not experience any lift!

Consider first the flow around a disk, as discussed in Examples 7.17 and 7.41. The disk potential (7.45) is a single-valued analytic function everywhere except at the origin $z = 0$. Therefore, the circulation integral (7.130) around any contour encircling the disk will vanish, and hence the disk experiences no net lift. This is more or less evident from Figure 7.12; the streamlines of the flow are symmetric above and below the disk, and hence there cannot be any net force in the vertical direction.

Any conformal map will maintain single-valuedness of the complex potentials, and hence preserve the zero-circulation property. In particular, all the flows past airfoils constructed in Example 7.43 also admit single-valued potentials, and so also have zero circulation integral. Such an airplane will not fly, because its wings have no lift. Of course, physical airplanes do fly, and so there must be some physical assumption we are neglecting in our treatment of flow past a body. Abandoning incompressibility or irrotationality would banish us from the paradise of complex variable theory to the vastly more complicated world inhabited by the fully nonlinear partial differential equations of fluid mechanics. Moreover, although air is slightly compressible, water is, for all practical purposes, incompressible, and, as we know, hydrofoils do experience lift when traveling through water.

The only way to introduce lift into the picture is through a (single-valued) complex velocity with a non-zero circulation integral, and this requires that its complex potential be multiply-valued. The one function that we know that has such a property is the complex logarithm

$$\lambda(z) = \log(a\,z+b), \qquad \text{whose derivative} \qquad \lambda'(z) = \frac{a}{a\,z+b}$$

is single-valued away from the singularity at $z = -\,b/a$. Thus, we are naturally led to

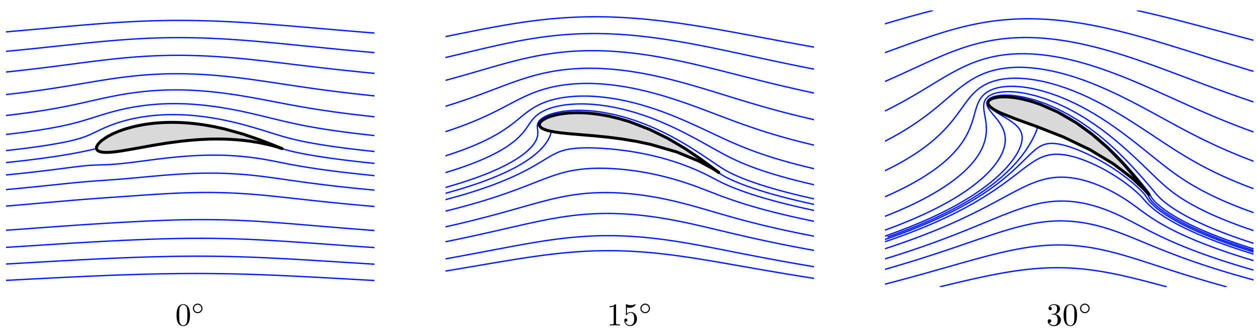

Figure 7.37. Kutta Flow Past a Tilted Airfoil.

introduce the family of complex potentials

$$\chi_\gamma(z) = z + \frac{1}{z} + \mathrm{i}\,\gamma \log z. \tag{7.133}$$

According to Exercise ■, the coefficient γ must be real in order to maintain the no flux boundary conditions on the unit circle. By (7.126), the circulation is equal to the real part of the integral of the complex velocity

$$f_\gamma(z) = \frac{d\chi_\gamma}{dz} = 1 - \frac{1}{z^2} + \frac{\mathrm{i}\,\gamma}{z}\,, \tag{7.134}$$

which remains asymptotically 1 at large distances. By Cauchy's Theorem 7.49 coupled with formula (7.124), if C is a curve going once around the disk in a counter-clockwise direction, then

$$\oint_C f_\gamma(z)\,dz = \oint_C \left(1 - \frac{1}{z^2} + \frac{\mathrm{i}\,\gamma}{z}\right) dz = -2\pi\gamma.$$

Therefore, when $\gamma \neq 0$, the circulation integral is non-zero, and the cylinder experiences a net lift. In Figure 7.36, the streamlines for the flow corresponding to a few representative values of γ are plotted. The asymmetry of the streamlines accounts for the lift experienced by the disk. In particular, assuming $|\,\gamma\,| \leq 2$, the stagnation points have moved from ± 1 to $\pm\sqrt{1 - \frac{1}{4}\gamma^2} - \frac{1}{2}\,\mathrm{i}\,\gamma$.

When we compose the modified potentials (7.133) with the Joukowski transformation (7.101), we obtain a complex potential for flow around the corresponding airfoil — the image of the unit disk. The conformal mapping does not affect the value of the complex integrals, and hence, for any $\gamma \neq 0$, there is a nonzero circulation around the airfoil under the modified fluid flow, and at last our airplane will fly!

However, we now have a slight embarrassment of riches, having designed flows around the airfoil with an *arbitrary* value $-2\pi\gamma$ for the circulation integral, and hence an arbitrary amount of lift! Which of these possible flows most closely realizes the true physical version? In his 1902 thesis, the German mathematician Martin Kutta hypothesized that Nature chooses the constant γ so as to keep the velocity of the flow at the trailing edge of the airfoil finite, which requires that the trailing edge, $\zeta = 1$, be a stagnation point. Sample flows for the airfoil of Figure 7.31 are depicted in Figure 7.37. As long as the attack angle ϕ is of moderate size, the resulting flow and lift is in fairly good agreement with experiments. Further developments and refinements can be found in several references, including [**12**, **56**, **67**, **71**].

All of the preceding examples can be interpreted as planar cross-sections of three-dimensional fluid flows past an airplane wing oriented in the longitudinal z direction. The wing is assumed to have a uniform cross-section shape, and the flow not dependent upon the axial z coordinate. For sufficiently long wings flying in laminar (non-turbulent) flows, this model will be valid away from the wing tips. Understanding the dynamics of more complicated airfoils with varying cross-section and/or faster motion requires a fully three-dimensional fluid model. For such problems, complex analysis is no longer applicable, and, for the most part, one must rely on large scale numerical integration. Only in recent years have computers become sufficiently powerful to compute realistic three-dimensional fluid motions — and then only in reasonably mild scenarios†. The two-dimensional versions that have been analyzed here still provide important clues to the behavior of a three-dimensional flow, as well as useful initial approximations to the three-dimensional airplane wing design problem.

Cauchy's Integral Formula

Cauchy's Theorem 7.49 forms the cornerstone of almost all applications of complex integration. The fact that we can move the contours of complex integrals around freely — as long as we do not cross over singularities of the integrand — grants us great flexibility in their evaluation. An important consequence of Cauchy's Theorem is the justly famous *Cauchy integral formula*, which enables us to compute the value of an analytic function at a point by evaluating a contour integral around a closed curve encircling the point.

Theorem 7.55. *Let $\Omega \subset \mathbb{C}$ be a bounded domain with boundary $\partial\Omega$, and let $a \in \Omega$. If $f(z)$ is analytic on Ω, then*

$$f(a) = \frac{1}{2\pi\,\mathrm{i}} \oint_{\partial\Omega} \frac{f(z)}{z-a}\,dz. \tag{7.135}$$

Remark: As always, we traverse the boundary curve $\partial\Omega$ so that the domain Ω lies on our left. In most applications, Ω is simply connected, and so $\partial\Omega$ is a simple closed curve oriented in the counter-clockwise direction.

It is worth emphasizing that Cauchy's formula (7.135) is *not* a form of the Fundamental Theorem of Calculus, since we are reconstructing the function by *integration* — not its anti-derivative! The closest real counterpart is the Poisson Integral Formula (4.126) expressing the value of a harmonic function in a disk in terms of its values on the boundary circle. Indeed, there is a direct connection between the two results resulting from the intimate bond between complex and harmonic functions.

† The definition of "mild" relies on the magnitude of the Reynolds number, [**12**], an overall measure of the flow's complexity.

Proof: We first prove that the difference quotient

$$g(z) = \frac{f(z) - f(a)}{z - a}$$

is an analytic function on all of Ω. The only problematic point is at $z = a$ where the denominator vanishes. First, by the definition of complex derivative,

$$g(a) = \lim_{z \to a} \frac{f(z) - f(a)}{z - a} = f'(a)$$

exists and therefore $g(z)$ is well-defined and, in fact, continuous at $z = a$. Secondly, we can compute its derivative at $z = a$ directly from the definition:

$$g'(a) = \lim_{z \to a} \frac{g(z) - g(a)}{z - a} = \lim_{z \to a} \frac{f(z) - f(a) - f'(a)\,(z - a)}{(z - a)^2} = \tfrac{1}{2}\, f''(a),$$

which follows from Taylor's Theorem (or l'Hôpital's rule). Knowing that g is differentiable at $z = a$ suffices to establish that it is analytic on all of Ω. Thus, we may appeal to Cauchy's Theorem 7.49, and conclude that

$$\begin{aligned} 0 = \oint_{\partial\Omega} g(z)\, dz &= \oint_{\partial\Omega} \frac{f(z) - f(a)}{z - a}\, dz = \oint_{\partial\Omega} \frac{f(z)}{z - a}\, dz - f(a) \oint_{\partial\Omega} \frac{dz}{z - a} \\ &= \oint_{\partial\Omega} \frac{f(z)}{z - a}\, dz - 2\pi\,\mathrm{i}\, f(a), \end{aligned}$$

where the second integral was evaluated using (7.124). Rearranging terms completes the proof of the Cauchy formula. *Q.E.D.*

Remark: The proof shows that if, in contrast, $a \notin \overline{\Omega}$, then the Cauchy integral vanishes:

$$\frac{1}{2\pi\,\mathrm{i}} \oint_{\partial\Omega} \frac{f(z)}{z - a}\, dz = 0.$$

If $a \in \partial\Omega$, then the integral does not converge.

Let us see how we can apply this result to evaluate seemingly intractable complex integrals.

Example 7.56. Suppose that you are asked to compute the contour integral

$$\oint_C \frac{e^z\, dz}{z^2 - 2z - 3}$$

where C is a circle of radius 2 centered at the origin. A direct evaluation is not easy, since the integrand does not have an elementary anti-derivative†. However, we note that

$$\frac{e^z}{z^2 - 2z - 3} = \frac{e^z}{(z + 1)(z - 3)} = \frac{f(z)}{z + 1} \qquad \text{where} \qquad f(z) = \frac{e^z}{z - 3}$$

† At least not one listed in any integration tables, e.g., [**51**]. A deeper result, [**26**], confirms that its anti-derivative *cannot* be expressed in closed form using elementary functions.

is analytic in the disk $|\,z\,| \leq 2$ since its only singularity, at $z = 3$, lies outside the contour C. Therefore, by Cauchy's formula (7.135), we immediately obtain the integral

$$\oint_C \frac{e^z\,dz}{z^2 - 2\,z - 3} = \oint_C \frac{f(z)}{z+1}\,dz = 2\,\pi\,\mathrm{i}\,f(-1) = -\,\frac{\pi\,\mathrm{i}}{2\,e}\,.$$

Note: Path independence implies that the integral has the same value on any other simple closed contour, provided it is oriented in the usual counter-clockwise direction and encircles the point $z = 1$ but not the point $z = 3$.

Derivatives by Integration

The fact that we can recover values of complex functions by integration is noteworthy. Even more amazing‡ is the fact that we can compute *derivatives* of complex functions by *integration* — turning the Fundamental Theorem on its head! Let us differentiate both sides of Cauchy's formula (7.135) with respect to a. The integrand in the Cauchy formula is sufficiently nice so as to allow us to bring the derivative inside the integral sign. Moreover, the derivative of the Cauchy integrand with respect to a is easily found:

$$\frac{\partial}{\partial a}\left(\frac{f(z)}{z-a}\right) = \frac{f(z)}{(z-a)^2}\,.$$

In this manner, we deduce an integral formulae for the derivative of an analytic function:

$$f'(a) = \frac{1}{2\,\pi\,\mathrm{i}}\oint_C \frac{f(z)}{(z-a)^2}\,dz, \tag{7.136}$$

where, as before, C is any simple closed curve that goes once around the point $z = a$ in a counter-clockwise direction§. Further differentiation yields the general integral formulae

$$f^{(n)}(a) = \frac{n\,!}{2\,\pi\,\mathrm{i}}\oint_C \frac{f(z)}{(z-a)^{n+1}}\,dz \tag{7.137}$$

that expresses the n^{th} order derivative of a complex function in terms of a contour integral.

These remarkable formulae can be used to prove our earlier claim that an analytic function is infinitely differentiable, and thereby complete the proof of Theorem 7.9.

Example 7.57. Let us compute the integral

$$\oint_C \frac{e^z\,dz}{z^3 - z^2 - 5\,z - 3} = \oint_C \frac{e^z\,dz}{(z+1)^2(z-3)}\,,$$

around the circle of radius 2 centered at the origin. We use (7.136) with

$$f(z) = \frac{e^z}{z-3}\,, \qquad \text{whereby} \qquad f'(z) = \frac{(z-4)\,e^z}{(z-3)^2}\,.$$

‡ Readers who have successfully tackled Exercise ■ may be less surprised by this fact.

§ Or, more generally, any closed curve that has winding number $+1$ around the point $z = a$.

Since $f(z)$ is analytic inside C, the integral formula (7.136) tells us that

$$\oint_C \frac{e^z\,dz}{z^3 - z^2 - 5\,z - 3} = \oint_C \frac{f(z)}{(z+1)^2}\,dz = 2\,\pi\,\mathrm{i}\,f'(-1) = -\,\frac{5\,\pi\,\mathrm{i}}{8\,e}\,.$$

